THE UNIVERSITY OF MICHIGAN

INDUSTRY PROGRAM OF THE COLLEGE OF ENGINEERING

PLATE EFFICIENCIES AND MASS TRANSFER FOR VALVE TRAYS AND TRAYS WITH LARGE PERFORATIONS

Robert H. Miller

A dissertation submitted in partial fulfillment
of the requirements for the degree of
Doctor of Philosophy in the
University of Michigan
1958

March, 1959

IP-360

Doctoral Committee:

Professor Brymer Williams, Chairman
Professor Julius T. Banchero
Assistant Professor Kenneth F. Gordon
Professor Victor L. Streeter
Professor Robert R. White

ACKNOWLEDGEMENTS

The author wishes to express his appreciation to the following people who materially aided him during the course of the investigation:

To Professor Brymer Williams, whose advice and counsel served as a constant guide.

To the members of the Doctoral Committee, for their many suggestions and help in planning the work.

To Messrs. Cleatis Bolen, Frank Drogosz, and William Hines, who helped with the construction and modification of the experimental equipment.

To Mr. Robert Norman and Mr. Keith Coats, for aid in programming and operation of the IBM 650 computer.

To Mr. John Begley, who was always willing to take time from his own work to discuss problems as they arose.

To the Phillips Petroleum Company, Allied Chemical Corporation, and the Research Committee of the American Institute of Chemical Engineers, for their fellowship grants.

To the Industry Program of the College of Engineering for preparation and printing of the dissertation.

TABLE OF CONTENTS

TABLE OF CONTENTS (CONT'D)

LIST OF TABLES

LIST OF TABLES (CONT'D)

LIST OF FIGURES

LIST OF FIGURES (CONT'D)

LIST OF FIGURES (CONT'D)

SUMMARY

The purpose of the study was to obtain plate efficiency, mass transfer, and hydraulic data for the valve and perforated trays, and ascertain if their performance could be predicted from presently available data on bubble cap trays. Two types of tray design were investigated using two systems in which the resistance to mass transfer is controlled by the vapor phase.

The valve tray contained nine 7/8-inch holes fitted with 1-1/2-inch valves stamped from 18 gauge sheet and located on a 2-1/2-inch square pitch. The perforated tray was identical to the valve tray except that the valves were not used. The trays were installed in a rectangular column previously used by the Tray Efficiency Program of the American Institute of Chemical Engineers. The tray was 7-1/2 inches wide and 13 inches long from inlet downcomer to overflow weir. A splash baffle was installed upstream from the weir to smooth the liquid flow and to confine the bubbling action. The splash baffle limited the length of the active tray to 11-13/16 inches. The front of the column was fitted with a glass window so that the bubbling action on the tray could be observed.

Data for the humidification of air with water, using the valve tray, covered an operating range in which the weir height was 1-1/2 and 3-1/2 inches, liquid rate was from 8 to 24 gallons per minute, and gas velocity varied from 1 to 5 feet per second, based on the active area of the tray. For the absorption of ammonia from air by water, using both the valve tray and the perforated tray, the weir height was 2 and

3-1/2 inches, liquid rate was from 8 to 32 gallons per minute, and gas velocity varied from 1 to 5 feet per second.

It was found that the Murphree vapor efficiency for both systems investigated increases with either an increase of weir height or an increase of liquid rate. At a weir height of 3-1/2 inches, the efficiency was almost independent of vapor rate if the tray was in the stable operating range. At weir heights of 1-1/2 and 2 inches, the efficiency decreased as the vapor rate was first increased. As the vapor rate was further increased, the efficiency remained constant or increased slightly.

The weeping limit of the perforated tray was found to be primarily a function of the vapor velocity through the holes, with values falling in the range of from 30 to 40 feet per second. Liquid mixing was greater for the perforated tray than for the valve tray, but in each case was not as large as that previously found for bubble cap trays. The entrainment was greater for the perforated tray than for the valve tray.

The mass transfer data for the two systems were correlated by the following equations:

Humidification, Valve Tray

$$N_G = 5.84(Z_f - Z_c)^{0.475}\ u^{-0.382}\ Z_w^{0.183}$$

Ammonia Absorption, Valve Tray

$$N_G = 4.97(Z_f - Z_c)^{0.621}\ u^{-0.458}\ Z_w^{0.287}$$

Ammonia Absorption, Perforated Tray

$$N_G = 3.72(Z_f - Z_c)^{0.650}\ u^{-0.459}\ Z_w^{0.407}$$

where N_G is the number of individual gas phase transfer units; Z_f is

the froth height, feet; Z_c is the clear liquid height, feet; u is the gas velocity based on the active bubbling area, feet per second; and Z_w is the height of the overflow weir, inches. It was found that the inclusion of weir height as an independent variable improved the correlation over that obtained using the same form but omitting weir height.

Performance of the valve and perforated trays can be estimated from existing correlations for bubble cap trays. The estimates can be improved by use of correction factors that were determined and found to be a function of tray design and weir height.

INTRODUCTION

The use of bubble cap plate towers in the petroleum and chemical industries has been standard for thirty to thirty-five years. In recent years, as costs have risen, manufacturers have begun to investigate other types of vapor-liquid contacting devices in the hope of reducing their equipment and operating expenses. Many new plate designs have appeared, and their designers claim that the new plates have operating characteristics which make them superior to bubble cap plates. In addition, perforated plates, whose use dates back to the 1830's, have been reinvestigated and their use is beginning to increase.

The present research was designed to investigate two types of plate design and compare their performance with bubble cap plates. The designs selected were the valve plate and a perforated plate in which the size of the perforations was three to four times as large as those normally used.[29] The research was carried out in a rectangular column which had previously been used to investigate bubble cap plates. Two experimental systems were used: humidification of air and the absorption of ammonia from air by water. The first system is one in which all of the resistance to mass transfer is in the vapor phase. In the second, the majority of resistance is in the vapor phase, but some liquid phase resistance is present. The amount of liquid phase resistance varies with the operating conditions and ranged from a negligible amount to about fifteen per cent of the total resistance. As both the column and the systems have been previously investigated with bubble cap plates, a direct comparison can be made between the performance of bubble cap plates and the valve and perforated plate.

VAPOR-LIQUID CONTACTING APPARATUS

The use of vapor-liquid contacting apparatus in the chemical engineering field is of great importance. It is the basis of many types of separations. These separations can be broken down into three major categories[17]:

> Distillation, where heat is used to drive off vapors from the liquid, the vapors being later condensed; Absorption, where the material being transferred passes from the vapor phase to the liquid phase; and Stripping or Desorption, where the material being transferred passes from the liquid phase to the vapor phase.

The types of apparatus that can be used to effect the separations are multitudinous, although the packed tower and plate tower are the ones that have been used most frequently. The packed tower consists of a column shell which is filled with material so constructed as to break up the liquid flow and provide a large liquid surface area to contact the rising vapors. Many types of packing material have been used such as coke, stone, ceramic rings and saddles, glass helices and other proprietary types. The use of packed towers is normally limited to towers having a diameter of less than two or three feet as the larger towers can be more economically constructed by using plates.

In the plate tower, the column shell contains horizontal plates spaced at fixed intervals. Liquid flows across the plate where it is contacted by the rising vapors and passes to the tray below via downcomers. The method of contacting the vapor and liquid varies with the

plate design, the most simple being the perforated plate. The perforated plate contains a large number of small holes, usually from 1/8 to 1/4-inch in diameter, through which the vapor passes. The vapor is thus broken up into small bubbles which provide good contacting with the liquid. The passage of the vapors through the perforations prevents the liquid from leaking through the holes as long as the vapor velocity through the holes is above a minimum value. This minimum value fixes the lower operating condition if effective separation is to be maintained. Although the perforated plates have been used for many years, it was believed that their operating range was small; and their use was restricted to specialized separations such as those in which the liquid contained a large amount of suspended solid material. More recently it has been found[41] that when properly designed they have a wide range of stable, efficient operation, and they are being used more and more in the chemical and petroleum industry.[29].

Until the time when the perforated plates started to return to favor, the standard type of design was the bubble cap plate. The bubble cap plate contains a large number of holes into which are fitted risers to conduct the vapors from the space beneath the plate. Over the risers are mounted caps. Caps are available in a large number of shapes and sizes with the hemispherical and cylindrical-shaped caps normally used, although bell-shaped and rectangular caps are sometimes used. In commercial equipment, the caps normally range from 2-1/2 to 6 inches in diameter. The lower edge or skirt of the cap usually contains a large number of slots or serrations. Vapor from the riser is diverted downward by the cap and issues from the slots or serrations. An overflow weir is

installed at the outlet of the plate to insure that the skirts of the caps are below the liquid level on the plate.

Although the plate columns described provide intimate contacting between the liquid and vapor and have the advantage of essentially counter current flow, their operation sometimes presents problems. Each tray has an associated pressure drop of the vapor stream. Approximately, this is the sum of the pressure drop of a dry tray, i.e., with no liquid flow, and the pressure drop due to the liquid present on the tray when operating. This pressure drop may be on the order of several inches of water per plate. In most cases, this does not present much of a problem with towers operating at atmospheric or high pressure, but with vacuum towers with large numbers of plates a high pressure drop through the column can cause the bottom temperature to be high enough to cause damage to a heat sensitive product. The high pressure at the base of the column can,in some cases, decrease the relative volatility of the materials being separated and increase the difficulty of the separation.[26]

Another factor of concern is the stability of the operating plates. A plate is called stable if all bubble caps or perforations are functioning. The liquid flowing across the plate has a hydraulic gradient. If the length of liquid path is long or if the liquid rates are high, the hydraulic gradient may be large enough to prevent the upstream caps or perforations from bubbling. In extreme cases, it may cause liquid to "dump" or "back trap" through the upstream caps or perforations to the plate below. Unstable operation can be eliminated by proper design[12,26,33], and in large columns multipass plates are often used

to reduce the length of the liquid path and, consequently, the hydraulic gradient.

Unfortunately, the vapor is never completely separated from the liquid on the plate and will carry some liquid to the plate above in the form of a fine mist or spray. Liquid may also be carried over due to the splashing and agitation of liquid on the plate. The liquid reaching the tray above is called entrainment. If the entrainment becomes large, the effectiveness of the separation is decreased. Entrainment can be decreased by increasing the plate spacing, but this results in a taller and more expensive tower. It can also be decreased by lowering the allowable vapor velocity in the column, but this results in either limiting the vapor handling capacity or a column of larger diameter. Thus the economic aspect is also important and may well determine the column design.

If the column does not provide sufficient vapor and liquid handling capacity, it will not operate properly. If vapor handling capacity is limiting, the column will flood. If liquid handling capacity is limiting, the column will prime. The result in either case is that the column fills with liquid and separation ceases.

In the many years that plate towers have been in use, a large number of individual designs have evolved. Until recently, few of them have been used in commercial equipment. As the cost of manufacturing, operating and maintaining columns continues to rise, manufacturers are looking for less expensive ways to obtain the desired separations. In general, the new trays have been designed along one or more of the following categories:

1. Increase the degree of contacting between the liquid and vapor phases, or maintain the degree of contacting over a wider range of liquid and vapor flow rates, and thus increase the capacity of a given piece of equipment.
2. Decrease the vapor pressure drop through the plate.
3. Decrease the liquid hydraulic gradient across the plate.
4. Decrease the entrainment produced by the plate.

Unfortunately, the four categories are interrelated and the improvement of one category may result in unsatisfactory performance in one or more of the other categories. Thus, a satisfactory design is usually a compromise to obtain the best results for a given set of operating conditions. In the following section, a description will be given of some of the newer plate designs presently available.

PLATE DESIGNS

Most of the new plate designs are proprietary developments and have seen relatively limited service. Whether or not they will replace bubble cap or perforated plates remains to be seen. Some of the designs that will be described are not new, but are being investigated in the attempt to improve performance or increase capacity. Sketches of the plates are presented in Figure 1.

Baffles[27] - This is a type of construction that has been used for some time for easy separations. Baffles are used instead of trays. They are of the disc and doughnut type or segmental cross baffles which extend over half of the tower area set at 180° to each other. This equipment has a low pressure drop and high capacity, but performance is not as good as bubble cap plates.

Benturi[27,38,63] - In this design, a series of bent venturis (hence the name) are used to convey the vapor. They have roughly a 90° bend and discharge the vapor in a horizontal plane in the same direction as the liquid flow. Vertical perforated baffles are located above the plate to reduce entrainment.

Dual Flow[27] - This is a variation of the perforated plate. However, the holes are much larger and downcomers are not used, the holes passing both vapor upwards and liquid downwards.

Flexitray[27,63] - This is one of the valve trays and is also a modification of the perforated plate. The plate contains a number of large holes about two inches in diameter. The holes are covered by a disc that rises off the plate as vapor flows through the column. A retaining spider prevents horizontal motion of the disc and

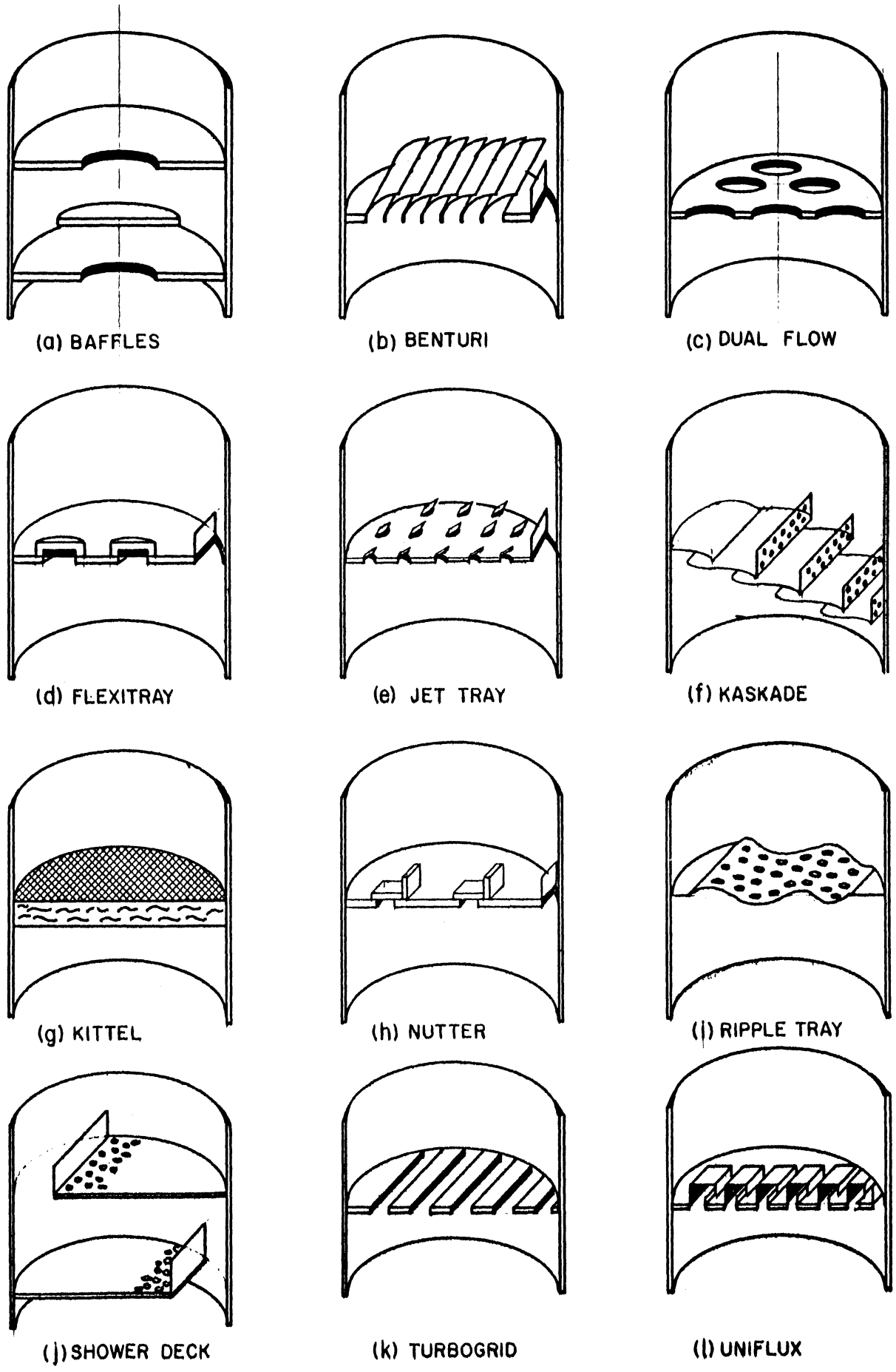

Figure 1. Various Types of Plates

limits the amount of vertical travel. A wider range of operating conditions is enhanced by using discs of different weights in adjacent rows.

Jet Tray[27] - This may also be thought of as a modified perforated plate. Incomplete circular cuts are made in the plate and the metal bent upward. The cuts are made so that the vapor issuing from them is directed across the tray in the direction of liquid flow. Overflow weirs are not used.

Kaskade[27,30] - This is somewhat similar to the Benturi design. Instead of venturis they consist of a series of S-shaped baffles which are set on their sides and arranged stepwise across the path of liquid flow. A nearly vertical perforated baffle is attached to the lower part of the S-shaped unit. Vapor rising through the S portion of the baffles impinges against the perforations and carries along the liquid which flows down the steps.

Kittel[27] - A unit is made from several sheets of expanded metal plates. The cuts in the metal are made at various angles so that the desired flow pattern can be obtained. Downcomers are not used, and the unit passes both liquid and vapor.

Nutter[27,48] - This type is similar to the Flexitray; however, the holes in the plate are rectangular and are located at right angles to the path of liquid flow. The holes are covered with an angle-shaped valve with the vertical leg on the downstream side. As vapor flow increases in the column, the valve starts to lift, pivoting on the apex of the angle. Liquid flowing over the plate will also help to pivot the valve. If the vapor flow is further increased, the valve will lift completely off the plate. Brackets limit the rise of the valve unit and prevent horizontal motion.

Ripple[7,27,35] - In this design, weirs and downcomers are not used. The tray is perforated in the flat much like a perforated tray and then bent into a series of sinusoidal waves. The plates are installed with the wave axis rotated 90° on adjacent plates. Increased capacity is claimed as the holes in the bottom of the waves will preferentially pass liquid while those in the top will preferentially pass vapor.

Shower Deck[27] - This is an older design and a modification of the baffle type. The column contains a number of horizontal baffles that occupy most of the tower cross section. At the edge of the baffle is a dam which prevents liquid from overflowing. Adjacent to the dam is a series of perforations which allow the liquid to flow through the plate and be broken up into drops which contact the rising vapors. Each succeeding tray is turned 180° from the adjacent one. The operating characteristics are similar to the baffle columns, and they are used for the same types of service.

Turbogrid[23,27,38,56] - This design is simple in construction and consists of a grid of parallel slots that cover the entire cross-sectional area of the column. Weirs and downcomers are not used. The slots can be stamped from metal plate or can be the spaces between parallel bars. Adjacent trays are installed with the slots at right angles to each other.

Uniflux[13-15,27,38] - The basic elements of the Uniflux tray are a series of S-shaped members with slots along one face. These are installed on their sides in an overlapping manner at right angles to the path of liquid flow. The spaces between the members act as bubble cap

risers and the slots as bubble caps. They have been operated both with and without downcomers.

METHODS FOR EXPRESSING PERFORMANCE

Of the several ways available to express the performance of vapor-liquid contacting devices, the one most frequently used is the efficiency concept. If the degree of contacting of the liquid and vapor on a plate were perfect, the liquid and vapor leaving the plate would be in equilibrium; and such a plate is called an equilibrium plate or ideal plate. Unfortunately the plates in use do not produce equilibrium streams, and the term efficiency has been introduced to describe the actual performance. Three separate efficiencies have been defined: overall column efficiency, Murphree plate efficiency, and point efficiency. The choice of which efficiency to use depends on the individual situation, although under certain conditions the three are related as will be shown later.

Overall Column Efficiency

If all of the plates in a given column operate as ideal plates, the number of such plates required to effect a given separation can be readily calculated by methods based on a set of material and energy balances.[10,17,52,54] As the actual plates are not ideal plates, the number of actual plates required for the separation will be different. The ratio of these two numbers is termed the overall column efficiency. Thus

$$E_o = \frac{\text{Number of Ideal Plates}}{\text{Number of Actual Plates}}, \qquad (1)$$

where

E_o = overall column efficiency.

Drickamer and Bradford[28] investigated the performance of columns operating with petroleum and similar hydrocarbon materials and found their performance could be expressed by the following empirical relationship.

$$E_o = 18 - 60 \log \mu \qquad (2)$$

where

μ = molal average viscosity of feed at the average column temperature, centipoises.

O'Connell[49] added the relative volatility of the key components as a correlating factor and improved the correlation and extended its range of applicability. His correlation is normally presented in graphical form as a plot of overall column efficiency versus the product of relative volatility times molal average viscosity.[17,54,60]

Later investigators[37,71] have added data in the same type of plot while Chu[21,22] has added the liquid to vapor mass ratio and submergence to improve the correlation.

Unfortunately the overall column efficiency does not appear to be a simple function of the variables listed above, and in order to obtain a better prediction of column performance other methods have been used and will be described later.

Murphree Plate Efficiency

Murphree[46] defined the approach to equilibrium on a plate. Although first developed for a single bubble, it is now applied to the entire plate. The Murphree plate efficiency can be defined in terms of either the vapor or liquid compositions. Using vapor compositions, the

efficiency of plate n (numbered from the bottom of the column) is

$$E_{MV} = \frac{y_{n-1} - y_n}{y_{n-1} - y_n^*} \tag{3}$$

where

E_{MV} = Murphree vapor efficiency for plate n

y_{n-1} = average concentration of solute in vapor leaving the plate below plate n, mole fraction

y_n = average concentration of solute in vapor leaving plate n, mole fraction

y_n^* = concentration of solute in vapor that would be in equilibrium with the average concentration of solute in liquid leaving plate n, mole fraction.

In terms of liquid compositions, the efficiency is

$$E_{ML} = \frac{x_n - x_{n+1}}{x_n^* - x_{n+1}} \tag{4}$$

where

E_{ML} = Murphree liquid efficiency for plate n

x_n = average concentration of solute in liquid leaving plate n, mole fraction

x_{n+1} = average concentration of solute in liquid leaving the plate above plate n, mole fraction

x_n^* = concentration of solute in liquid that would be in equilibrium with the average concentration of solute in the vapor leaving plate n.

Thus, it can be seen for either definition the Murphree plate efficiency is the ratio of the actual concentration gain to that theoretically possible if the liquid and vapor streams leaving the plate were at equilibrium.

By setting up a material balance around plate n, a relationship between the Murphree vapor efficiency and Murphree liquid

efficiency can be obtained[59]

$$E_{MV} = \frac{E_{ML}}{E_{ML} + \frac{mG_M}{L_M}(1 - E_{ML})} \tag{5}$$

or

$$E_{MV} = \frac{E_{ML}}{E_{ML} + \frac{H}{P}\frac{G_M}{L_M}(1 - E_{ML})} \tag{6}$$

where

G_M = superficial molar mass velocity of vapor, lb mole/hr-sq ft, based on column cross section

L_M = superficial molar mass velocity of liquid, lb mole/hr-sq ft, based on column cross section

m = slope of the equilibrium curve, dy^*/dx

H = Henry's Law constant, atm/mole fraction

P = pressure on tray, atm.

If the operating and equilibrium lines are straight and E_{MV} is constant throughout the column, a relationship between E_{MV} and E_o, the overall column efficiency, can be obtained.[44]

$$E_o = \frac{\ell n[1 - E_{MV}(\frac{mG_M}{L_M} - 1)]}{\ell n \frac{mG_M}{L_M}} \tag{7}$$

If liquid from the plate is being entrained by the vapor stream, the change in composition of the latter will not be as great as if there were no entrained liquid. The apparent efficiency of the plate will be lower than the plate operating under the same conditions but with no entrainment. Colburn[24] has derived an expression relating the apparent efficiency and the plate efficiency when no entrainment is present. An

approximate form of this expression is

$$E_a = \frac{E_{MV}}{1 + \epsilon \frac{G_M}{L_M} E_{MV}} \tag{8}$$

where

E_a = apparent vapor plate efficiency in the presence of entrainment, and

ϵ = moles liquid entrained per mole dry vapor.

This expression is rigorous only for the case where the operating and equilibrium lines are parallel and the liquid is completely mixed. However, it can be used for cases where the operating and equilibrium lines are not widely divergent. In cases where there is great divergence between operating and equilibrium lines, the exact expression given by Colburn should be used.

Point Efficiencies

Whereas the Murphree vapor efficiency was defined over the entire tray, the vapor point efficiency is defined over a vertical line above a given point on the tray.

$$E_{OG} = \frac{y'_{n-1} - y'_n}{y'_{n-1} - y'^*_n} \tag{9}$$

where

E_{OG} = the vapor point efficiency, and the primes indicate vapor concentrations at points lying on a vertical line through the tray.

This is equivalent to taking the liquid as well mixed in the vertical direction but not necessarily in the horizontal direction. It can readily be seen that if the liquid on the tray is completely mixed, then the

Murphree vapor efficiency and the vapor point efficiency will be equal, or $E_{MV} = E_{OG}$.

Analogously a liquid point efficiency is defined over a horizontal line in the direction of liquid flow.

$$E_{OL} = \frac{x'_n - x'_{n+1}}{x'^*_n - x'_{n+1}} \tag{10}$$

where

E_{OL} = the liquid point efficiency, and the primes indicate liquid samples lying on a horizontal line.

This is equivalent to taking the vapor to be well mixed in the horizontal direction but not necessarily in the vertical direction. This might be true in a case where the gas composition changes so little that value of x'^*_n is essentially constant, but in the majority of cases this is a questionable assumption.

It should be noted that the physical models used in the expression for point efficiencies are not compatible. It is not surprising, therefore, that difficulty arises when the two models are assumed to exist simultaneously.

LIQUID MIXING

The relationship between plate and point efficiency depends greatly on the degree of liquid mixing on the plate. As has been stated previously, if the liquid on the plate is completely mixed, $E_{MV} = E_{OG}$. If the liquid is unmixed or partially mixed, a different relationship will result. Likewise, if the vapor is completely mixed and of uniform composition at all vertical levels, the Murphree liquid plate efficiency will be equal to the liquid point efficiency, or $E_{ML} = E_{OL}$.

Lewis[43] investigated three types of liquid and vapor flow patterns and obtained relationships between the Murphree plate efficiency and the point efficiency, which was assumed to remain constant across the plate. One type was the case of vapor of uniform composition entering the plate and contacting liquid that flows across the plate without mixing. This is often referred to as the "plug flow model". The relationship he obtained is

$$E_{MV} = \frac{L_M}{mG_M} \left[\exp\left(E_{OG} \frac{mG_M}{L_M}\right) - 1\right] \qquad (11)$$

where

$$\exp(x) = e^x.$$

The other types involved non-mixing of the vapor between plates and non-mixing of the liquid flowing in various directions on successive plates. These appear to be much more artificial models, and the relationships will not be presented here. Of the three models, only the plug flow type has found much acceptance and appears to be reasonably valid in large columns under conditions of low vapor and high liquid loadings.

In actual operation, most plates operate somewhere in the range between plug flow and completely mixed flow. Several models have been developed to describe the degree of mixing and the relationship between point and plate efficiencies.

Kirschbaum[39,40] and Gautreaux and O'Connell[31] have proposed a model in which the plate is considered to be composed of a number of completely mixed pools or stages. By assuming that the liquid and vapor loads are equal for each pool, the equilibrium relationship is linear, and E_{OG} is constant across the plate, they have derived relationships between point and plate efficiency. The equation presented by Gautreaux and O'Connell is in much simpler form than that of Kirschbaum and is

$$E_{MV} = \frac{L_M}{mG_M}\left[\left(1 + \frac{mG_M}{L_M}\frac{E_{OG}}{n}\right)^n - 1\right] \qquad (12)$$

where

n = number of pools or stages on the plate.

If the tray is completely mixed, the number of pools is one and Equation (12) reduces to $E_{MV} = E_{OG}$. However, if plug flow exists, an infinite number of pools would be required. Under such conditions Equation (12) is indeterminate, but in the limit reduces to Equation (11).

Attempts to correlate the number of pools on a plate have not met with much success. In the absence of other data Gautreaux and O'Connell recommend the use of one pool per foot of liquid travel on the plate.

Warzel[66] and Oliver and Watson[50] have postulated a mixing model based on a fictitious liquid stream of quantity (C-1)L which is

recycled from the overflow weir back to the liquid inlet without contacting the vapor stream. Thus, the net flow of liquid across the tray is CL, and the relation between point and plate efficiency is

$$E_{MV} = \frac{C}{\lambda} \left[\exp\left(\frac{\lambda E_{OG}}{C}\right) - 1\right] \tag{13}$$

where

$\lambda = \frac{mG_M}{L_M}$ the ratio of slopes of the equilibrium and operating lines, and

$$C = \frac{x_n - x_{n+1}}{x_n - x_e} \tag{14}$$

where

x_e = concentration of solute in the liquid at a point on plate n between the inlet and the first row of caps, mole fraction.

If the liquid on the tray is completely mixed, then x_n and x_e are identical and C becomes infinite. If plug flow exists, x_{n+1} and x_e are identical as the liquid has not yet been contacted by the vapor, and C is unity.

Crozier[25] derived a mixing model in which the turbulence of the vapor bodily carries liquid from a point on the plate to another point upstream. Using a differential difference equation he obtained the relationship

$$E_{MV} = \frac{1+\gamma}{\lambda} \left[\exp\left(\frac{\lambda E_{OG}}{1+\gamma}\right) - 1\right] \tag{15}$$

where

γ = mixing parameter, defined as

$$\gamma = \frac{x_{n+1} - x_n}{x_e - x_n} - \frac{x_{n+1}}{x_e} \tag{16}$$

It can be seen that the result is similar to that obtained by Warzel.[66] The net liquid flow across the tray is $(1+\gamma)L$. For a completely mixed liquid γ becomes infinite, and for the plug flow case γ is zero.

Although Crozier also measured his mixing parameter by a dye decay technique, both his and Warzel's model suffer from the fact that their mixing parameters are defined in terms of exit liquid concentration. As the exit liquid concentration is a function of the efficiency, the mixing parameter must also be dependent on the efficiency.

Anderson[6] and Robinson[55] have derived equations relating plate and point efficiency based on the eddy diffusion concept. They postulate that material is transported from point to point in the froth by eddies as well as by bulk flow. Anderson obtained the relationship

$$1+\lambda E_{MV} = \frac{1 - A_1/M}{(1-A_1/A_2)\exp A_1} + \frac{1 - A_2/M}{(1-A_2/A_1)\exp A_2} \qquad (17)$$

where

$$A_1 = \frac{M}{2} + \sqrt{\frac{M^2}{4} + \lambda E_{OG} M}$$

$$A_2 = \frac{M}{2} - \sqrt{\frac{M^2}{4} + \lambda E_{OG} M}$$

$$M = \frac{S^2}{D_E t_L}$$

and

S = plate length, ft.

D_E = eddy diffusivity, $ft^2/sec.$

t_L = liquid residence time, sec.

He used a boundary condition that related the liquid concentration at the tray entrance to the entering liquid concentration and to material transferred by eddy diffusion to the tray boundary.

Robinson used as boundary conditions the relationships that at the exit of the tray the liquid concentration gradient was zero and the liquid concentration was that overflowing the weir. The expression he obtained is

$$E_{MV} = \frac{E_{OG}[1 - \exp(-A_1)]}{A_1(1-A_1/A_2)} + \frac{E_{OG}[1 - \exp(-A_2)]}{A_2(1-A_2/A_1)} \qquad (18)$$

where the nomenclature is the same as for Equation (17).

Wharton[69], Stone[61], Brown[18], and Byfield[19] have obtained some data on the eddy diffusivity on sieve and bubble cap plates with values falling in the range of 70 to 150 ft^2/hr. Unfortunately the amount of data presently available does not allow Equations (17) and (18) to be readily used.

Johnson and Marangozis[36] postulate a model in which the liquid that passes a given point on the plate consists of a layer on the plate floor and that carried by splashing from points both upstream and downstream. This is similar to the model of Crozier[25] who used unidirectional splashing. They define a parameter in terms of the fraction splashed in each direction and the distance from which the liquid was splashed

$$\beta = Q_F W_F - Q_B W_B \qquad (19)$$

where

β = mixing parameter, and

Q_F = fraction of liquid rate splashing downstream

Q_B = fraction of liquid rate splashing upstream.

W_F = normalized distance of downstream liquid splashing.

W_B = normalized distance of upstream liquid splashing.

The general solution for their differential equation contains two constants which they evaluate using vapor concentrations obtained above the entrance and exit of the plate. It was found that one of the constants was several orders of magnitude smaller than the other and could be considered to be zero for the operating range studied. They thus obtained the result

$$E_{MV} = \frac{E_{OG}(1 - e^{-A_2})}{A_2} \tag{20}$$

where

$$A_2 = \frac{1}{2\beta} - \sqrt{\frac{1}{4\beta^2} + \frac{\lambda E_{OG}}{\beta}}$$

A_2 arises from the auxiliary quadratic equation, and it can be seen that mathematically the splashing model is identical to the eddy diffusivity model with $\beta = 1/M$.

It should be mentioned that Equation (20) can also be obtained from the differential equation by using the boundary conditions $x = x_n$ at the exit of the tray and $\frac{dx}{dw} = 0$ at $w = \infty$. The latter boundary condition is artificial as w is the normalized distance along the tray and has the value $w = 1$ at the tray exit. If one uses the same boundary conditions as Robinson, the solution is identical to Equation (18). Thus, measurement of the splashing on a tray is another way of obtaining eddy diffusivity data.

In presenting the work of Johnson and Marangozis, their equations have been normalized. If their correlation for β is used, it should be normalized before being used with the equations presented herein.

Although the models and equations listed previously were derived for use on bubble cap or perforated plates, they are equally applicable for all types of plate columns. The variation of the mixing parameters with plate design has not been investigated to much extent. The author has obtained some data with a valve tray and a perforated tray with large holes which will be presented later.

INTERPHASE MASS TRANSFER

As correlations of efficiencies per se have not given the desired accuracy, investigators have turned to the basic concepts of mass transfer in order to describe the performance of vapor-liquid contacting devices. The two film, or two resistance, theory proposed by Whitman[70] and the additivity of resistances presented by Lewis and Whitman[42] have served as the model. This model is based on the assumption that on each side of the gas-liquid interface there is a film, and the mass transfer between the two phases is controlled by the resistances in these films. Gordon and Sherwood[32] have shown that the two film theory is in fact dependent on the validity of three assumptions: (1) the rate of mass transfer within each phase is proportional to the difference in concentrations in the main body of the fluid and at the interface; (2) the phases are at equilibrium at the interface, i.e., no interfacial resistance; and (3) the holdup of diffusing solute in the film or region near the interface is negligible with respect to the total amount of material being transferred.

If the above assumptions are valid, then the steady state rate equations can be written

$$N_A = K_{OG}(p_G - p^*) = K_{OL}(c^* - c_L) = k_G(p_G - p_i) = k_L(c_i - c_L) \qquad (21)$$

where

N_A = rate of mass transfer, lb moles/hr-sq ft

K_{OG} = overall gas phase mass transfer coefficient, lb moles/hr-sq ft-atm

K_{OL} = overall liquid phase mass transfer coefficient, lb moles/hr-sq ft - lb moles/cu ft

k_G = individual gas phase mass transfer coefficient, lb moles/hr-sq ft - atm

k_L = individual liquid phase mass transfer coefficient, lb moles/hr-sq ft - lb moles/cu ft

p_G = partial pressure of solute in gas phase, atm

p_i = partial pressure of solute in gas at the interface, atm

p^* = partial pressure of solute in gas in equilibrium with liquid, atm

c_L = concentration of solute in liquid, lb moles/cu ft

c_i = concentration of solute in liquid at the interface, lb moles/cu ft

c^* = concentration of solute in liquid in equilibrium with gas, lb moles/cu ft

Now, if Henry's Law is applicable so that $p_i = Hc_i$ and $p^* = Hc_L$, then the interfacial values in Equation (21) can be eliminated to yield

$$\frac{1}{K_{OG}} = \frac{1}{k_G} + \frac{H}{k_L} \tag{22}$$

and

$$\frac{1}{K_{OL}} = \frac{1}{k_L} + \frac{1}{Hk_G} \tag{23}$$

Analogously if the vapor-liquid equilibrium is presented in the standard y-x form, then Equations (22) and (23) become

$$\frac{1}{K_{OG}} = \frac{1}{k_G} + \frac{Pm}{\rho_{ML} k_L} \tag{24}$$

and

$$\frac{1}{K_{OL}} = \frac{1}{k_L} + \frac{\rho_{ML}}{Pmk_G} \tag{25}$$

where

m = slope of the equilibrium curve, dy^*/dx

P = total pressure, atm

ρ_{ML} = liquid molal density, lb moles/cu ft

Since the mass transfer coefficients are analogous to conductances, the left hand side of Equations (22) through (25) represents the overall resistance to mass transfer, and the individual terms on the right hand side represent the resistance of the individual films.

The Relationship Between Mass Transfer Coefficients and Efficiencies

Consider the fluid streams in an element of an absorber or distillation column as shown in Figure 2.

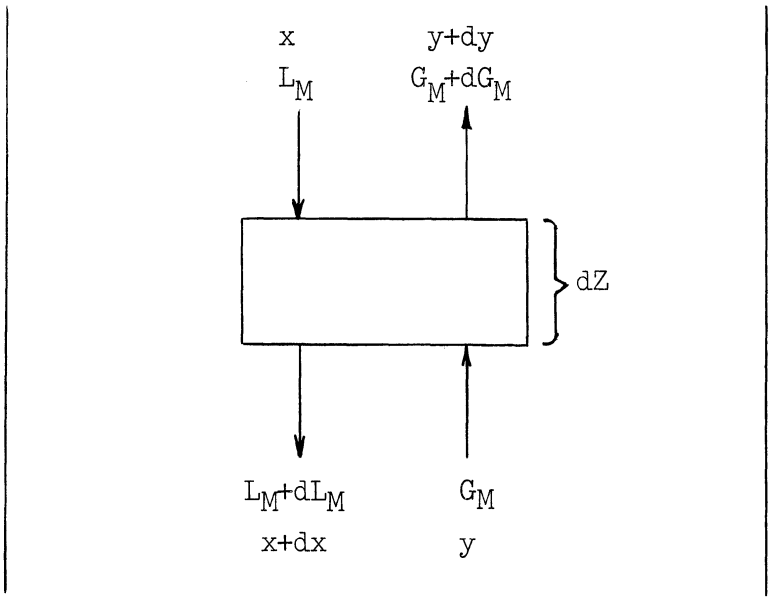

Figure 2. Fluid Streams in an Absorber or Distillation Column

A material balance around the element gives the rate of mass transfer as

$$dN_A = d(G_M y) = - d(L_M x) \tag{26}$$

But the rate of mass transfer can also be expressed in terms of mass transfer coefficients

$$dN_A = K_{OG}a'(y^*-y)PdZ = k_G a'(y_i-y)PdZ \tag{27}$$

$$dN_A = K_{OL}a'(x-x^*)\rho_{ML}dZ = k_L a'(x-x_i)\rho_{ML}dZ \tag{28}$$

where

a' = interfacial area, sq ft/cu ft of gas and liquid holdup.

Now if the gas rate is constant as is essentially so in distillation and for absorption from a dilute gas, then $d(G_M y) = G_M dy$. By combining Equations (26) and (27) one obtains

$$\frac{K_{OG}a'P}{G_M} dZ = \frac{dy}{y^*-y} \tag{29}$$

Considering $K_{OG}a'P/G_M$ constant, the integration is carried out over the mass transfer zone to obtain

$$\frac{K_{OG}a'PZ}{G_M} = \int_{y_o}^{y_1} \frac{dy}{y^*-y} \equiv N_{OG} \tag{30}$$

where

N_{OG} = the number of overall gas phase transfer units.

Also

$$H_{OG} \equiv \frac{Z}{N_{OG}} = \frac{G_M}{K_{OG}a'P} \tag{31}$$

where

H_{OG} = the height of an overall gas phase transfer unit, ft.

These equations defining the transfer unit and height of a transfer unit were originally proposed by Chilton and Colburn[20] for use in a packed column, but their usage is now applied to plate columns as well.

When y* is constant, the integration can be carried out analytically with the limits $y = y_o$ at $Z = 0$ and $y = y_1$ at $Z = Z$ to yield

$$N_{OG} = \frac{K_{OG}a'PZ}{G_M} = - \ell n \left(\frac{y^*-y_1}{y^*-y_o}\right) = - \ell n \, (1 - E_{OG}) \quad (32)$$

Under conditions when an inert carrier gas is present and the gas rate varies as in the absorption from an ammonia-air stream, then $d(G_M y)$ is given by $(G_M)_{avg} \frac{dy}{1-y}$ and N_{OG} is then defined as

$$N_{OG} = \frac{K_{OG}a'PZ}{(G_M)_{avg}} = \int_{y_o}^{y_1} \frac{dy}{(1-y)(y^*-y)} \quad (33)$$

Likewise if y* is constant, integration of the right hand side yields

$$N_{OG} = \frac{K_{OG}a'PZ}{(G_M)_{avg}} = \frac{1}{y^*-1} \ell n \left\{\frac{(1-y_o)(y^*-y_1)}{(1-y_1)(y^*-y_o)}\right\} = \frac{1}{y^*-1} \ell n \left\{\frac{1-y_o}{1-y_1} (1-E_{OG})\right\} \quad (34)$$

The expressions for the number of overall liquid phase and individual gas and liquid phase transfer units are similarly obtained and are presented in Table I.

It should be mentioned that several other definitions of interfacial area have been used. These are a, the square feet of interfacial area per cubic foot of gas holdup, and $\bar{a}$, the square feet of interfacial area per cubic foot of liquid holdup. Accordingly, the vertical distance over which the integration is performed will vary depending on which volume the interfacial area is based. This is shown in Table II.

TABLE I

SUMMARY OF THE NUMBER OF TRANSFER UNITS

BASIS	SYMBOL	ABSORPTION(1)	DISTILLATION(1)
OVERALL GAS PHASE	N_{OG}	$\frac{K_{OG}a'PZ}{(G_M)_{avg}} = \int_{y_o}^{y_1} \frac{dy}{(1-y)(y^*-y)} = \frac{1}{y^*-1} \ell n \left\{ \frac{1-y_o}{1-y_1} \frac{y^*-y_1}{y^*-y_o} \right\}$	$\frac{K_{OG}a'PZ}{G_M} = \int_{y_o}^{y_1} \frac{dy}{y^*-y} = - \ell n \left\{ \frac{y^*-y_1}{y^*-y_o} \right\}$
OVERALL LIQUID PHASE	N_{OL}	$\frac{K_{OL}a'\rho_{ML}Z}{(L_M)_{avg}} = \int_{x_1}^{x_2} \frac{dx}{(1-x)(x^*-x)} = \frac{1}{x^*-1} \ell n \left\{ \frac{1-x_1}{1-x_2} \frac{x^*-x_2}{x^*-x_1} \right\}$	$\frac{K_{OL}a'\rho_{ML}Z}{L_M} = \int_{x_1}^{x_2} \frac{dx}{x^*-x} = - \ell n \left\{ \frac{x^*-x_2}{x^*-x_1} \right\}$
INDIVIDUAL GAS PHASE	N_G	$\frac{k_Ga'PZ}{(G_M)_{avg}} = \int_{y_o}^{y_1} \frac{dy}{(1-y)(y_i-y)} = \frac{1}{y_i-1} \ell n \left\{ \frac{1-y_o}{1-y_1} \frac{y_i-y_1}{y_i-y_o} \right\}$	$\frac{k_Ga'PZ}{G_M} = \int_{y_o}^{y_1} \frac{dy}{y_i-y} = - \ell n \left\{ \frac{y_i-y_1}{y_i-y_o} \right\}$
INDIVIDUAL LIQUID PHASE	N_L	$\frac{k_La'\rho_{ML}Z}{(L_M)_{avg}} = \int_{x_1}^{x_2} \frac{dx}{(1-x)(x_i-x)} = \frac{1}{x_i-1} \ell n \left\{ \frac{1-x_1}{1-x_2} \frac{x_i-x_2}{x_i-x_1} \right\}$	$\frac{k_La'\rho_{ML}Z}{L_M} = \int_{x_1}^{x_2} \frac{dx}{x_i-x} = - \ell n \left\{ \frac{x_i-x_2}{x_i-x_1} \right\}$

(1) Integrated forms obtained by assuming that y^*, y_i, x^* and x_i remained constant.

TABLE II

INTERFACIAL AREAS AND CORRESPONDING INTEGRATION LIMITS

Area	Lower Limit	Upper Limit
a' = sq ft/cu ft gas and liquid holdup	$Z = 0$	$Z = Z_f$
a = sq ft/cu ft gas holdup	$Z = Z_c$	$Z = Z_f$
$\bar{a}$ = sq ft/cu ft liquid holdup	$Z = 0$	$Z = Z_c$

where

Z_f = froth height

Z_c = clear liquid height

If the interfacial area $\bar{a}$ is used in the definition of N_{OL} given in Table I, the factor $\frac{\rho_{ML} Z_c}{L_M}$ has units of time. This represents the liquid residence time of a plate having an area of one square foot. Accordingly, N_{OL} can be defined

$$N_{OL} = K_{OL}\bar{a}t_L \tag{35}$$

where

t_L = liquid residence time, sec

$K_{OL}\bar{a}$ = overall liquid phase mass transfer coefficient, (lb moles/sec-sq ft-lb moles/cu ft)(sq ft/cu ft), or sec^{-1}

and similarly

$$N_L = k_L\bar{a}t_L \tag{36}$$

where

$k_L\bar{a}$ = individual liquid phase mass transfer coefficient, sec^{-1}

The gas phase coefficients can also be defined on a concentration basis leading to

$$N_{OG} = K'_{OG} a t_G \tag{37}$$

and

$$N_G = k'_G a t_G \tag{38}$$

where

t_G = gas residence time = $\frac{(Z_f - Z_c)\rho_{MG}}{G_M}$, sec

ρ_{MG} = molar gas density, lb moles/cu ft

$K'_{OG}a$ = overall gas phase mass transfer coefficient, sec^{-1}

$k'_G a$ = individual gas phase mass transfer coefficient, sec^{-1}.

It can be readily seen that the two definitions for K_{OG} are related by

$$K'_{OG} = K_{OG} RT \tag{39}$$

where

R = ideal gas law constant, $\frac{\text{atm-cu ft}}{\text{lb mole-}^\circ\text{R}}$

T = absolute temperature, $^\circ$R

A similar relationship holds for k_G and k'_G .

In practice the bubbling action on a plate is so complex that it is impossible to determine accurately the interfacial area for mass transfer. For this reason the area is combined with the mass transfer coefficient, for example $K'_{OG}a$, and the resulting expression is also termed a mass transfer coefficient.

The relationship between overall and individual transfer units can be obtained by substituting the definitions listed in Table I into Equations (24) and (25) to obtain

$$\frac{1}{N_{OG}} = \frac{1}{N_G} + \frac{\lambda}{N_L} \tag{40}$$

and

$$\frac{1}{N_{OL}} = \frac{1}{N_L} + \frac{1}{\lambda N_G} \tag{41}$$

In a similar manner using Equations (22) and (23), one obtains

$$\frac{1}{N_{OG}} = \frac{1}{N_G} + \frac{H\rho_{ML}G_M}{PL_M N_L} \tag{42}$$

and

$$\frac{1}{N_{OL}} = \frac{1}{N_L} + \frac{PL_M}{H\rho_{ML}G_M N_G} \tag{43}$$

As with the expressions for mass transfer coefficients, the left hand side of Equations (40) to (43) is proportional to the total resistance to mass transfer while the terms on the right hand side are proportional to the individual phase resistances. Thus, a system in which the gas phase resistance is larger than the liquid phase resistance is termed a gas phase controlling system and vice versa.

If liquid phase resistance is zero as in the case of vaporization of pure liquids, the system is said to be a pure gas phase resistance system. In systems where the solubility of the gas is very small as in the carbon dioxide-water or oxygen-water systems, the Henry's Law constant is so large that the gas phase resistance is often negligible. However, this assumes that the values of N_L and N_G are of the same order of magnitude. Much work has been done on this premise, and it appears to be a valid assumption. These systems are not, however, pure liquid phase resistance systems. Such a system might be a gas which is sparingly soluble in a liquid that has no vapor pressure--a rather artificial system, to say the least.

The Effects of Concentration on Mass Transfer

In the previous presentation of the equations concerning mass transfer, it was assumed that there was no variation of diffusion rate with concentration. The theory of molecular diffusion in gases indicates that this assumption may not be valid in some cases.

In the case of equimolar counter current diffusion, the theory based on Fick's Law states[65] that the amount of material transferred per unit time per unit area is

$$N_A = \frac{D_G(p_1-p_2)}{RT\ z} \tag{44}$$

so

$$k_G = \frac{D_G}{RTz} \tag{45}$$

where

D_G = molecular gas diffusivity

R = ideal gas law constant

z = length of element through which diffusion takes place

p_1, p_2 = partial pressure of the diffusing gas at the extremities of the element.

However, in the case of a material diffusing through a layer of non-diffusing gas, the relationship is[65]

$$N_A = \frac{D_G P(p_1-p_2)}{RTp_{BM}z} \tag{46}$$

so

$$k_G = \frac{D_G P}{RTp_{BM}z} \tag{47}$$

where

P = total pressure

p_{BM} = logarithmic mean partial pressure of the non-diffusing gas = $(p_{B2}-p_{B1})/\ell n(p_{B2}/p_{B1})$

Thus, it appears that the expressions listed in Table I are valid for cases where equalmolar counterdiffusion is present but may not be so in absorption or desorption.

Analogously, in liquid diffusion through a stagnant layer, a ρ_{ML}/c_{BM} term is included in which the denominator represents the logarithmic mean concentration of the non-diffusing liquid. This term cannot be justified on the basis of the kinetic theory of liquids, but is included on the assumption that liquid diffusion is similar to gaseous diffusion.

By substituting $(1-y)_f$ for p_{BM} and $(1-x)_f$ for c_{BM}, the equation for the number of transfer units can be written[52]

$$N_{OG} = \frac{K_{OG}a'Z(1-y)_f}{G_M} = \int \frac{(1-y)_f}{(1-y)(y^*-y)}\,dy \qquad (48)$$

$$N_{OL} = \frac{K_{OL}a'Z(1-x)_f}{L_M} = \int \frac{(1-x)_f}{(1-x)(x^*-x)}\,dx \qquad (49)$$

$$N_G = \frac{k_Ga'Z(1-y)_f}{G_M} = \int \frac{(1-y)_f}{(1-y)(y_i-y)}\,dy \qquad (50)$$

$$N_L = \frac{k_La'Z(1-x)_f}{L_M} = \int \frac{(1-x)_f}{(1-x)(x_i^*-x)}\,dx \qquad (51)$$

where

$(1-y)_f$ = logarithmic mean of $1-y$ and $1-y^*$, and

$(1-x)_f$ = logarithmic mean of $1-x$ and $1-x^*$.

Thus, the relationships between the transfer units are

$$\frac{1}{N_{OG}} = \frac{1}{N_G} + \frac{\lambda(1-x)_f}{N_L(1-y)_f} \tag{52}$$

$$\frac{1}{N_{OL}} = \frac{1}{N_L} + \frac{(1-y)_f}{(1-x)_f \lambda N_G} \tag{53}$$

If y^* is constant, then the integral in Equation (48) can be evaluated analytically. By replacing $(1-y)_f$ by the definition for the logarithmic mean, one obtains

$$N_{OG} = \int_{y_o}^{y_1} \frac{[(1-y)-(1-y^*)]}{(\ell n \frac{1-y}{1-y^*})(1-y)(y^*-y)} dy \tag{54}$$

and by combining terms and factoring

$$N_{OG} = \int_{y_o}^{y_1} \frac{dy}{(1-y)\ \ell n \frac{1-y}{1-y^*}} \tag{55}$$

Use a change of variables, $q = \frac{1-y}{1-y^*}$, to obtain

$$N_{OG} = \int_{\frac{1-y_1}{1-y^*}}^{\frac{1-y_o}{1-y^*}} \frac{dq}{q\ \ell n\ q} \tag{56}$$

the solution of which is

$$N_{OG} = \ell n \left\{ \frac{\ell n(\frac{1-y_o}{1-y^*})}{\ell n(\frac{1-y_1}{1-y^*})} \right\} \tag{57}$$

In many cases, the solute concentration is not large, and the logarithmic mean can be replaced by the arithmetic mean without

appreciable error. Thus, the expression for N_{OG} becomes

$$N_{OG} = \int_{y_o}^{y_1} \frac{[(1-y)+(1-y^*)]}{2(1-y)(y^*-y)}\, dy \tag{58}$$

If y^* is constant, this may be integrated to obtain[59]

$$N_{OG} = \frac{1}{2}\, \ell n \left\{\frac{1-y_1}{1-y_o}\right\} - \ell n(1-E_{OG}) \tag{59}$$

For cases where the solute concentration is low or for equimolar counter diffusion, the relationships given in Table I and Equations (40) through (43) can be used.

In practice the expressions involving p_{BM}/P or c_{BM}/ρ_{ML} are not often used. Usually these ratios are relatively close to unity and the precision of diffusivity data and correlation of mass transfer coefficients have not been sufficiently exact to justify their usage. In addition, Westkaemper[68] conducted studies on the evaporation of carbon tetrachloride into air-carbon tetrachloride mixtures in which the concentration of carbon tetrachloride varied up to 65 mole per cent. He found that the data could be correlated equally well either with or without the p_{BM}/P variable and concluded that this term had not been established as being fundamental. His work was performed by passing the gas stream over a relatively quiescent liquid in a rectangular channel and may not be directly applicable to the studies in a plate column where a more complex type of vapor-liquid contacting takes place. Studies of this nature in plate columns are needed to determine whether or not the theory is valid in this type of equipment.

APPLICATION OF MASS TRANSFER DATA TO PREDICT EFFICIENCIES

The previous sections have described the relationship between the quantities in the mass transfer concept and efficiencies. In this section it will be shown how one might use these quantities to predict the performance of actual equipment.

The basic values that will be needed are data on mass transfer in the individual phases. This might come from a correlation of N_G and N_L, or alternatively $k_G a$ and $k_L \bar{a}$. Use of the former would be easier as hydraulic data are required to convert the latter by the equations

$$N_G = \frac{k_G a P (Z_f - Z_c)}{G_M} \tag{60}$$

$$N_L = \frac{k_L \bar{a} \rho_{ML} Z_c}{L_M} \tag{61}$$

The correlating equations should be functions of the physical properties of the system and ideally would be applicable to all types of plate design. This is the approach that was used by the American Institute of Chemical Engineers research program on bubble cap plates, and it is hoped that their results can be applied to other plates without major modifications.

Once the individual phase properties have been determined, the performance on the overall basis can be computed by Equation (40)

$$\frac{1}{N_{OG}} = \frac{1}{N_G} + \frac{\lambda}{N_L} \tag{40}$$

From the number of overall gas phase transfer units, the point efficiency can be obtained by Equation (32) for distillation

systems or systems where the gas flow rate does not change appreciably

$$N_{OG} = -\ell n(1-E_{OG}) \tag{32}$$

To obtain the Murphree plate efficiency, one must have some knowledge of the degree of mixing expected. This will vary, of course, with the particular system, size of equipment, liquid and vapor flow rates, etc. At the present time the mixing problem has not been solved completely, and the engineer must rely a good deal on his own judgment. Let it be said, however, that the Murphree plate efficiency can be obtained by

$$E_{MV} = \varphi(E_{OG}) \tag{62}$$

where

φ is some function of the degree of mixing.

If the equilibrium and operating lines are straight, then the overall column efficiency is computed by Equation (7)

$$E_o = \frac{\ell n[1-E_{MV}(\lambda-1)]}{\ell n\lambda} \tag{7}$$

Thus, although the path to be followed in obtaining efficiencies is straightforward, it is not without its pitfalls.

The above method is illustrated in the Fourth Annual Report of the A. I. Ch. E. Research Committee[5] where the performance of a 4-ft diameter distillation column, operated by Fractionation Research Inc., separating cyclohexane and n-heptane is predicted from data obtained in a 2-ft diameter column with the systems acetone-benzene and oxygen-water. Mixing was described by using the method of Gautreaux and O'Connell[31] with n taken as 1.2. A Murphree vapor efficiency of 86.9 per cent was predicted, which compares to an experimental value of 85.4 per cent.

CORRELATIONS OF MASS TRANSFER DATA

Until recently, the majority of mass transfer investigations were carried out in equipment other than plate columns. Packed columns were often used as were wetted wall columns. In addition, mass transfer from various geometrical shaped objects such as spheres, cylinders and plates, was also studied. The results can be found in the standard texts such as Sherwood and Pigford[58], Treybal[64], and Perry[51].

The most comprehensive work on plate columns has been done under the auspices of the American Institute of Chemical Engineers. Although this work has been performed exclusively with bubble cap plates, it is hoped that the results will be able to be applied to other plates as well. Unfortunately, the program is still in progress and the final results are not yet available.

However, the work performed by Warzel[66], Ashby[9], and Begley[11] in this program has been correlated. These investigators used the same column as the author. They used bubble cap plates while the present investigation was carried out with a valve plate and a perforated plate with large holes. Since only the plate design was varied, a direct comparison can be made between bubble cap plates and those used in the present investigation.

Gas Phase Resistance

Ashby conducted experiments on the adiabatic vaporization of pure liquids. The liquids used were water, isobutyl alcohol, and methyl isobutyl ketone, while the gases were air, helium, nitrogen, and Freon 12 (dichlorodifluoromethane). A constant liquid rate of 8 gallons per

minute and a weir height of 1-1/2 inches were used. The gas velocity based on the active tray area varied from 0.6 to 7.5 feet per second.

He found that the data could be correlated by

$$N_G = 0.297 \left(\frac{\mu_G}{\rho_G D_G}\right)^{-0.23} \left(\frac{D_s u \rho_G}{\mu_G}\right)^{-0.33} \left(\frac{D_s \rho_G \sigma}{\mu_G^2}\right)^{0.16} \left(\frac{h_L}{D_s}\right)^{0.62} \left(\frac{\rho_L}{\rho_G}\right)^{-0.01} \left(\frac{\mu_L}{\mu_G}\right)^{-0.005} \tag{63}$$

If the second and third dimensionless groups are combined and the last two groups with very small exponents are eliminated, a much simpler form is obtained

$$N_G = 0.253 \left(\frac{\mu_G}{\rho_G D_G}\right)^{-0.23} \left(\frac{\sigma}{D_s u^2 \rho_G}\right)^{0.16} \left(\frac{h_L}{D_s}\right)^{0.62} \tag{64}$$

where

D_s = bubble cap slot width

D_G = gas diffusivity

σ = surface tension

u = vapor velocity based on active tray area

h_L = vertical distance between bottom of slot opening and top of liquid flowing over weir

ρ_G, ρ_L = density of gas and liquid

μ_G, μ_L = viscosity of gas and liquid

As the groups in the above equations are dimensionless, any set of consistent units can be used.

Ashby found that his correlation would not predict the ammonia absorption and desorption data of Warzel, the average deviation being

-40 per cent. Warzel operated at liquid rates of from 4 to 32 gallons per minute and with weir heights of 2 and 3-1/2 inches, while the gas velocity varied from 1 to 4.7 feet per second. Although Ashby reasoned that the correction for liquid phase resistance in the ammonia-air-water system had not been properly applied, Begley found that this reasoning was not supported and that the failure was due to the choice of h_L/D_s as a correlating variable.

Begley adiabatically vaporized cyclohexanol and ethylene dibromide into nitrogen to find the effect of liquid properties on mass transfer. Operating conditions were in the same range as mentioned previously. He found that his data and the data of Ashby and Warzel could be correlated by

$$N_G = 4528 \left(\frac{Z_f - Z_c}{D_s}\right)^{0.532} \left(\frac{\mu_G}{\rho_G D_G}\right)^{-0.892} \left(\frac{D_s u \rho_G}{\mu_G}\right)^{-0.408} \left(\frac{\rho_L}{\rho_G}\right)^{-0.070} \left(\frac{\mu_L}{\mu_G}\right)^{-0.694} \left(\frac{D_s \sigma \rho_L}{\mu_L^2}\right)^{-0.370} \qquad (65)$$

The average absolute deviation was 11.6 per cent with the maximum being 31.8 per cent.

Begley performed an intercorrelation analysis on Equation (65) to find how much a change in one dimensionless group would affect each of the others. He found that about 86 per cent of the change in the surface tension group $\frac{D_s \sigma \rho_L}{\mu_L^2}$ could be accounted for by the change in the viscosity ratio μ_L/μ_G. No significant intercorrelation was found among the remaining groups. He then recorrelated the data omitting the surface

tension group as a variable. The resulting equation had approximately twice the deviation as Equation (65) although if only Ashby's and Warzel's data were used, the deviation was about the same as when the surface tension group was used. Begley thus concluded that the dimensionless group form of a correlating equation might not be able to be extrapolated beyond the range of variables studied, and a second type of correlation was performed.

This latter correlation was based on graphical analysis and the previously presented relationship

$$N_G = k'_G a t_G = k'_G a \frac{Z_f - Z_c}{u} \tag{38}$$

Using this definition for $k'_G a$ Gerster[4] was able to correlate Ashby's data by the expression

$$k'_G a = C\, u^{0.23} \tag{66}$$

where

$C = 18.19\, D_G^{0.33}$, and

D_G = gas diffusivity sq ft/hr

u = linear gas velocity based on bubbling area, ft/sec.

Begley used Ashby's and Warzel's data as well as his own to obtain the correlation

$$k'_G a = 523.9 \frac{D_G^{0.526}\, F^n}{\rho_L^{0.834}\, (Z_f - Z_c)^{0.28}} \tag{67}$$

where

$n = 0.852\, (\mu_L/\rho_L)^{0.238}$

F = F-factor $= u\sqrt{\rho_G}$

ρ_G, ρ_L = gas and liquid density, lb/cu ft

μ_L = liquid viscosity lb/ft-hr

$Z_f - Z_c$ = gas holdup, cu ft/sq ft

Equation (67) can also be expressed in terms of N_G by using Equation (38) to obtain

$$N_G = 523.9 \frac{D_G^{0.526} \rho_G^{0.5} F^{n-1} (Z_f - Z_c)^{0.72}}{\rho_L^{0.834}} \qquad (68)$$

Liquid Phase Resistance

Begley was unable to completely correlate his liquid phase resistance systems because of the uncertainty of the diffusivity data of high viscosity systems. However, he did obtain the form of the correlation which is

$$k_L\bar{a} = \beta' D_L^{1/2} (\mu_L/\rho_L)^{\alpha} F^{0.575} \qquad (69)$$

where

β' and α are functions of the liquid kinematic viscosity, μ_L/ρ_L, sq ft/hr, and

D_L = liquid diffusivity, sq ft/hr.

The value of α appears to have the value 0.5 at high viscosities, and decreases as the kinematic viscosity is decreased. The value of β' is also a function of kinematic viscosity but cannot be specified in general because of the uncertainty in the diffusivity data mentioned above.

However, Begley also analyzed Warzel's data on the absorption and desorption of carbon dioxide in water where the diffusivity is better known. From these results a correlation is obtained that appears to be valid for aqueous solutions whose kinematic viscosity is close to

that of pure water at temperatures near 25°C. The correlation obtained is

$$k_L\bar{a} = 55.4\ D_L^{1/2}\ F^{0.575} \tag{70}$$

or alternatively in terms of N_L

$$N_L = 55.4\ D_L^{1/2}\ F^{0.575}\ t_L \tag{71}$$

where

t_L = liquid contact time, sec.

APPARATUS

The apparatus used in the present study was designed and constructed by personnel of the Department of Chemical and Metallurgical Engineering for use in the Tray Efficiency Research Program sponsored by the American Institute of Chemical Engineers.[2,3,5] It has been used for tray efficiency studies by Warzel[66], Ashby[9], and Begley[11]. Although their work was done exclusively with bubble cap trays, modification of the equipment to use valve trays and perforated trays was relatively simple and will be described later. A description of the bubble cap trays will also be included, as a comparison between these trays and trays used by the author will be made.

The basic equipment was a rectangular column containing five trays. Only one active tray was used in the present study. Vapor and liquid handling systems were arranged so that both streams could be either recirculated or run on a once-through basis. A general view of the column and some of the auxiliary equipment is shown in Figure 3. Blowers for vapor circulation were located on the floor above, while pumps for liquid circulation can be seen in the area behind the test column. Figures 4 and 5 show simplified flow diagrams for use in humidification and ammonia absorption, respectively.

The size and shape of the test tray was designed with specific requirements in mind. A short liquid path was used in the hope that the liquid on the tray would be completely mixed. It was found, however, that mixing was not complete and concentration gradients did exist. The author also found this to be true with the trays investigated. A rectangular shape was used as it was desired to have uniform liquid

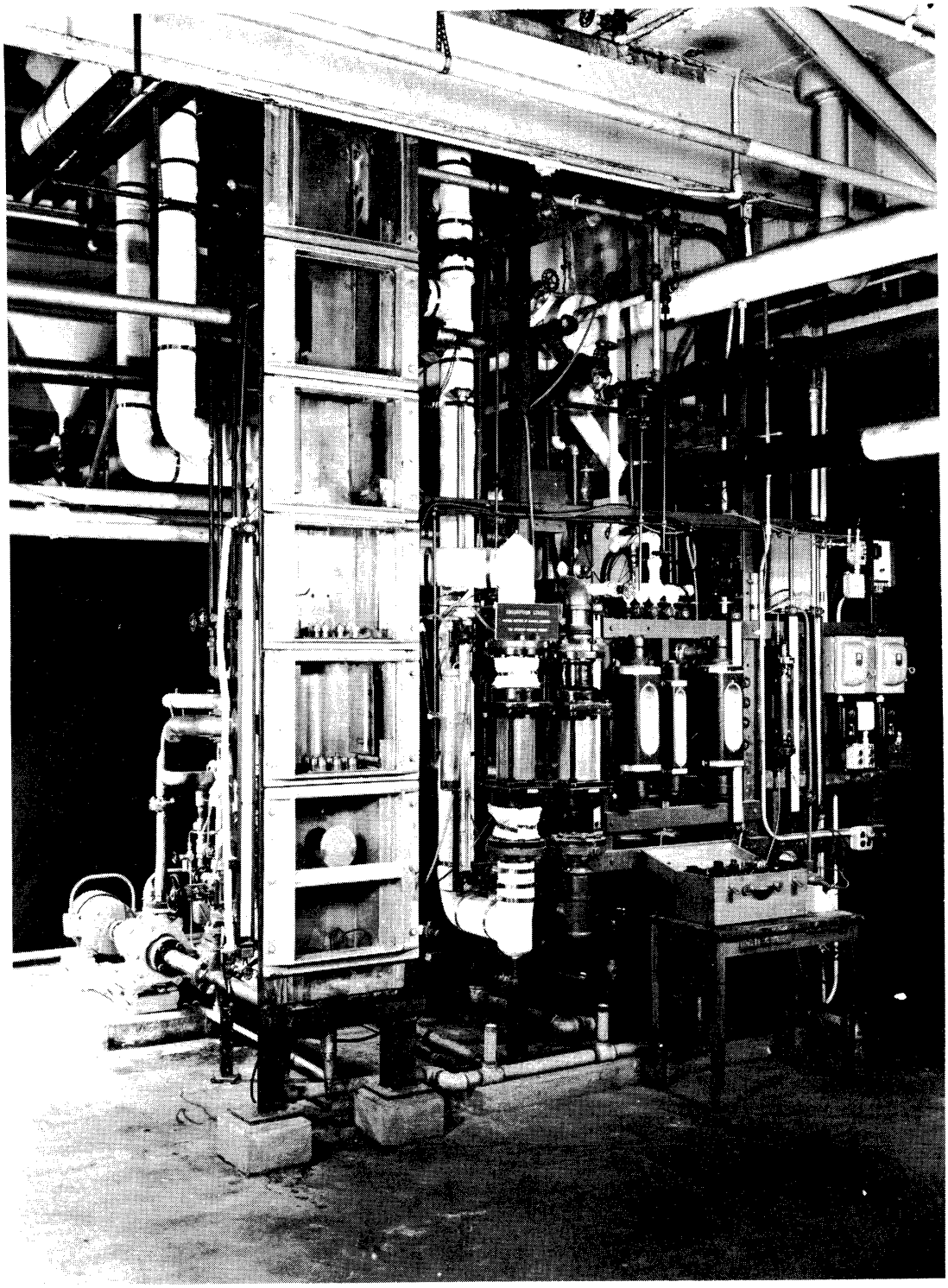

Figure 3. General View of Column

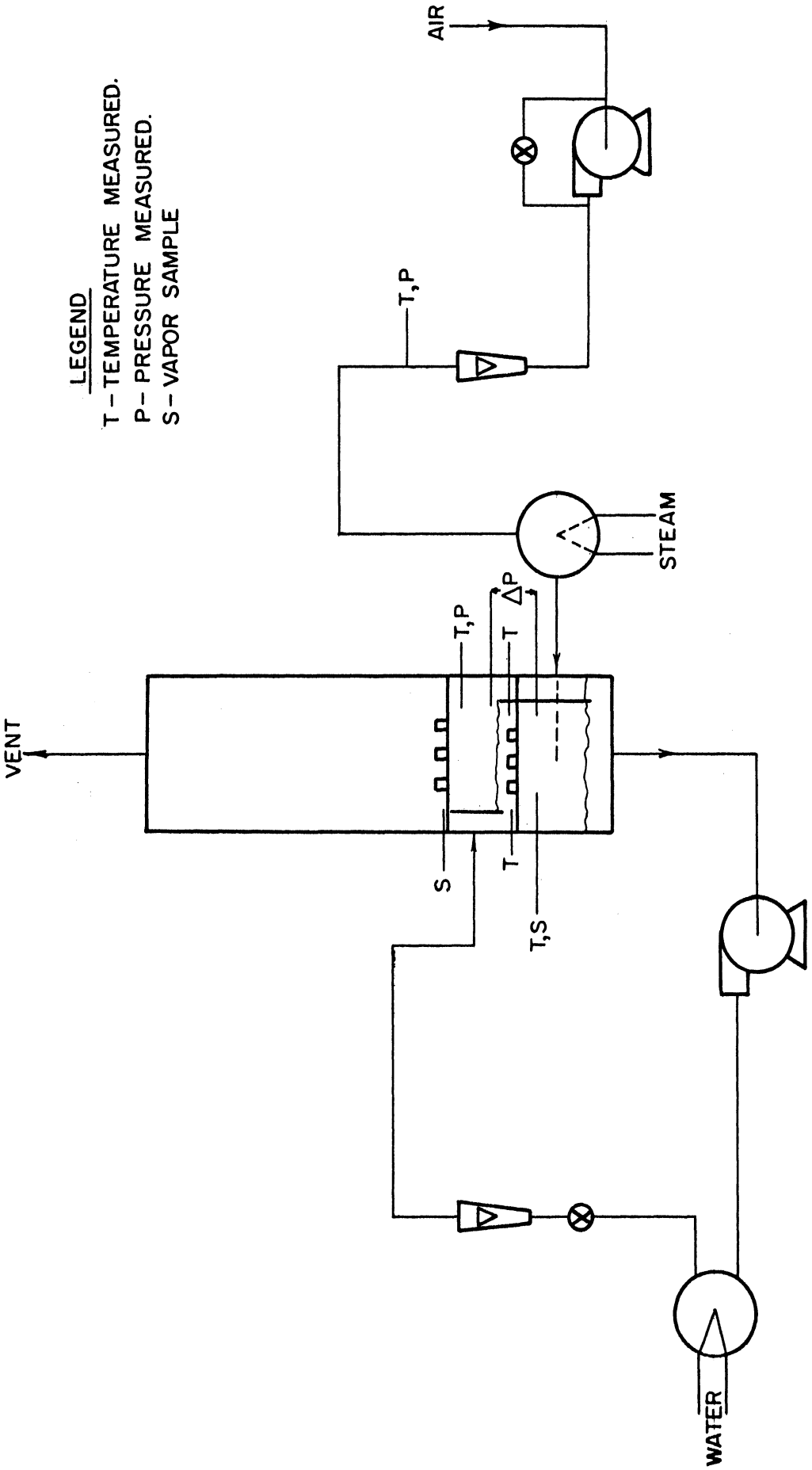

Figure 4. Simplified Flow Diagram for Humidification

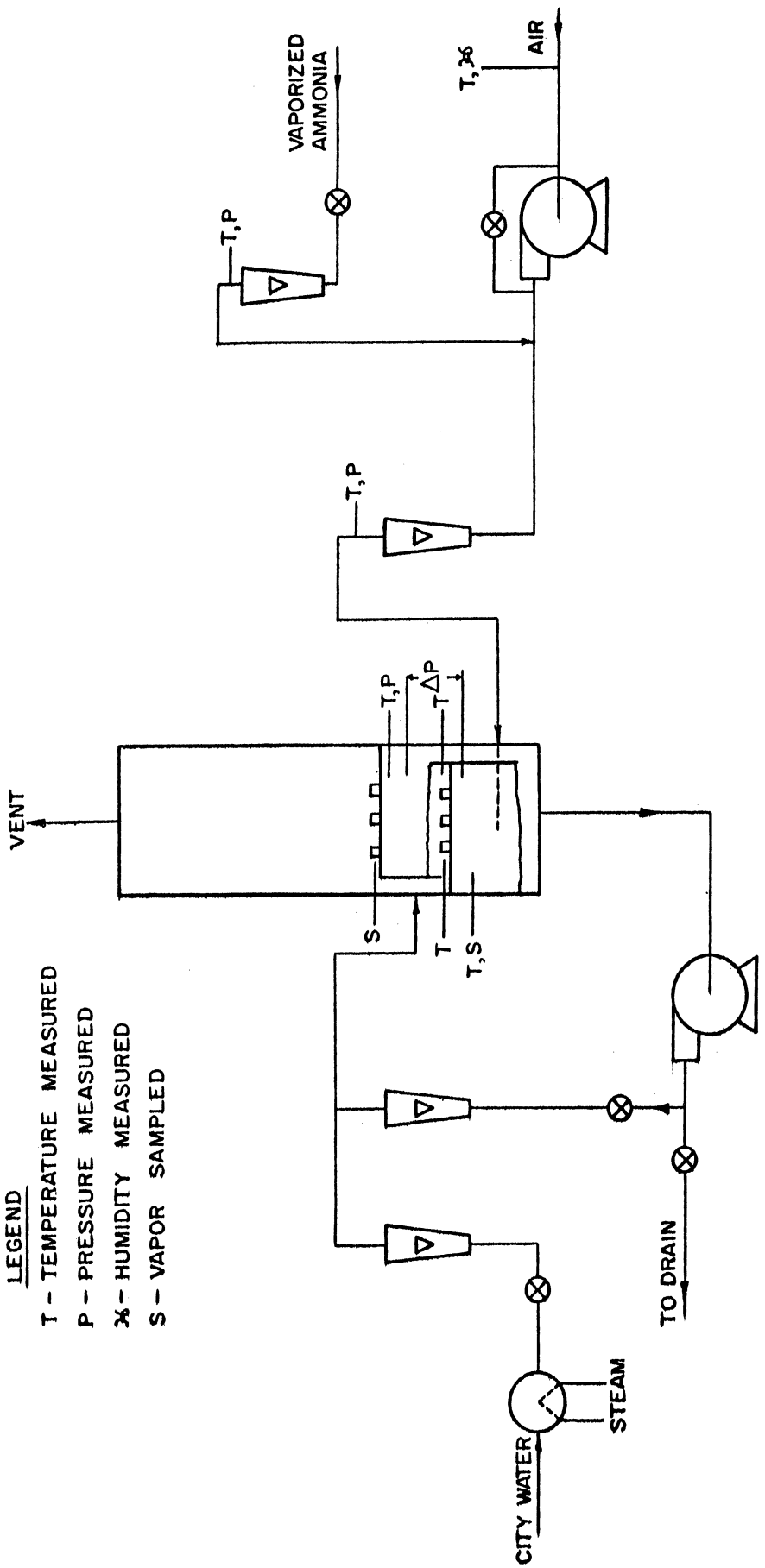

Figure 5. Simplified Flow Diagram for Ammonia Absorption

distribution even though this shape prevented operation at greater than atmospheric pressure. This shape also made visual observation easier as the front of the column could be fitted with glass or Plexiglas windows. Nine bubble caps were located in three rows on a square pitch with a center-to-center spacing of 2-1/2 inches. This gave one cap which was completely surrounded by active caps.

The Test Column

The test column was constructed previous to this work and had been used by Warzel[66], Ashby[9], and Begley[11]. Warzel gives complete details on the column's design and construction which will be summarized here. A single piece of 3/16-inch Incoloy sheet approximately 10 feet long and 37 inches wide was bent by the Central Boiler and Manufacturing Company of Detroit, to form a channel 17-1/2 inches wide and 7-1/2 inches deep. The channel had a 2-inch flanged lip on each side against which the windows could be seated. The trays, inlet and outlet weirs, and splash baffles were made removable. The remaining Incoloy members, top, bottom, downcomers, plate support, and front braces, were welded in permanently. The column was tack-welded inside a frame of 4 x 4 x 1/2-inch mild steel angle which added rigidity to the column as well as providing support for the steel window frames. Figure 6 shows the column during construction and Figure 7 gives the details of the construction.

Bubble Cap Trays - The bubble cap trays used previously contained nine 1-1/2-inch bubble caps on a 2-1/2-inch square pitch. The complete tray layout is given in Figure 8. Figure 9 shows the removable trays and installation details. The bubble caps were manufactured by

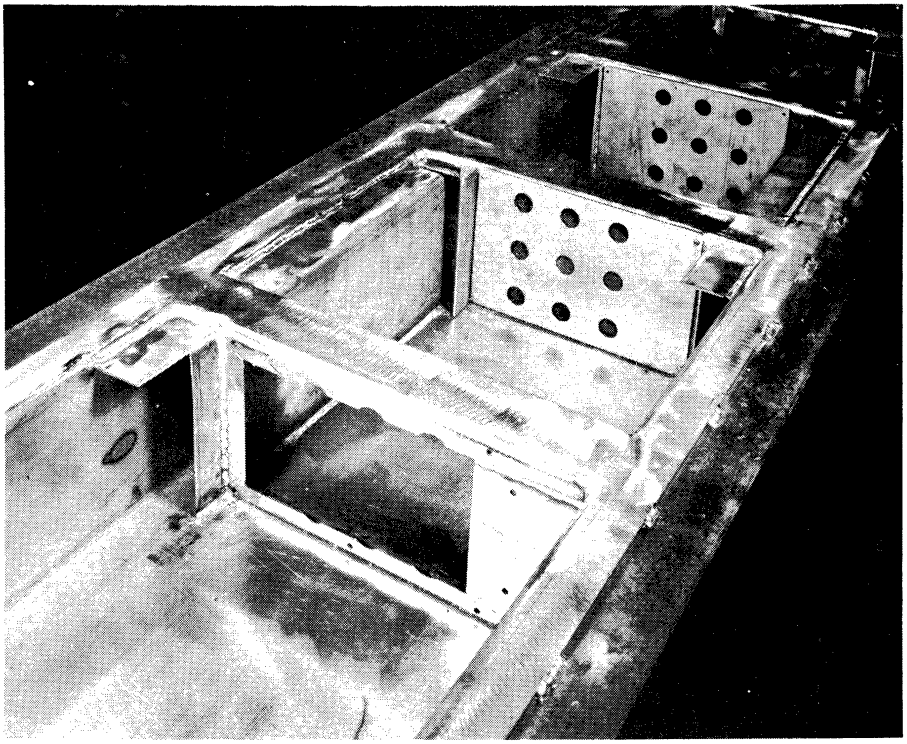

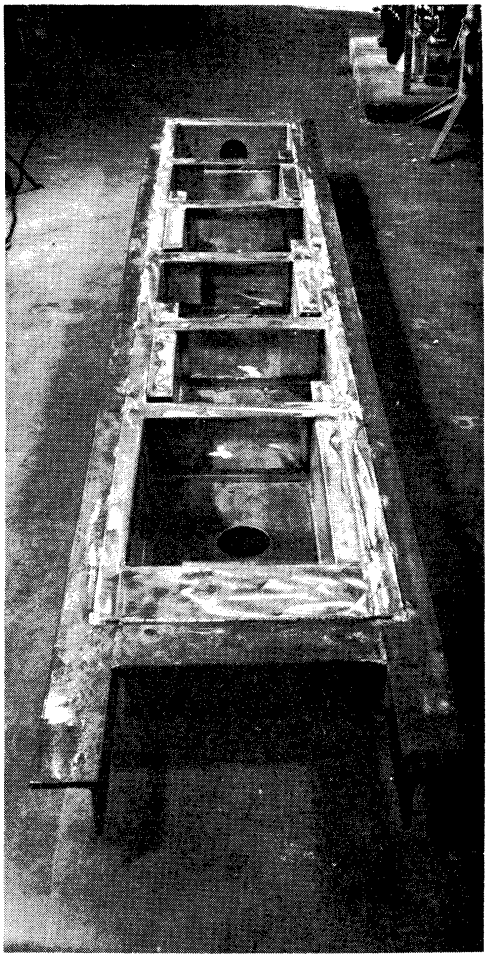

Figure 6. Test Column During Construction

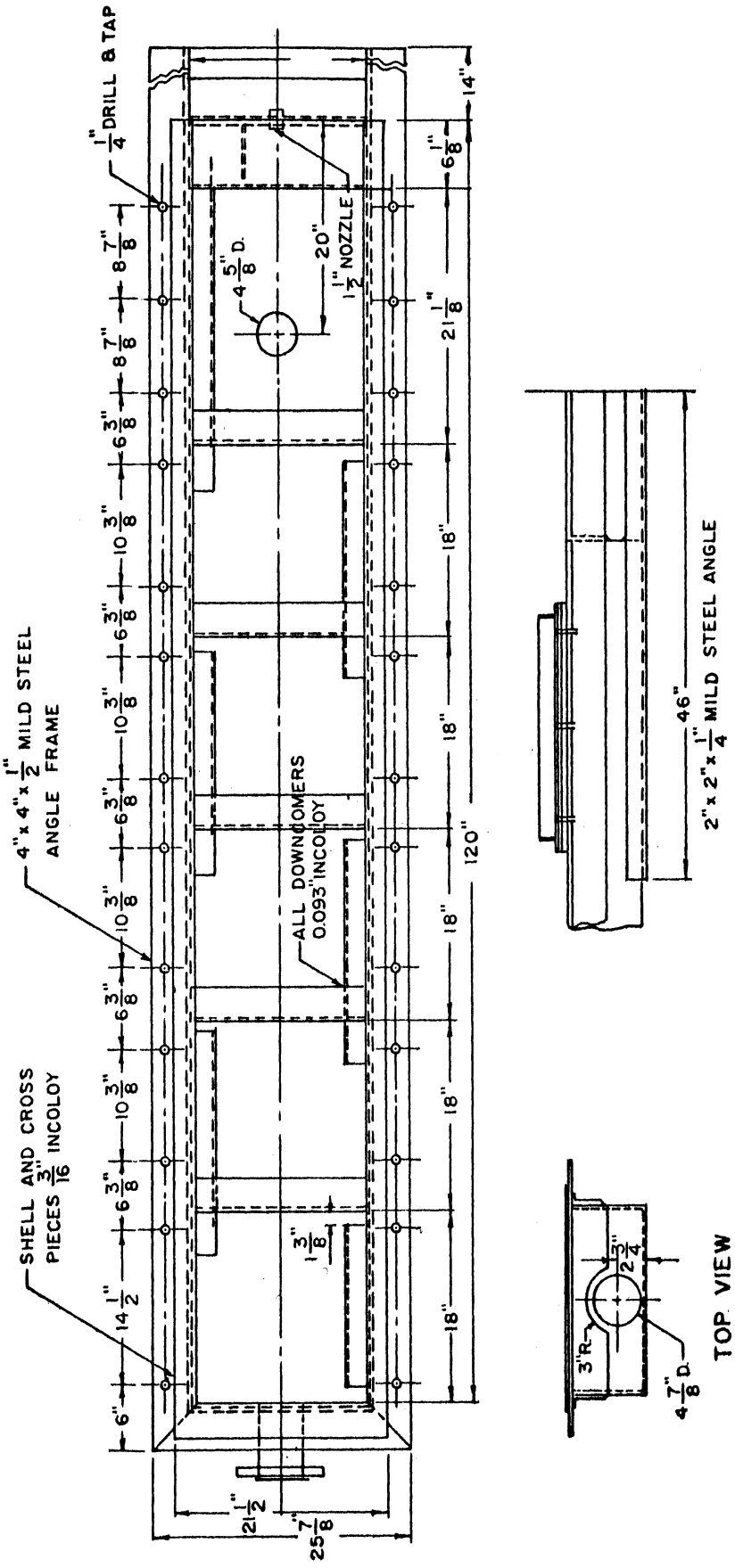

Figure 7. Column Construction Details

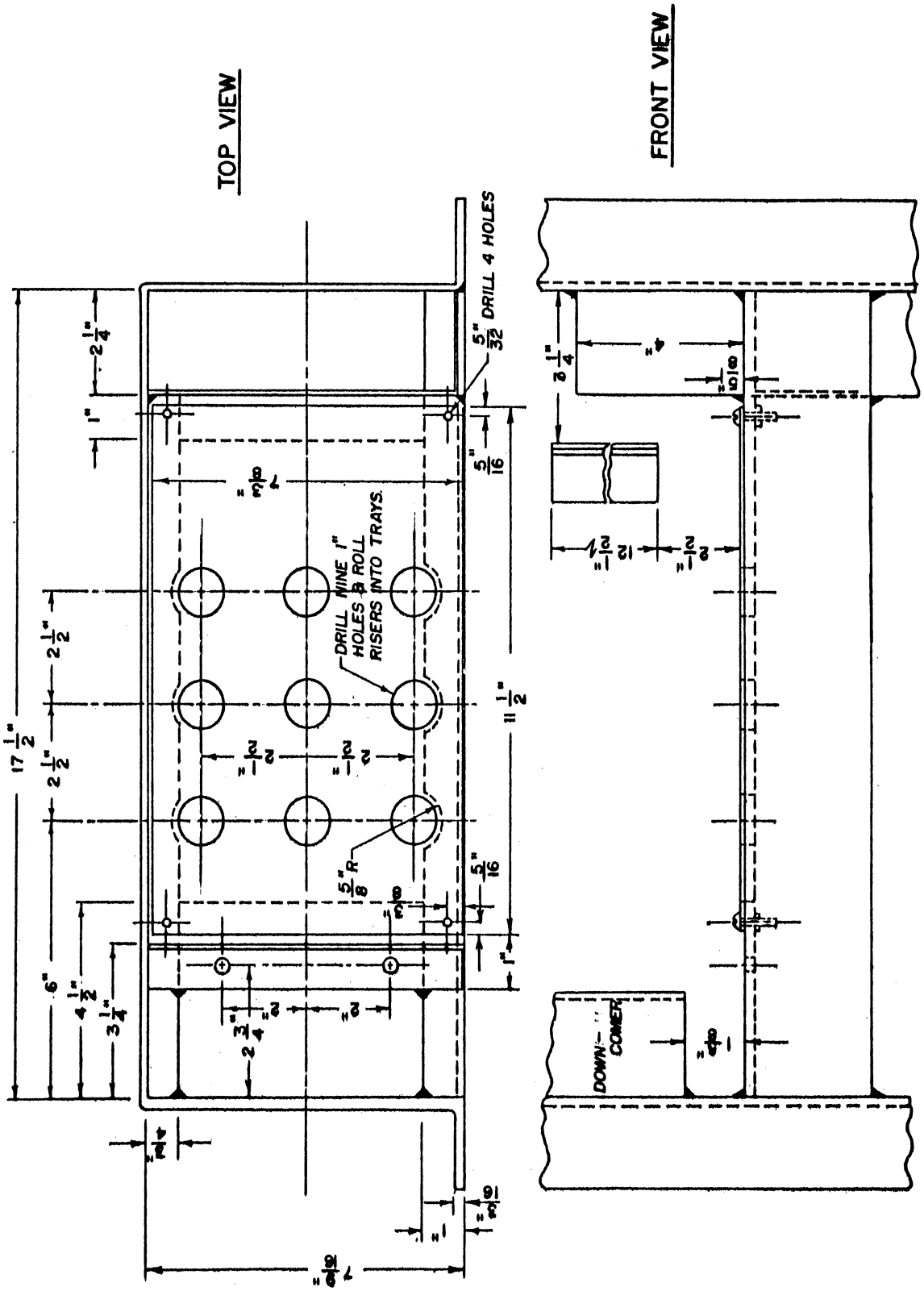

Figure 8. Bubble Cap Plate Layout

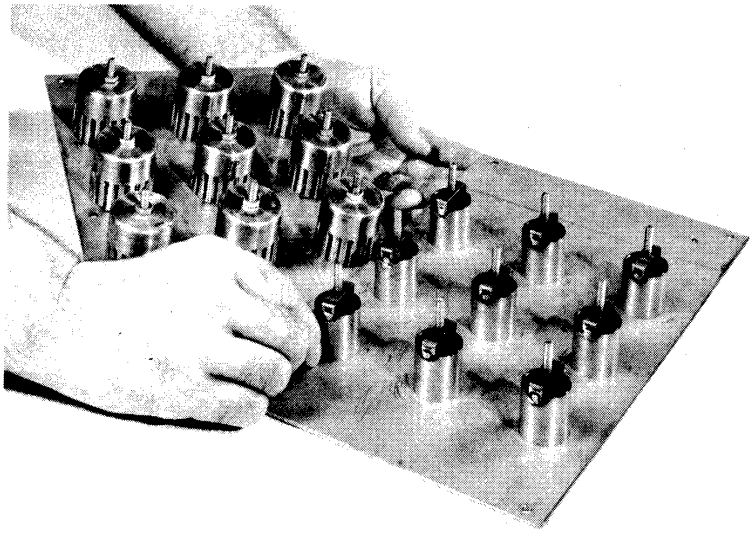

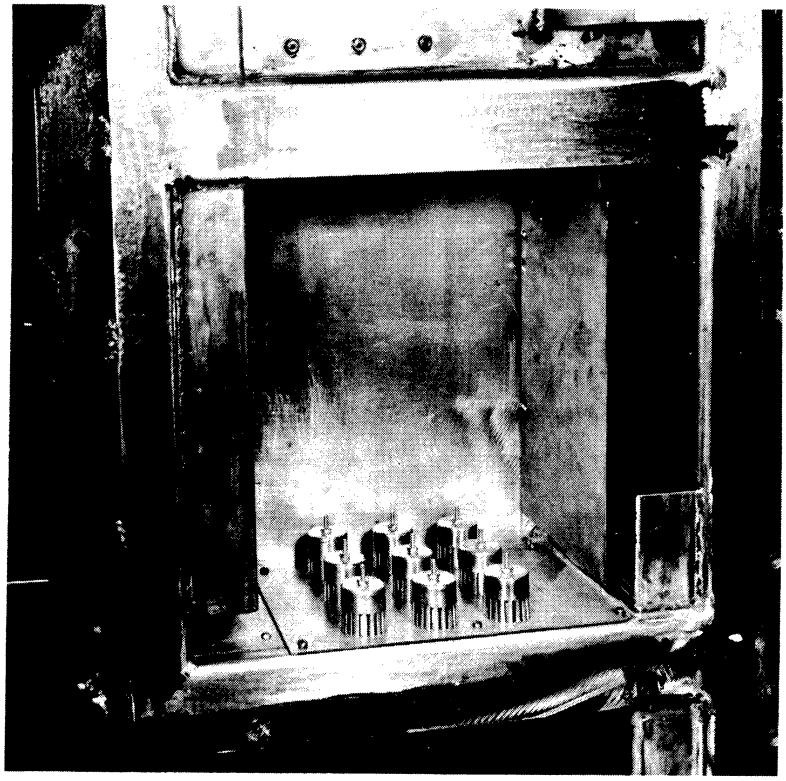

Figure 9. Removable Trays and Tray Installation

Fritz Glitsch & Sons, Dallas, Texas, from type 304 stainless steel. Their dimensions are listed in Table III.

Valve Tray - The valve tray was designed to be as geometrically similar to the bubble cap tray as possible. Nine 1-1/2-inch valves were used on a 2-1/2-inch square pitch. The vertical rise of the valve was such that in the fully open position the peripheral area under the edge of the valve was essentially the same as the slot area for the bubble cap trays. The perforations in the tray floor were the same diameter as the inside diameter of the risers on the bubble cap tray. The tray was fabricated of type 302 stainless steel by personnel of the Chemical and Metallurgical Engineering Department. The valve discs were stamped from 18 gauge type 302 stainless steel by Ann Arbor Machinery Company. Stainless steel machine screws were used to hold the yokes and spacers in place. Taps in the tray floor were provided so that the height of the liquid on the tray could be measured. By a suitable valve and tee arrangement these taps were also used to withdraw liquid samples from the tray floor during the ammonia absorption runs. The taps were constructed by cutting a stainless steel Swagelock 1/4-inch tubing connector in half and welding it to the underside of the tray. A 3/16-inch hole was drilled through the tray from the underside using the bore of the connector as a centering device. After the tray had been mounted in the column, 1/4-inch stainless tubing was connected to the taps and led to the liquid manometers and the sampling lines. Figure 10 shows the construction details of the tray, and Figure 11 shows the assembled tray. Table IV summarizes the dimensions of the valve tray.

TABLE III

CHARACTERISTICS OF THE BUBBLE CAP TRAY LAYOUT

Cap		
	Diameter (O.D.)	1-1/2 inch
	Height	1-1/2 inch
	Metal Thickness	1/16 inch
Slot		
	Height	3/4 inch
	Width	1/8 inch
	Number, per cap	18
	Area, per cap	0.0117 sq ft
	Area, per plate	0.105 sq ft
	Area, fraction of bubbling area	0.171
Risers		
	Diameter (O.D.)	1 inch
	Diameter (I.D.)	7/8 inch
	Area, per cap	0.00417 sq ft
	Area, per plate	0.0375 sq ft
	Area, fraction of bubbling area	0.061
Weir(variable)		
	Length	7-3/8 inches
	Height	3-1/2 and 2 inches
Splash Baffle (variable)		
	Length	7-3/8 inches
	Clearance above tray floor	4 and 2-1/2 inches
Downcomer		
	Size	7-3/8 x 2-1/8 inches
	Area, cross sectional	0.137 sq ft
Bubbling Area (taken as space between downcomer and splash baffle)		
	Width	7-1/2 inches
	Length	11-13/16 inches
	Area	0.615 sq ft
Tray Spacing		18 inches

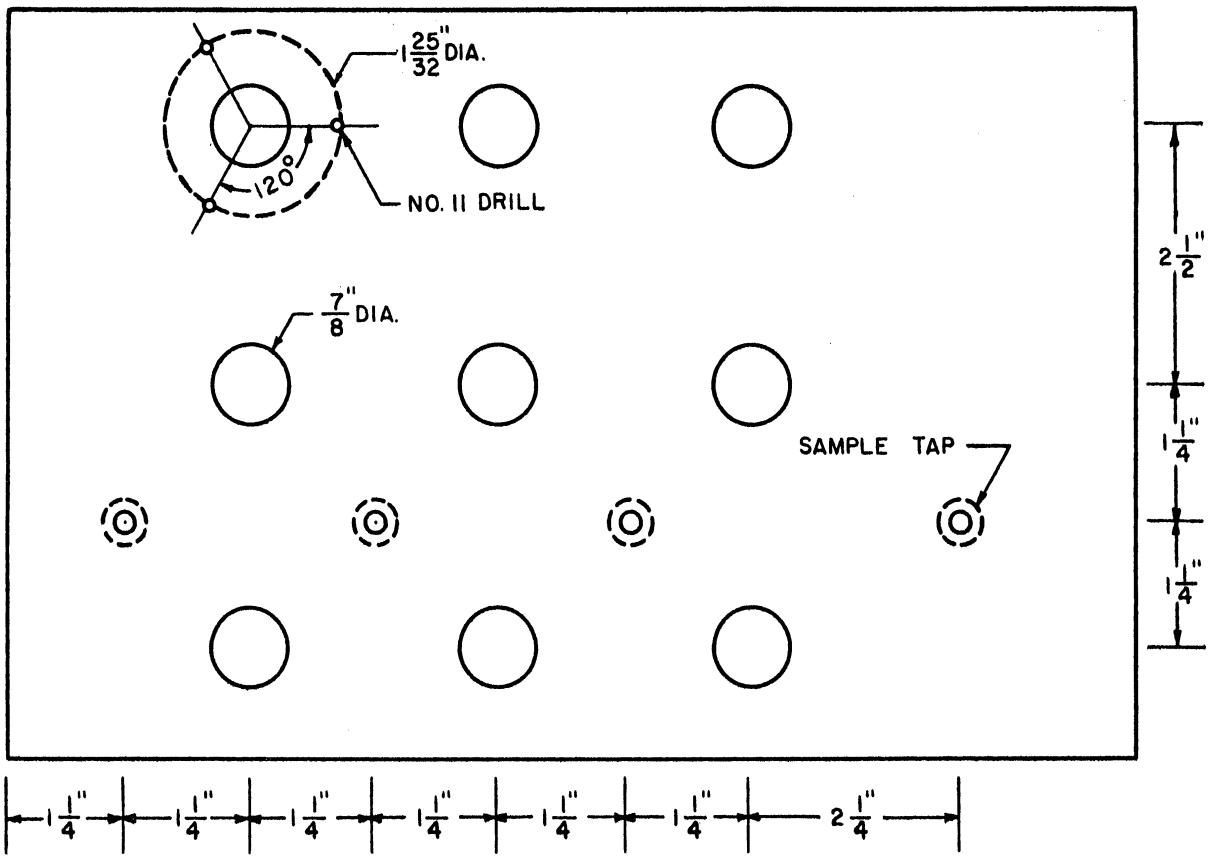

TRAY FLOOR – $7\frac{5}{16}$" x $11\frac{1}{2}$" x 11 GA. TYPE 302 STAINLESS STEEL

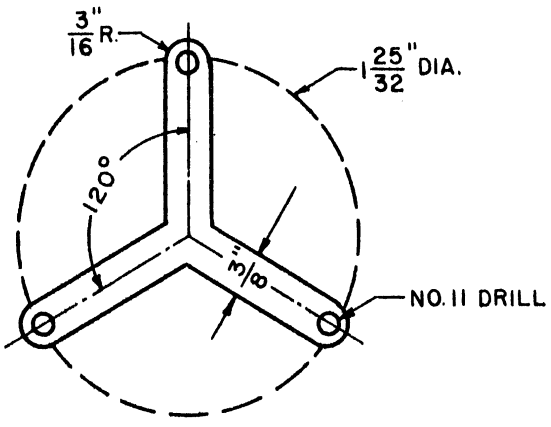

YOKES – 9 REQ.
18 GA. 302 S.S.

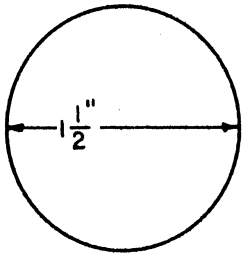

VALVES – 9 REQ.
18 GA. 302 S.S.

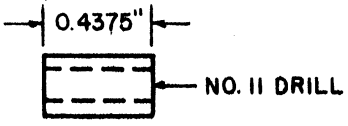

SPACERS – 27 REQ.
1/4" 304 S.S. TUBING

Figure 10. Valve Tray Details

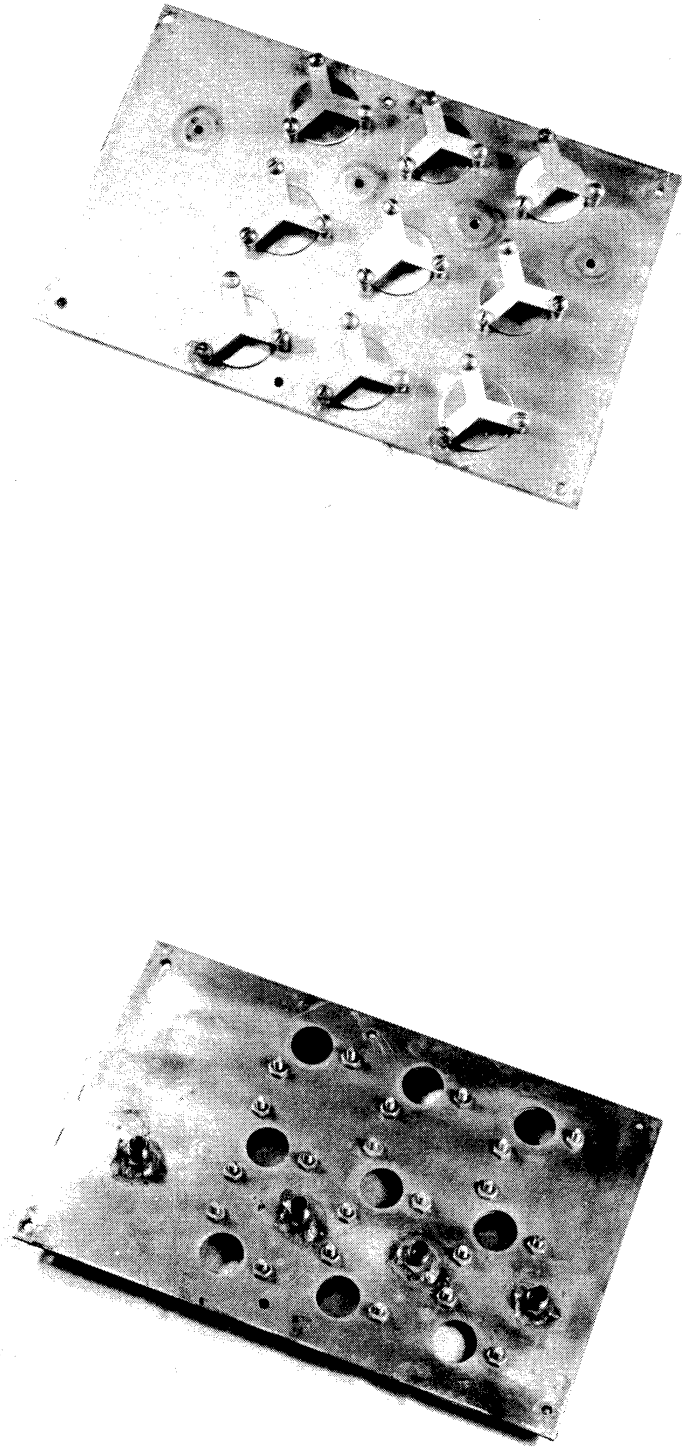

Figure 11. Top and Bottom Views of Assembled Valve Tray

TABLE IV

DIMENSIONS OF THE VALVE TRAY

Perforations	
Diameter	7/8 inch
Spacing	2-1/2 inches square pitch
Number, per tray	9
Area, per tray	0.0375 sq ft
Area, fraction of bubbling area	0.061
Tray thickness	11 gauge (0.125 inch)
Valves	
Diameter	1-1/2 inches
Metal thickness	18 gauge (0.0475 inch)
Height of vertical travel	0.390 inch
Peripheral area, per valve	0.0128 sq ft
Peripheral area, per tray	0.115 sq ft
Peripheral area, fraction of bubbling area	0.187

Perforated Tray - The perforated tray was essentially a valve tray without the valves and yokes. Nine 7/8-inch holes were drilled on a 2-1/2-inch square pitch. Sampling taps were installed as on the valve tray. Figure 12 shows the perforated tray installed in the column. Table V summarizes the dimensions of the perforated tray. The trays were installed in the column using Teflon sheet and epoxy resin as a gasket.

TABLE V

DIMENSIONS OF THE PERFORATED TRAY

Hole Diameter	7/8 inch
Spacing	2-1/2 inches square pitch
Number, per tray	9
Area, per tray	0.0375 sq ft
Area, fraction of bubbling area	0.061
Tray thickness	11 gauge (0.125 inch)

Weirs - Adjustable overflow weirs were used to control the liquid level on the tray. These weirs were constructed of 1/16-inch stainless steel in the shape of a channel which fitted inside the downcomer. In preparing the column for operation, a weir of the appropriate height was fitted inside the downcomer, adjusted for proper height, leveled, and bolted to the wall of the downcomer beneath the tray. Liquid leakage was prevented by sealing all joints with epoxy resin. The downcomers were completely enclosed to avoid an extra seal between the downcomer and the glass face of the window. Accordingly, the length of the outlet weirs was 7-1/8 inches as compared to the full column width of

Figure 12. Perforated Tray Installed in Column

7-1/2 inches. This did not appear to have any effect on the flow patterns observed on the tray. Although the column was designed to use an inlet weir, it was found that its use caused the upstream slots on the first row of caps to remain inactive. To prevent this, the weir was not used on the bubble cap tray, with the valve tray, or perforated tray.

Splash Baffle - During all runs using this column, a splash baffle was installed one inch upstream of the overflow weir with the top of the baffle 1/2 inch above the top of the weir. The baffle was made of 1/16-inch Incoloy and was 12-1/2 inches long by 7-3/8 inches wide. It was supported by bolting to a piece of angle welded to the back of the column. A piece of Tygon tubing was used as a gasket between the edge of the baffle and the glass window to prevent leakage. Warzel[66] found that without the baffle, liquid would splash unevenly over the weir. In addition, at high vapor rates the froth would not maintain a reasonably steady level but would flow over the weir into the downcomer with a steep gradient.

Windows - Previously, difficulty had been encountered in maintaining a good seal between the windows and the face of the column. As only one active tray was used for most studies with the column, Begley[11] replaced the Plexiglas windows with 3/8-inch stainless steel sheets which fitted between the window frames and the column face, and were welded to the frames for ease in installation. Since observations were to be made on trays 1 and 2, rectangular holes slightly smaller than the original window were cut in the stainless steel sheet and safety glass windows installed. This increased the width of the tray so a plate of safety glass was fitted to the inside of the window assembly on the

test tray to preserve the column dimensions. This was not done on tray 2 as this was not an active tray, and was only used to collect the entrained liquid in the vapor stream. The window assembly was bolted to the face of the column using Teflon tape and epoxy resin as a gasket. An access plate was cut in the assembly which covered the space beneath the first tray so that the trays could be changed and weirs could be adjusted without removing the assembly from the column.

Vapor Handling System

The vapor handling system consisted of two blowers operating in series, metering devices, a heat exchanger for regulating the temperature and an entrainment separator. Standard 3-inch galvanized pipe was used with both screwed and flanged fittings. Although the piping could be arranged for recirculation of the vapor stream, for the present investigation it was handled on a single pass basis.

Air from the laboratory was compressed in the first blower, metered, heated if desired, and fed to the test column. From the test column the air went to an entrainment separator, was compressed in the second blower, and fed to a vent line which exhausted outside the laboratory.

Blowers - Two identical blowers were used. They were brass two-lobe rotary blowers, type RCB, manufactured by the Sutorbuilt Corporation, Los Angeles. The blowers displaced 0.18 cubic foot per revolution with a maximum operating speed of 1800 revolutions per minute. The first blower was driven by a 10 h.p. electric motor, type K, serial P93912, manufactured by Robbins and Myers Co., Springfield, Ohio. The

second blower was driven by a 10 h.p. electric motor, type CSP, serial 5201, manufactured by Westinghouse Electric Company.

An Allis Chalmers variable speed drive was belted between the motor and the first blower. This gave approximately a three-fold change in blower speed. Fine control in air rate was accomplished by a gate valve in a 2-inch bypass line connected between the blower inlet and outlet. The second blower was belted directly to the motor and was primarily used to regulate the pressure in the column. A valved bypass line was installed as with the first blower. Although the air flow rate and column pressure were dependent upon settings of the individual blowers, no difficulty was encountered in obtaining the desired conditions.

Metering - Total vapor flow rate to the column was measured by a size 12 Fischer and Porter Flowrator, tube no. 12LL-25, serial no. D8-1609, figure no. 26P-E, Chemical and Metallurgical Department No. C17-200. The precision bore tube was calibrated for 0-200 cubic feet per minute of 0.877 gravity gas at 14.7 psia and 60°F. Warzel[66] checked the calibration of the meter and found it to be sufficiently accurate for measuring gas flow rates providing corrections for gas density were made.

Heat Exchanger - For the humidification runs the gas was heated in a Ross type SSCF, No. 804, 8-inch heat exchanger. The tube bundle was 4 feet long, and the header design gave four tube side passes while the shell side was baffled at one foot intervals. Construction was entirely of type 316 stainless steel. The gas flowed through the shell side while the heating medium passed inside the tubes. The exchanger was connected so that either steam or hot water could be used as the heating medium.

Entrainment Separator - A steel 55-gallon drum fitted with 3-inch pipe connections was used as an entrainment separator to collect any droplets not removed on the dry tray in the column.

Liquid Handling System

Two different flow patterns were used for the liquid handling system. For the humidification runs, distilled water was used and recirculated to the column. For the ammonia absorption runs, city water was normally used in a single pass system, although part of the liquid flow was recirculated for runs at the higher liquid rates. Flow diagrams for the two systems are shown in Figures 4 and 5. Both systems consisted of circulating pumps, meters, and control valves. For the humidification runs, a heat exchanger was used to maintain the liquid temperature at the desired level. For the absorption runs, city water was passed through a heat exchanger to raise the temperature of the water to test conditions.

Pumps - Two identical centrifugal pumps were installed. They were Durcopumps Model 40, series WS7RD-74 with 7-1/2-inch open impellers fabricated of Durimet 20, a stainless steel alloy, manufactured by the Duriron Company, Inc. The pumps were direct coupled to 3 h.p. induction motors, model 5K213B6228, manufactured by General Electric. The original rope-type packing glands in both pumps were replaced by Begley[11] with mechanical seals type DU3151/52, manufactured by the Durametallic Corporation, Kalamazoo, Michigan. This was done to eliminate packing gland grease as a possible source of contamination in the liquids. One pump was used to recirculate water to the column for the humidification runs or to both recirculate and discharge the water to the drain for the

absorption runs. The second pump was used to circulate city water to the column for the absorption runs.

Control Valves - The control valves were globe valves, Figure 2475 Flanged End, F and D, 150-lb., O S and Y, Bolted Bonnet fabricated of Durimet 20 by the Wm. Powell Company. For the absorption runs, a one-inch globe valve, drawing B16573 REV6, body and stem F8, catalog 9815, manufactured by Henry Vogt Machinery Co., Louisville, Kentucky, was used to control the water flowing to the drain, and thus maintain the desired liquid level in the base of the column.

Metering - Two identical size 8, series 700 Fischer and Porter Flowrators, tube no. B9-27-10/70G and float no. BSVT-93 were used to measure the liquid flow rates. They were calibrated from 10 to 100 per cent of maximum capacity (32 gallons of water per minute) in increments of one per cent. The first meter, serial W70-4024/1, was used to measure the flow rate of the recirculated stream. The second meter, serial 5601D1038B1, was used to measure the flow rate of city water fed to the column.

Piping - Standard 2-inch, Schedule 5, welding type, type 304 stainless steel pipe was used for all liquid piping, except for a 2-inch galvanized pipe which fed city water from the mains to the inlet of the circulating pump. Both flanged and welded joints were used.

Heat Exchangers - Two heat exchangers were used. The first was constructed from a 4-1/2-foot length of 2-inch stainless steel pipe, and contained 3 coils of 1/4-inch stainless steel tubing. Liquid flowed in the shell side and cooling water in the tubes. This was used only in the humidification runs to cool the liquid which had been heated by the

pump and maintain the desired operating temperature in the column. A brass heat exchanger was used to heat city water to the desired temperature before feeding the water to the test column. Steam was condensed at atmospheric pressure in the four-pass tube side while water flowed through the shell side. This exchanger was used only for the absorption runs.

Solute Gas Supply

For the ammonia absorption studies, liquid anhydrous ammonia was vaporized, metered, reduced in pressure, and introduced into the vapor line between the discharge of the first blower and the rotameter which measured the total vapor flow rate. Liquid ammonia was fed from a 150-lb cylinder through a check valve to a vaporizer. The vaporizer was constructed of a 3-foot length of 4-inch steel pipe, and contained a heating coil of 3/8-inch copper tubing in the bottom. The coil was heated by condensing steam at atmospheric pressure. An excess amount of steam was used to insure a steady flow rate of ammonia. If insufficient steam were used, the condensate would freeze and the ammonia flow from the cylinder would have to be shut off until all the liquid in the vaporizer had evaporated and the condensate had melted. The vaporizer was operated at a pressure of from 110-130 psig, corresponding to a saturation temperature of 55°-65°F. As the piping from the vaporizer was warm to the touch, it indicated that the ammonia was slightly superheated, and that the liquid was vaporized immediately. Apparently, there was little or no liquid hold-up in the vaporizer. The vaporizer was fitted with a pressure gauge and a spring loaded relief valve, 3/4-inch inlet, all iron,

No. 1118, manufactured by the Crane Co. The relief valve was set to open at 150 psi. Before use, the vaporizer was hydrostatically tested to 300 psi.

The vaporized ammonia was reduced to a pressure of about 20 psig before being metered and fed to the air stream. This was done by a Matheson No. 12A ammonia regulator. The regulator had an aluminum body and stainless steel internal fittings. Flow rate of the ammonia was controlled by a Metrol 1/4-inch steel needle valve. For a given flow rate, the valve setting in the ammonia cylinder had to correspond to the needle valve setting in order to maintain a steady pressure in the vaporizer. The ammonia was metered into the air stream by a Fischer and Porter Flowrator, serial V5-1200/1, tube B5-27-10/70G, float BSVT53. The beaded, precision bore tube was graduated in from 10 to 100 per cent of maximum capacity in increments of one per cent. The meter was calibrated using a Critical Flow Orifice Prover. Due to the temperature drop of the expanding gas and the rapid heat transfer through the aluminum body of the pressure regulator, the temperature of the ammonia metered to the air stream was within several degrees of room temperature, and remained very stable.

Sampling and Analytical Equipment - Humidification

The methods used for sampling and analysis varied with the system investigated. For the humidification runs, only vapor samples were required. The inlet vapor sample was taken by a 1/4-inch stainless steel probe located about three inches below the test plate. The outlet vapor sample was taken by a stainless steel probe located on the dry tray above the test tray. The location of the probe with respect to a

a modified bubble cap is shown in Figure 13. The tray above the test tray is referred to as a dry tray, as the liquid enters the column in the downcomer feeding the test tray, and is not contacted on the second tray. The only liquid which reaches the dry tray is that which is entrained with the vapor stream. Any liquid reaching the dry tray was withdrawn to prevent accumulation although the surface of the tray was often wet. Inlet and outlet vapor samples were withdrawn simultaneously through lines heated with electrical resistance wire, passed through drying tubes to absorb the water vapor, resaturated in bubblers, and the volume measured by wet test meters.

Drying Tubes - The drying tubes were 4-1/2-inch glass U-tubes fitted with ground glass stoppers and sidearms. They were filled with anhydrous calcium sulfate (Drierite) and quantitatively removed water vapor from the sample.

Wet Test Meters - Two wet test meters, serial nos. J5SS and H9SS, manufactured by Precision Scientific Co., and rated at 0.1 cubic foot per revolution, were used to measure the volume of the sample.

Balance - The drying tubes were weighed before and after sampling on a Christian Becker Projectomatic Balance model AB-1, using class S stainless steel weights. The balance and weights were checked against a second set of weights which had been calibrated by the National Bureau of Standards. It was found that no correction need be made to remain within a tolerance of $\pm$ 0.2 mg.

Sampling and Analytical Equipment - Absorption

The same sampling probes were also used for obtaining vapor samples in the absorption runs. From the column, the sampling lines

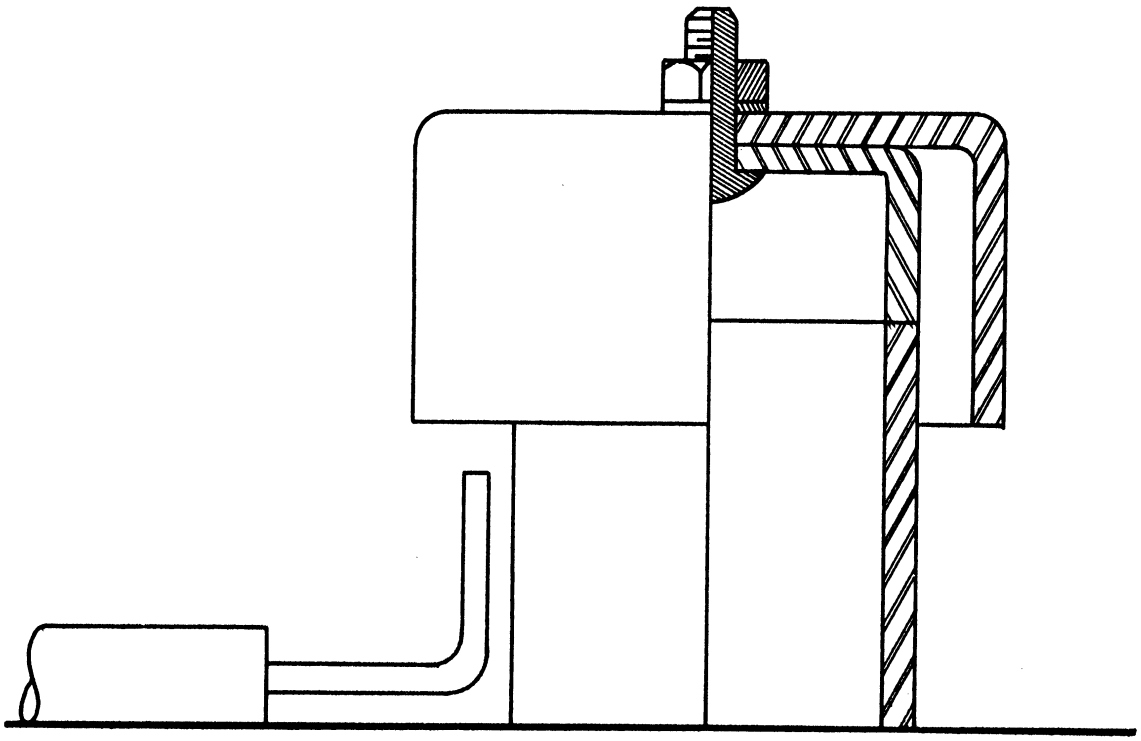

Figure 13. Position of Probe for Outlet Vapor Sample

ran to a train of bubblers where the ammonia reacted with an excess of hydrochloric acid solution. After passing through a water bubbler, the volume of the samples was measured in the wet test meters. The ammonia concentration in the samples was determined by back-titrating the unreacted hydrochloric acid.

Hydrochloric Acid Bubblers - The bubblers were 4-ounce glass bottles fitted with rubber stoppers and connected with rubber tubing.

A total of eight liquid samples were taken for each run. They were taken with a hypodermic syringe from sample lines fitted with rubber serum stoppers. The liquid sampling points are shown in Figure 14. After withdrawal, the samples were transferred to bottles containing an excess of hydrochloric acid. The samples were analyzed by back-titration of the excess acid.

Hypodermic Syringe - A Becton, Dickinson and Co., Yale B-D 50Y, 50 cc hypodermic syringe with a 3-1/2-inch no. 13 stainless steel needle was used. The plunger head was enclosed in an aluminum housing which was fitted with a push rod. At the desired sample volume, the push rod could be made to engage the shoulder of the sleeve by rotating the plunger slightly. No liquid could then be expelled from the syringe without further rotating the plunger. This insured a constant volume for all samples. The push rod length was adjusted so that the sample volume was approximately 50 cc, and the delivery was calibrated using a Kimble Normax burette no. 8275.

Liquid Sample Bottles - The liquid sample bottles were 8-ounce Boston round glass bottles, fitted with rubber serum stoppers.

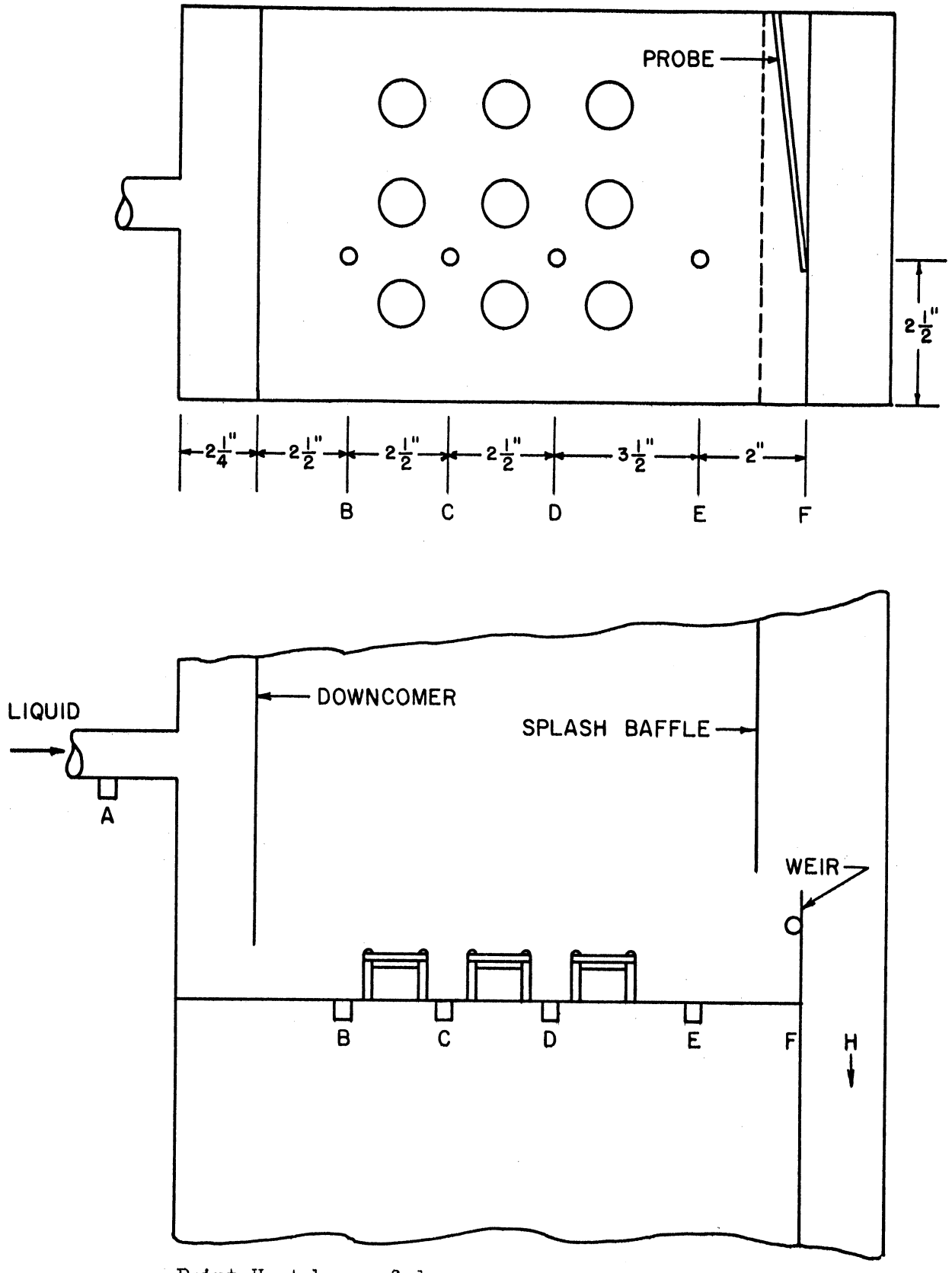

Point H at base of downcomer.
Point I in line to drain.

Figure 14. Liquid Sampling Locations

Burette - All titrations were performed with a 50 ml Kimble Normax burette no. 8275.

pH Meter - The end point of the titrations was determined using a Beckman pH meter model H-2, serial 82945, with a type 4990-80 glass electrode and type 8970-13 calomel reference electrode.

Stirrer - Agitation of the sample during titration was accomplished with a Labline magnetic stirrer, catalog no. 1250. The impeller was a polyethylene covered stirring bar placed in the 250-ml Griffin beaker holding the sample.

Auxiliary Equipment

Temperatures of the liquid entering and leaving the test tray were measured with 0-50°C mercury filled glass thermometers graduated to 0.1°C, and calibrated for 76 mm immersion. Similar 0-100°C thermometers were used to measure the temperature of the gas beneath the test tray and in the gas rotameter. The thermometers were checked against a National Bureau of Standards calibrated thermometer. Temperatures of the liquid leaving the rotameters and of the gas above the test tray were measured with copper-constantan thermocouples. The thermocouples were connected through a 11-point Mallory selector switch, and readings were taken with a Leeds and Northrup portable precision potentiometer, model 8662, serial no. 773919.

Pressures in the test column and in the gas rotameters were measured with mercury filled 30-inch Meriam manometers. The pressure drop across the test tray was measured with a water-filled 50-inch Meriam manometer.

The clear liquid heights at four positions on the tray floor were measured by manometers connected to the taps previously described. The lines above the manometer board were manifolded and vented to the vapor space above the test tray. The scale was zeroed by vertical adjustment of the manometer board so that corrections for capillary effect need not be applied.

The froth height on the tray was measured by a scale fastened to the face of the glass window.

MATERIALS

Ammonia - The anhydrous ammonia was manufactured by Barada and Page, Inc., and was obtained in 150-lb cylinders from the Davis Supply Co., Detroit.

Nitrogen - The water-pumped nitrogen used was obtained in 200 cubic feet cylinders from The Liquid Carbonic Corporation via the General Stores Department of the University of Michigan.

Air - Air from the laboratory was drawn into the blower suction, and after passing through the column, was exhausted via a vent line leading to the roof of the laboratory. This prevented the accumulation of ammonia in the laboratory. The laboratory compressed air lines were used to purge lines and dry equipment.

Water - Distilled water for the humidification runs was obtained from the Department of Chemical and Metallurgical Engineering. City water for the absorption runs was obtained from the mains in the laboratory. The city obtains its water from the Huron River and wells, and it is softened by the lime-soda process. A small amount of ammonia is added to remove the chlorine taste before the water is pumped to the mains. The analysis of a composite sample taken over a one-month period was obtained from the Ann Arbor Water Department, and is presented in Table VI.

Steam - Steam from the 60 psi main was throttled for use in the heat exchangers and normally condensed at atmospheric pressure.

Analytical Reagents - Stock solutions were made from reagent grade chemicals and distilled water. The normality of the solutions was determined by using standardization grade potassium acid phthalate as described by Willard and Furman[72] except that the pH of the end point was determined with a pH meter instead of with phenolphthalein.

TABLE VI

AVERAGE ANALYSIS OF ANN ARBOR WATER

Ions	Concentration, Parts per Million
Carbonate	15.0
Hydroxide	2.0
Calcium	18.8
Magnesium	9.2
Sodium and Potassium	10.6
Chloride	17.2
Sulfate	56.5
Iron	0
Residual Fluoride	1.1
Dissolved Solids	18.8
Total Hardness	83.0
Non-carbonate Hardness	50.0
Total Alkalinity, as calcium carbonate	33.0
pH	10.2

EXPERIMENTAL PROCEDURE

Basically, the experimental procedure consisted of selecting the operating conditions, starting the equipment, taking samples and operating data after steady state conditions had been reached, and analyzing the samples. The actual procedure differed in the humidification and absorption runs, and will be described in detail.

Procedure - Humidification Runs

Before operation, the column and all the lines were thoroughly cleaned to remove any organic material that might have been left from previous investigations. The valve tray was installed and the appropriate overflow weir was bolted in place. The variable speed drive on the first blower was adjusted to give a gas rate slightly higher than desired. The proper orifice was inserted in the inlet line to the second blower. The column was filled with distilled water to the proper level; the liquid recirculating pump was started and flow adjusted to the desired rate. The blowers were started and the two bypass valves adjusted to give the desired flow rate at a normal operating pressure. This operating pressure was from one to four inches of mercury on the test tray. The lower limit was fixed by the pressure drop through the sampling apparatus, and the upper limit was fixed by safety requirements.

The cooling water to the liquid heat exchanger was turned on and the water temperature adjusted to the desired level. The steam to the vapor heat exchanger was turned on to heat the air so that the water in the column would be at the adiabatic saturation temperature of the entering air stream. Because of the high heat capacity of the gas and

the vapor lines, it normally took several hours to obtain this temperature. While the gas stream was being heated, the wet and dry bulb temperatures of the air in the laboratory were taken with a sling psychrometer. From these temperatures and a psychrometric chart[53], the correct gas temperature to be used was determined.

While waiting for the gas stream to come up to temperature, the drying tubes were prepared. The U-tubes were filled with indicating Drierite and fitted with a glass wool plug to prevent any loss of material. A total of twelve tubes was prepared--three tubes for each inlet and outlet vapor sample of the duplicate runs. The tubes were weighed on the analytical balance and placed in a sample holder for transportation to the laboratory.

The sample line heaters were turned on. As the gas temperature approached the desired value, the steam flow was regulated until the temperature of the entering gas stream agreed with the correct value previously determined. Although it took a considerable time to reach the correct temperature, once it had been obtained, the temperature was very steady. The liquid temperature was rechecked and adiabatic operation confirmed by noting the constancy of temperature of the liquid entering and leaving the test tray.

After making any final adjustments in temperature, the drying tubes were connected in series to the sampling lines. The outlets of the drying trains were connected to water bubblers before being connected to a wet test meter. Before the actual sampling, the drying trains were briefly disconnected and the sampling lines purged with nitrogen to remove any water vapor that might have collected in them. The drying trains were reconnected and sampling was started, taking samples of both the

inlet and outlet vapor. The vapor samples taken had a volume of 0.5 cubic foot for most runs although for the series at a 3-1/2-inch weir height it was found that the reproducibility could be improved by taking a 1.0 cubic foot sample.

While the vapor samples were being withdrawn the fluid-dynamic and other operating data were recorded. These consisted of the pressure on the test tray and in the gas rotameter, temperatures of the liquid and gas entering and leaving the test tray and in the gas and liquid rotameters, the pressure drop across the tray, froth height above the tray floor, clear liquid heights at four positions on the tray, gas and liquid rotameter readings, and the atmospheric pressure.

After the runs had been completed, the U-tubes were removed to the balance room and re-weighed to determine the amount of water absorbed. It was found that usually the first drying tube removed over 95 per cent of the water vapor and the third tube showed no change in weight.

Procedure - Absorption Runs

As in the humidification runs, before operation the appropriate tray and weir were placed in the column. The city water circulating pump was turned on, and the flow rate adjusted to the operating value. As the column filled with water, the drain pump was started and the outlet valve adjusted to maintain the desired liquid level in the column beneath the test tray. The liquid level could be observed in a gauge glass, and the level was kept high enough to insure a liquid seal at the base of the downcomer leading from the test tray. As the capacity of the drain line was limited, at high liquid rates part of the liquid from the

column was recirculated to the column, mixing with the city water before entering the downcomer feeding the test tray. The steam line to the city water heat exchanger was opened and adjusted so that the temperature of the water entering the column was 77°F.

The blowers were adjusted as for the humidification runs and started. Steam to the ammonia vaporizer was turned on. The ammonia control valve was opened. The valve on the liquid ammonia cylinder was gradually opened and the pressure gauge on the vaporizer observed. As the pressure reached the operating range (110-135 psig), the cylinder valve was closed slightly and the control valve adjusted to give the desired flow rate. Usually several adjustments of the valves were required to obtain the desired flow rate, but, once obtained, delivery was very stable. The pressure regulator was adjusted to reduce the pressure of the vaporized ammonia to about 20 psig, and this setting was used for all runs. The steam flow to the vaporizer was adjusted to insure that a slight excess of steam was used. Too little steam would cause the condensed steam to freeze and plug the line; while, if too great an excess were used, difficulty would be encountered in maintaining the ammonia fed to the vapor line at a constant temperature. Once the ammonia rate was fixed, the total gas flow to the column was set at the desired level by regulating the bypass valves on the air blower.

The residence time of the gas on the plate was less than 0.5 second, and the residence time of the liquid less than 20 seconds. The column was operated for 20 minutes before sampling to insure steady state conditions had been reached. This time interval was sufficient as shown by the reproducibility of the check runs. While waiting for the column to reach steady state conditions, the sample line heaters were turned on and the lines purged with nitrogen.

The entrained liquid carried to the dry plate was removed by a probe connected to a water aspirator. A tared container was placed in this line to measure the amount of entrainment.

Once steady state conditions had been reached, sampling was begun. Inlet and outlet vapor samples were withdrawn simultaneously. The samples were passed through a train of bubblers containing hydrochloric acid, a water bubbler, and a wet test meter. The first acid bubbler contained sufficient acid to neutralize the ammonia in the sample. The remaining two served to insure all ammonia was removed. At the same time the vapor samples were being withdrawn, liquid samples were taken and operating data recorded.

Eight liquid samples were taken for each run. Seven of the sampling positions are shown in Figure 14. In addition, a sample was taken from the drain line leaving the column. A blank sample was taken to correct for the alkalinity of the city water. This was also sample A for the runs where water was not recirculated. If water were recirculated, a separate city water sample was taken.

The liquid samples were taken with a 50 cc hypodermic syringe from sample lines fitted with a serum stopper. Sampling was done at a slow rate to avoid trapping gas bubbles. If any bubbles were taken with the sample, they were expelled from the syringe before the sample was transferred to the liquid sample bottles. The liquid sample bottles contained an excess of hydrochloric acid.

The same operating and hydraulic data were taken as for the humidification runs. In addition, the wet and dry bulb temperatures at the blower inlet were taken so that a correction could be made for the

humidity of the laboratory air. The ammonia rotameter reading, temperature and pressure in the ammonia rotameter, and pressure in the ammonia vaporizer were also recorded.

The nominal size of the vapor sample taken was 0.4 cubic foot, while the liquid samples were 50 ml. It was found that these sample sizes gave good reproducibility and were convenient to analyze. The analysis was performed by transferring the sample to a 250-ml beaker and back-titrating the hydrochloric acid with sodium hydroxide. The samples were titrated to an end-point pH of 5.4 using a Beckman model H-2 pH meter. As the last two bottles in the gas train contained little or no ammonium ion, these samples were titrated to an end point of 7.0. The procedure followed was to record the volume of solution used and the pH as the end point was approached and passed. The correct volume of solution used was then determined from a graph of pH versus quantity of solution. The end point was very sharp; the addition of 0.02 ml of base caused a change of pH of 1.0 units.

The sodium hydroxide solution used had a nominal strength of 0.35 N and was prepared from reagent grade sodium hydroxide pellets by the procedure given by Willard and Furman.[72] The acid solution had a nominal strength of 1.0 N and was prepared from reagent grade hydrochloric acid by dilution with distilled water.

The sodium hydroxide was standardized with potassium acid phthalate. The hydrochloric acid was standardized using the sodium hydroxide. The standardizations were carried out one after the other to avoid any possible inaccuracies caused by change in concentration of the sodium hydroxide. In addition, the relative strengths of the

solutions were checked frequently and restandardized if the amount of base required to neutralize the acid varied by more than 0.02 ml out of a total of 30 ml.

EXPERIMENTAL RESULTS

General Observations

The action on the tray could be observed through the window that covered the front of the column. In addition, the access plate to the vapor space beneath the test tray was replaced by a Plexiglas window for some runs. This permitted the observer to see if liquid were weeping through the perforations in the tray floor.

When operating with the air water system, the appearance of the liquid and froth on the tray seemed to be similar to that observed when operating with bubble caps. At high liquid and gas rates there were two pronounced eddies. The liquid was bodily lifted in the center of the tray by the rising gas stream and returned to the tray floor at either extremity of the tray. Begley[11] had noticed this previously, especially with the high liquid viscosity of the cyclohexanol-nitrogen system, and took high speed motion pictures of the action.

Stable operation was observed at linear gas velocities of 2 feet per second or greater, where the gas velocity is based on the active tray area between the inlet downcomer and the splash baffle. At lower gas velocities the trays were not stable. When the valve tray was in use, it was found that at a gas velocity of one foot per second only five or six of the valves would be open; the remainder would be closed. The valves would be either fully open or completely closed. In no case was a valve observed operating in a partially opened position. The location of the closed valves varied randomly, and over a period of time one could observe various valves opening and closing with the total number

of operating valves remaining constant. Visual observation of the space beneath the tray showed the weepage to be negligible even when the tray was not stable.

With the perforated tray the instability at low vapor rates appeared in a different form. The holes would alternately pass liquid and vapor. This could also be confirmed by observing the underside of the tray even though the liquid and froth on the tray appeared to be relatively uniform. This latter uniformity was also an unstable condition. After a short period of time the liquid on the tray was distributed so that weeping occurred simultaneously through the three holes along one side of the tray. This caused liquid to flow crosswise to the net liquid flow and lowered the liquid level on the other side of the tray. This in turn decreased the hydrostatic head on one side while increasing it on the other. The weeping holes could not handle all of the liquid, and part of it struck the side of the column and was reflected in the opposite direction. This set up a liquid cycling pattern on the tray with the perforations in the rows along the side of the column alternately passing vapor and dumping liquid. Once this cycling process started, it could not be stopped unless the vapor velocity was increased above the point where the weepage stopped. The weeping limit occurred at a gas velocity of about 2 feet per second which corresponds to a velocity through the holes of about 32 feet per second. This latter value is in the range reported by Arnold et al.[8] for perforated plates with hole diameters ranging from 0.06 to 0.37 inch.

Hydraulic Data

The data obtained in the study divided into two categories: hydraulic data, and mass transfer data. The hydraulic data were taken while samples were being withdrawn. In addition, some hydraulic studies alone were made with the air-water system.

Pressure Drop - Although the pressure drop through the tray was not used as a correlating variable, it was observed so that a comparison with the bubble cap tray could be made. The dry tray pressure drop through the two trays investigated is shown in Figure 15. The pressure drop for the perforated tray was almost identical to that of the bubble cap tray of Warzel.(66) The valve tray pressure drop was slightly higher. Also there was a definite Bernoulli effect with the valves. As the valve started to rise, the gas flowing between the valve and the tray floor had a high velocity which lowered the pressure. This pressure differential between the gas above and beneath the valve would keep the valve from rising. This would continue until the impact force on the valve from the gas passing through the holes in the tray was sufficient to overcome the pressure differential due to the Bernoulli effect. This effect could have been eliminated by making the diameter of the valve closer to that of the hole, but it was desired to keep the geometry of the tray as close as possible to that of the bubble cap tray. It was found that as soon as liquid was fed to the tray, the Bernoulli effect stopped, and the valves were either fully open or fully closed.

Pressure drops through the operating trays are presented in Figures 16 and 17. These were taken during mass transfer studies of the ammonia-air-water system. Additional data on the air-water system at

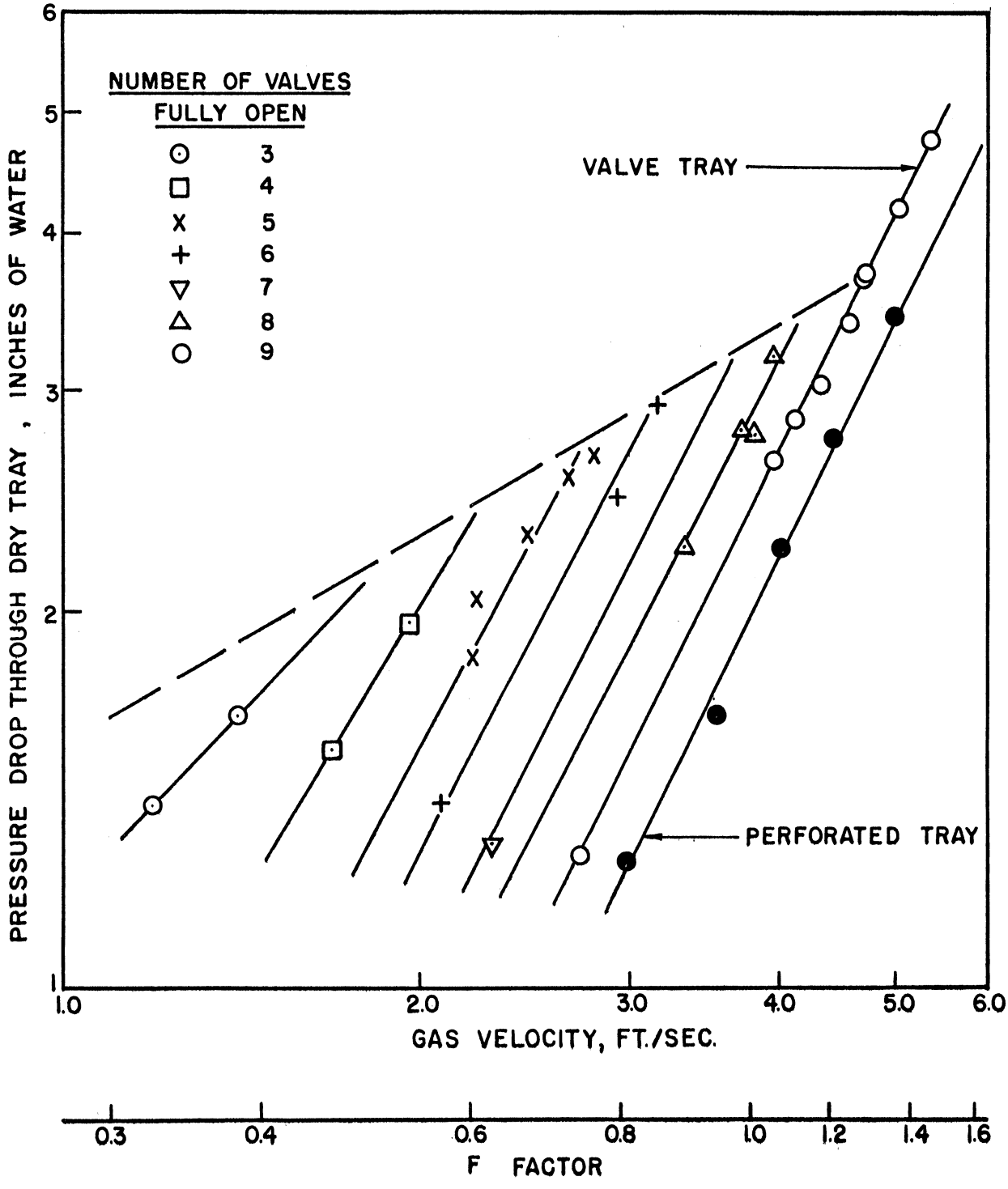

Figure 15. Dry Tray Pressure Drop for Valve and Perforated Trays

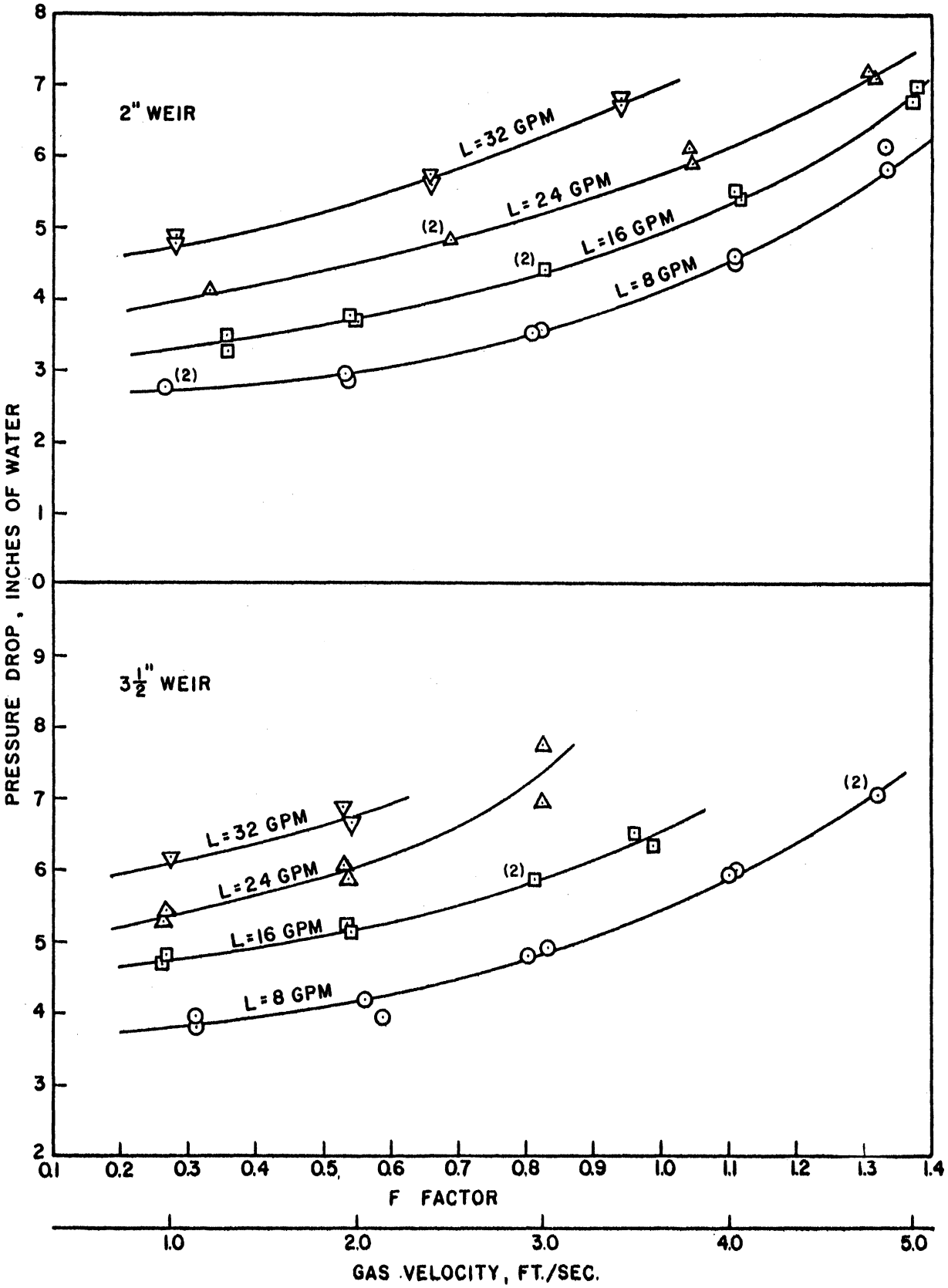

Figure 16. Pressure Drop for Valve Tray, Ammonia-Air-Water System

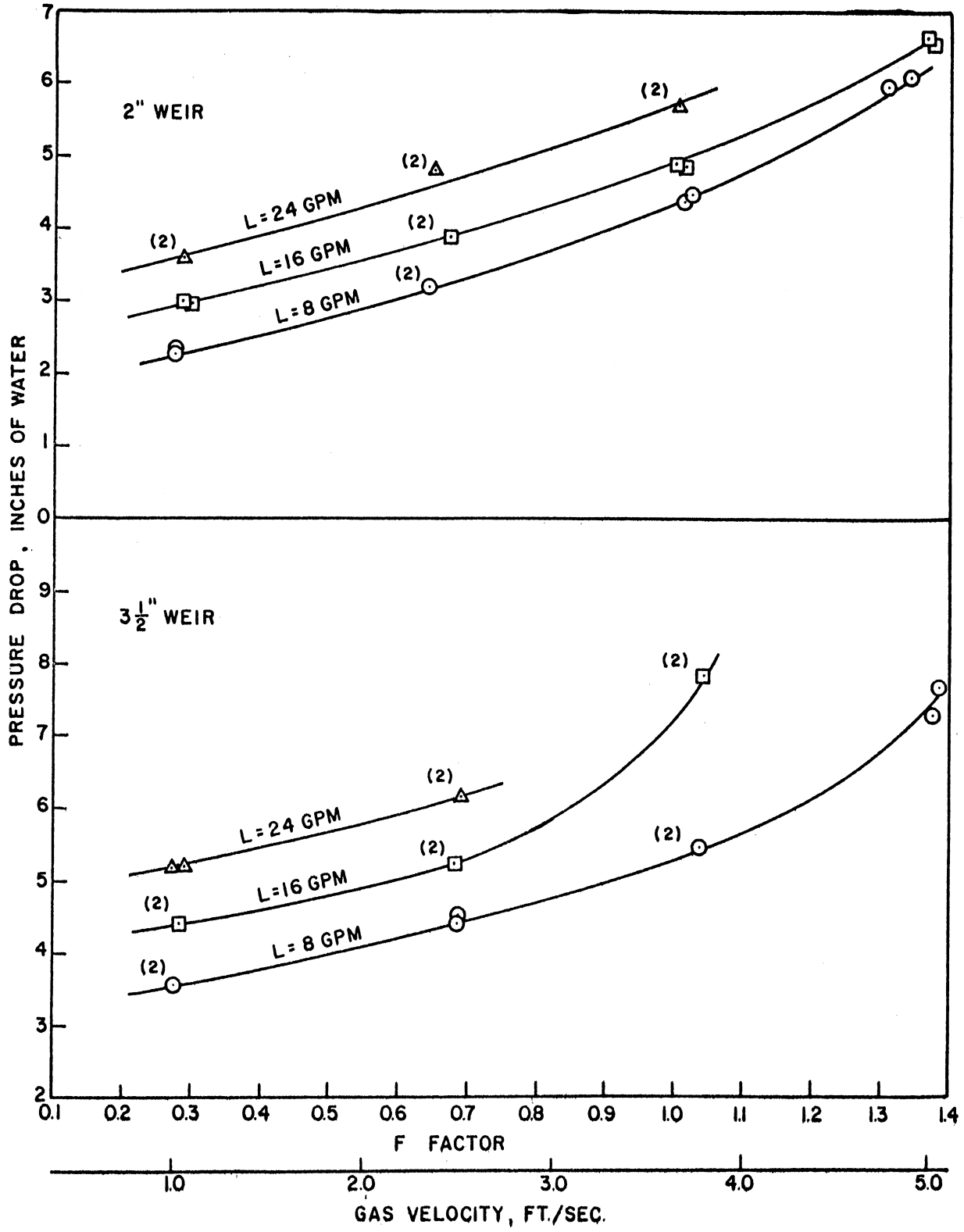

Figure 17. Pressure Drop for Perforated Tray, Ammonia-Air-Water System

slightly different parameters of liquid flow rate are presented in the Appendix. All data were taken with a splash baffle installed one inch upstream from the weir, with the lower edge one-half inch above the top of the weir. As only one tray was active, the flooding point could not be exactly determined. However, it appeared that flooding would occur when the pressure drop across the tray was about 8.5 inches of water, and would be caused by froth build up rather than by limited downcomer capacity.

Froth Height - The froth heights observed when operating with the ammonia-air-water system are presented in Figures 18 and 19. Additional data for the air-water system are presented in the Appendix. The measurements were obtained by comparing the height of the froth on the tray with a scale fixed to the window covering the front of the column. This measurement is the least precise of all the data observed, as the froth-gas interface was not at a constant level but fluctuated greatly due to the turbulence on the tray. The action was observed for a period of time, and the average value was recorded. Observations made by the author and Begley[11] checked within 1/4-inch in most cases; thus, even though the actual froth height may be slightly different from the recorded values, the readings are consistent.

It was found that the addition of ammonia to the gas stream caused the froth height to be lower than for the air-water system alone. This is similar to what was found by Warzel[66], but he reported the difference between the two systems to be slight. With ammonia in the system, the author found that the turbulence of the gas-liquid mixture on the tray did not appear to be as violent as for the air-water system.

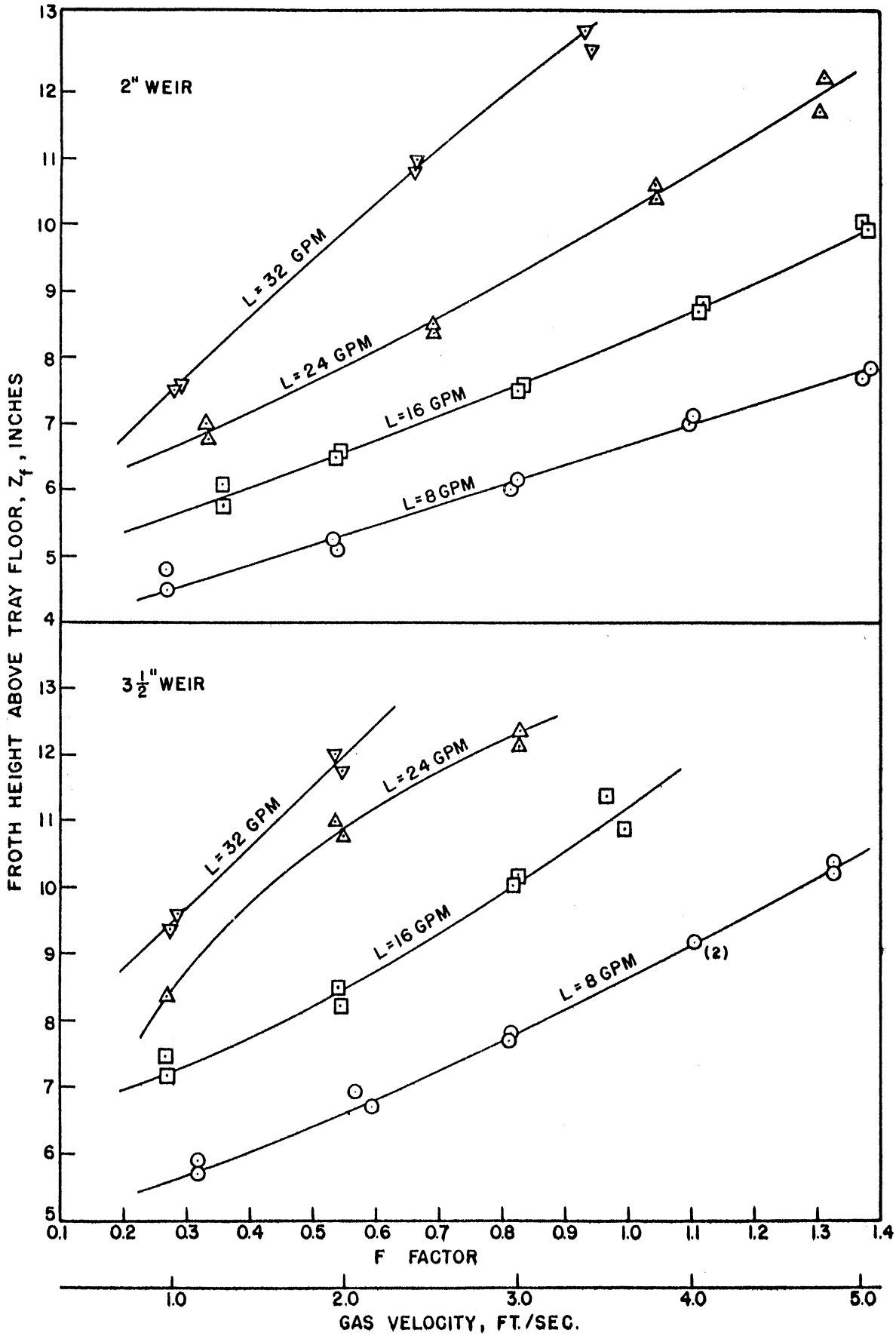

Figure 18. Froth Height for Valve Tray, Ammonia-Air-Water System

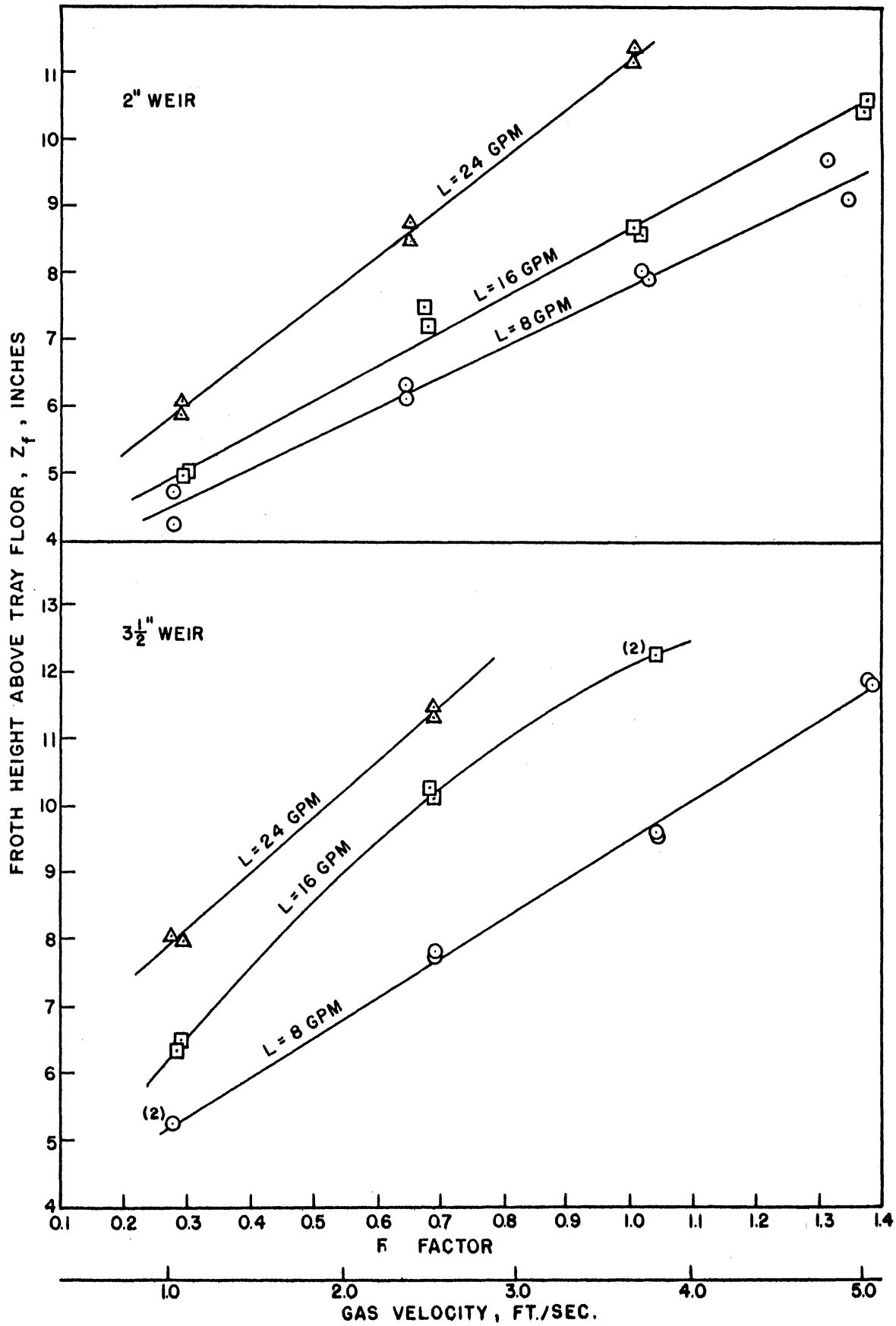

Figure 19. Froth Height for Perforated Tray, Ammonia-Air-Water System

As ammonia lowers the surface tension, it is possible that the local surface tension was lowered sufficiently to promote a more stable froth. This would also account for the lowered entrainment found for the ammonia-air-water system.

Clear Liquid Height - The clear liquid heights as indicated by the liquid manometers for the ammonia-air-water system are presented in Figures 20 and 21. The data plotted are the average heights for the two points in the active region of the tray, points C and D of Figure 14. It was found that these two points normally showed a clear liquid height lower than those at points B and D. The difference was usually a few tenths of an inch and increased with increasing liquid rate and weir height. This difference in liquid height can be explained by the large eddies previously mentioned. The eddies tended to accumulate liquid at the inlet and exit of the tray and, thus, the clear liquid heights would be higher at these points. It was found that the addition of ammonia to the gas stream had no effect on clear liquid height. Additional data for the air-water system is presented in the Appendix.

Gas Holdup - The gas holdup on the tray was computed by subtracting the clear liquid height from the froth height. Values obtained for the ammonia-air-water system are presented in Figures 22 and 23. Values for the air-water system may be computed from froth height and clear liquid height data presented in the Appendix. As the clear liquid height does not vary a great deal for a given liquid rate, the curves of gas holdup will have the same general shape as those for froth height.

Relative Froth Density - The relative froth density is the ratio of the clear liquid height to the froth height. The computed values for

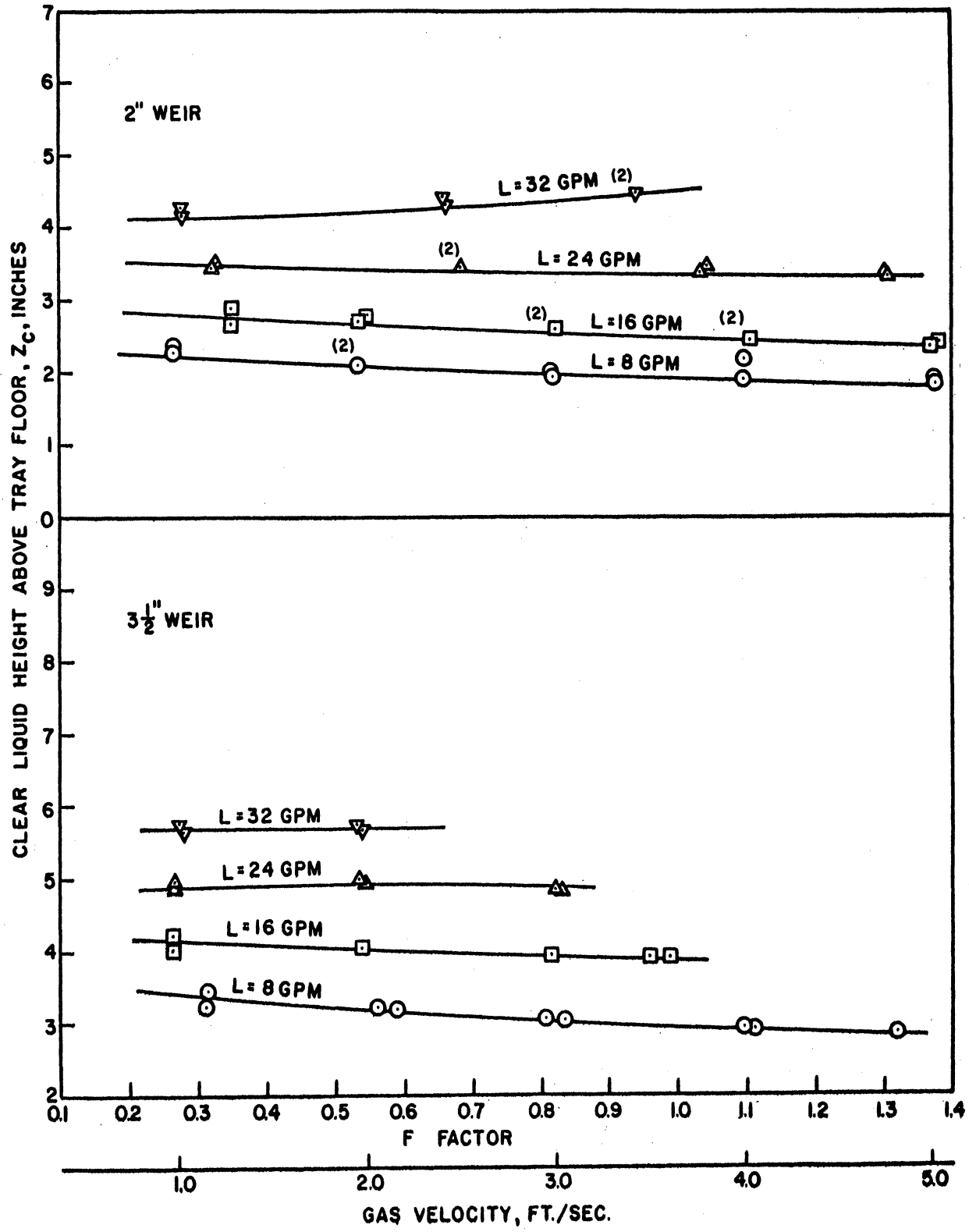

Figure 20. Average Clear Liquid Height for Positions C and D on Valve Tray, Ammonia-Air-Water System

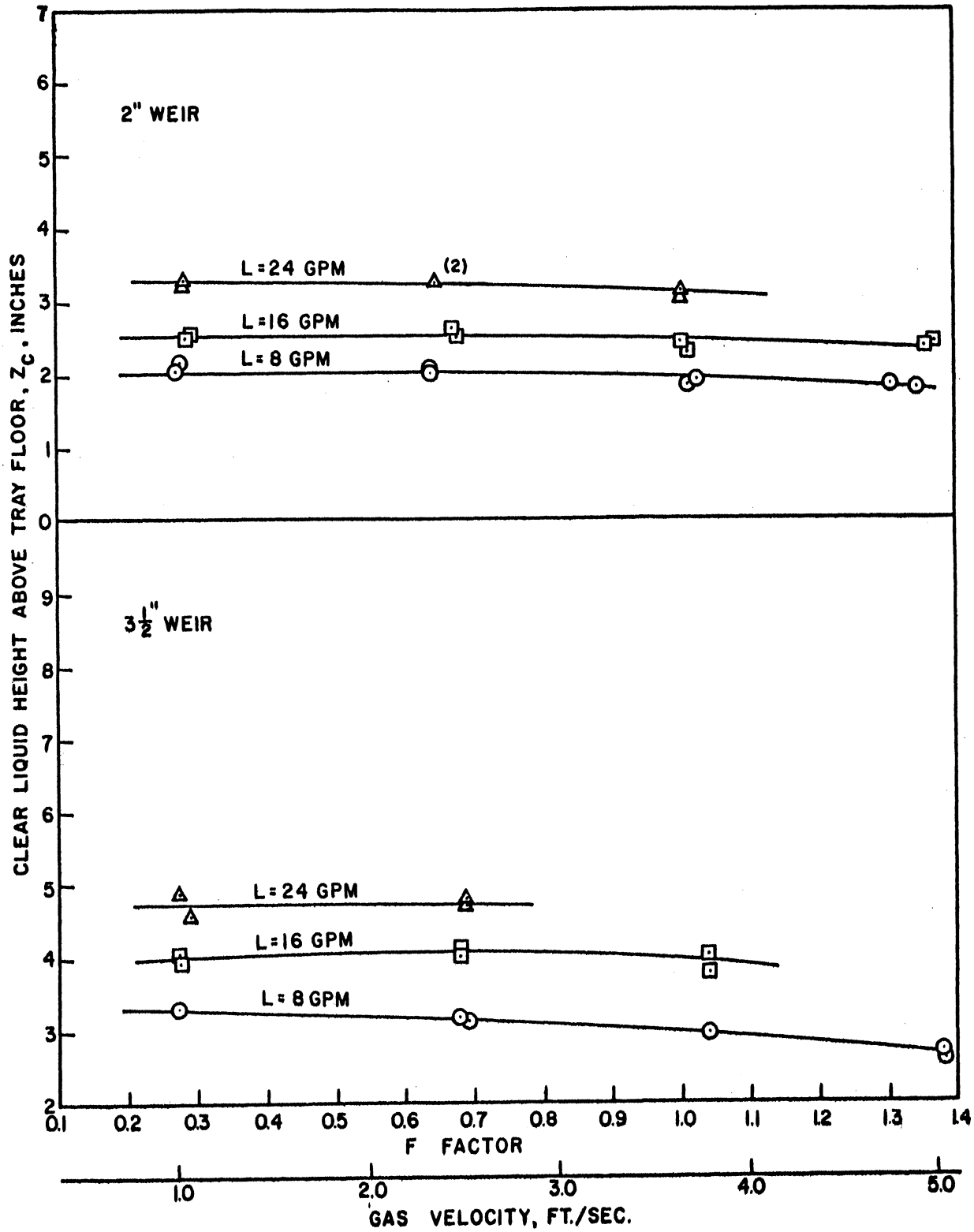

Figure 21. Average Clear Liquid Height for Positions C and D on Perforated Tray, Ammonia-Air-Water System

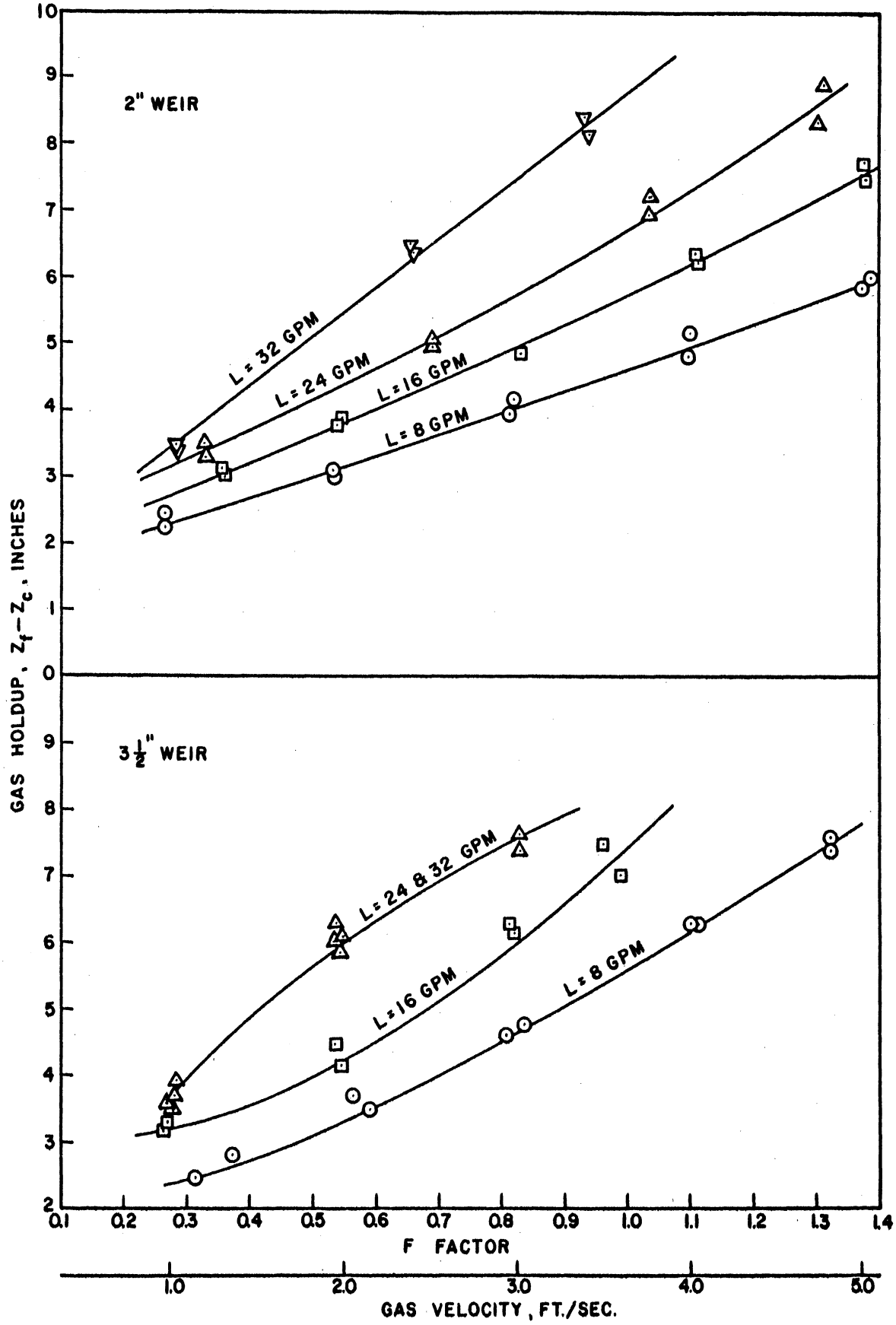

Figure 22. Gas Holdup on Valve Tray, Ammonia-Air-Water System

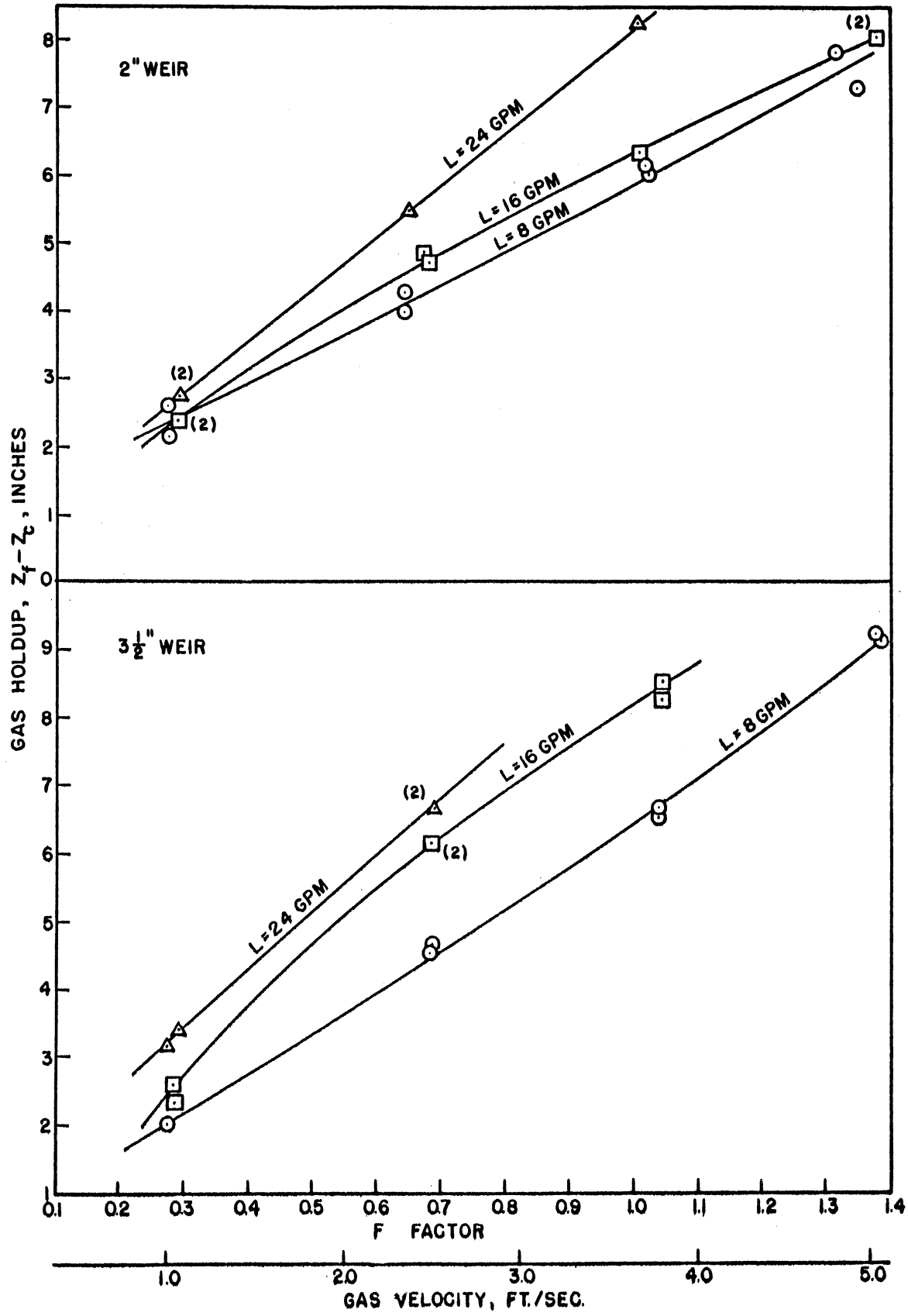

Figure 23. Gas Holdup on Perforated Tray, Ammonia-Air-Water System

the ammonia-air-water system are presented in Figures 24 and 25. It can be seen that for a given gas rate and weir height, the relative froth density is quite insensitive to liquid rate.

The lines drawn through the data in Figures 24 and 25 have been replotted on Figure 26 to show the effect of weir height and tray design. From the latter figure, it is apparent that over most of the operating range the relative froth density is greater for the valve tray than for the perforated tray. This difference is very slight and a single curve could be drawn to represent both trays within the precision of the data. The higher weir also causes an increased relative froth density, but the curves through the data have the same shape and are almost parallel.

Entrainment - The entrained liquid from the test tray carried to the dry tray was withdrawn by a probe located on the tray floor. This prevented the accumulation of liquid on the dry tray. The entrained liquid was collected in a tared container, and the results for the ammonia-air-water system are presented in Figures 27 and 28 where the entrainment, ϵ, is expressed as moles of liquid per mole of vapor.

Entrainment was not measured for the air-water system, as operating conditions were limited to those with negligible entrainment to avoid gas sampling difficulties. When operating with ammonia, a small amount of entrainment in the vapor sample would not appreciably affect the composition. Water would have no effect, and the quantity of dissolved ammonia would be negligible unless the sampling probe were immersed in liquid, a condition that did not occur. With the air-water system, a small amount of entrained liquid in the vapor sample would

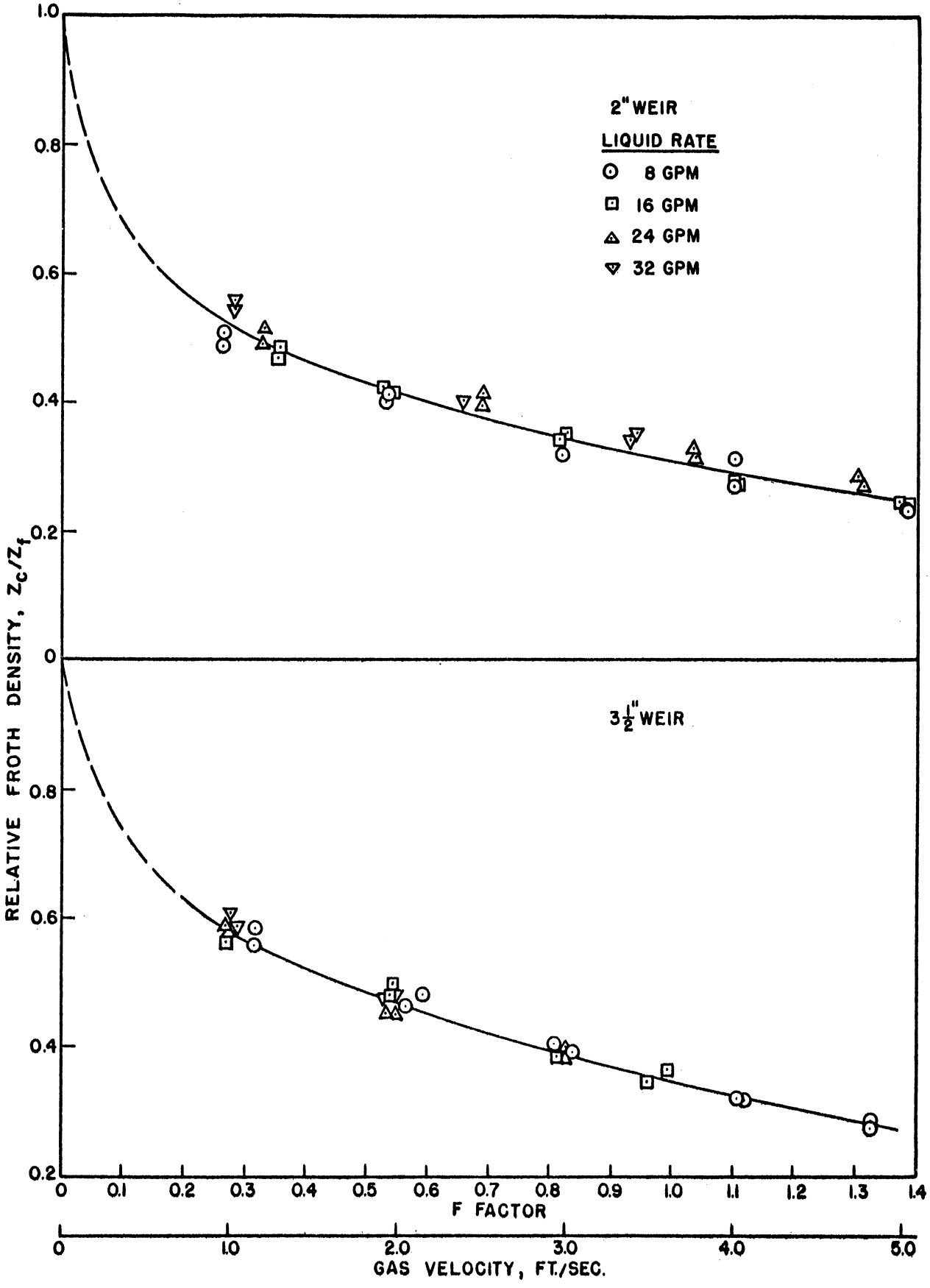

Figure 24. Relative Froth Density for Valve Tray, Ammonia-Air-Water System

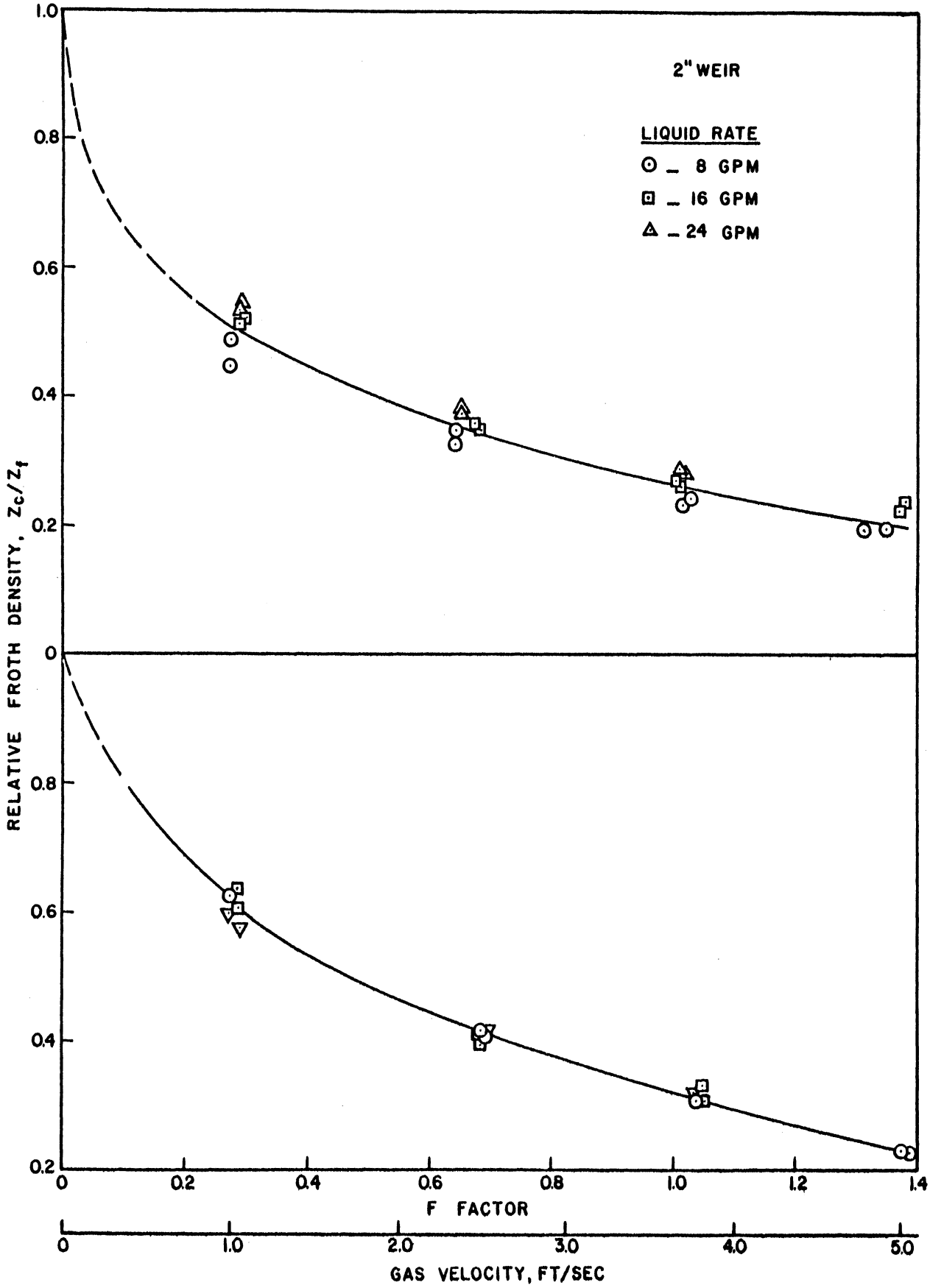

Figure 25. Relative Froth Density for Perforated Tray, Ammonia-Air-Water System

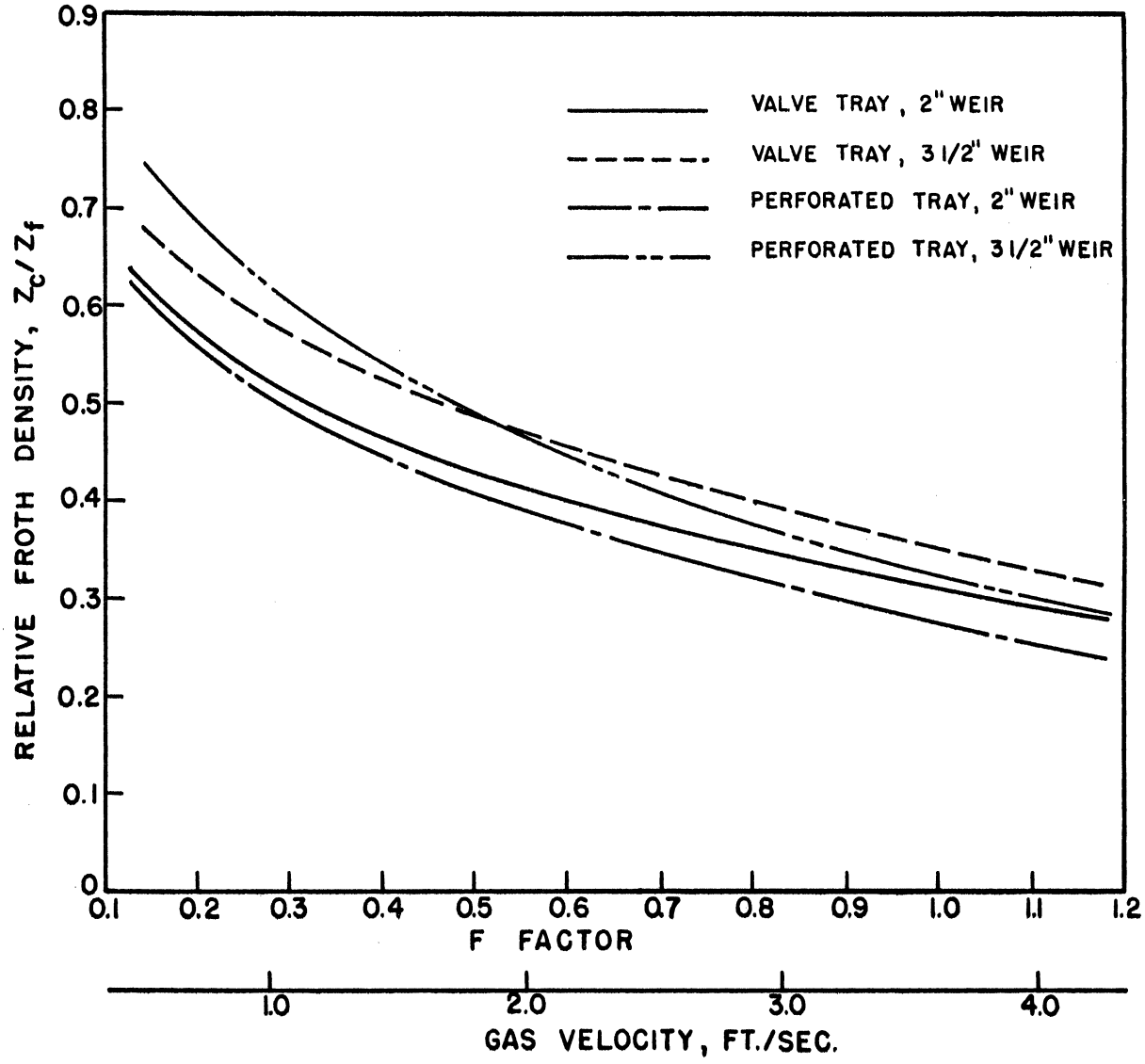

Figure 26. Relative Froth Density with Ammonia-Air-Water System

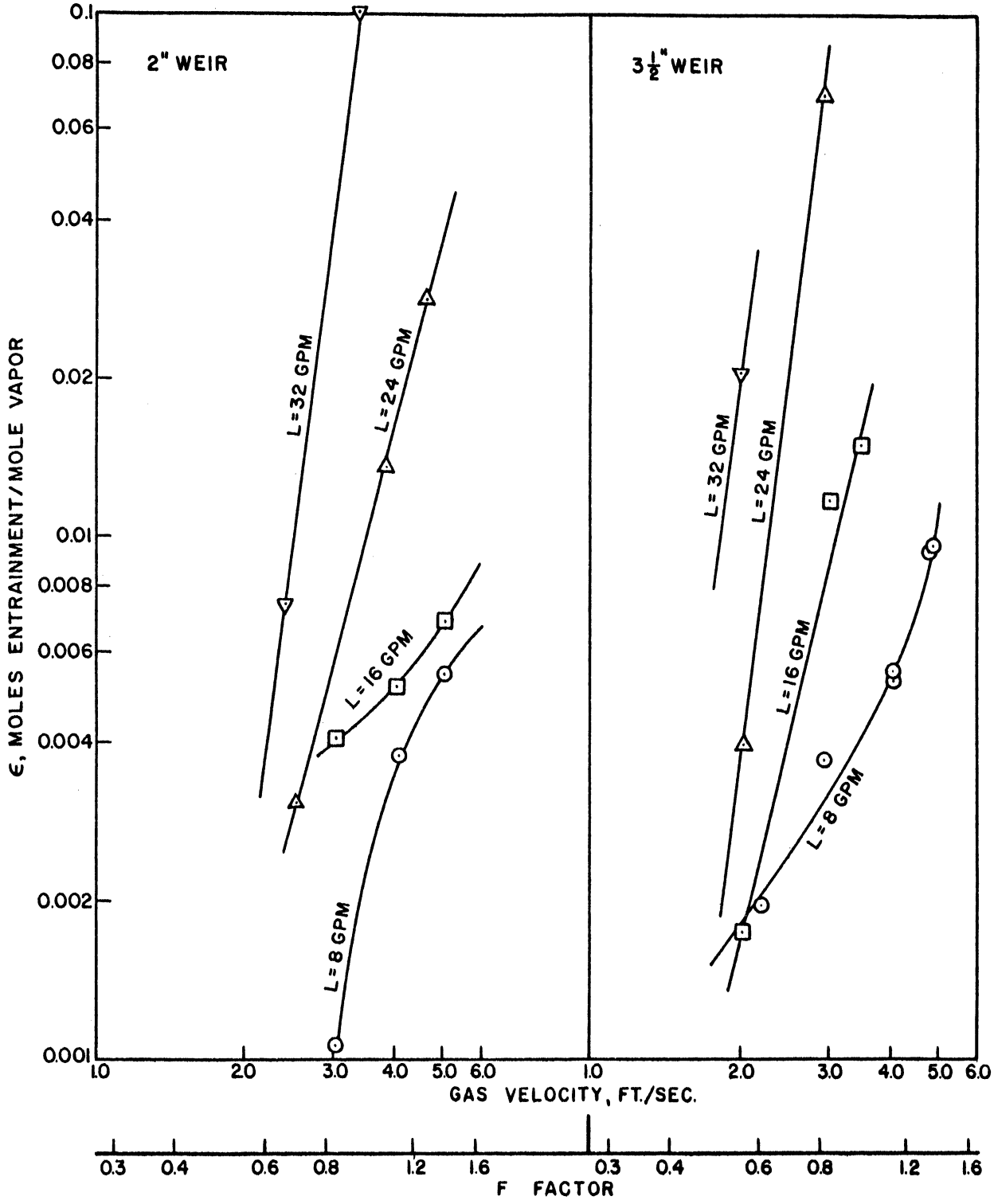

Figure 27. Entrainment with Valve Tray, Ammonia-Air-Water System

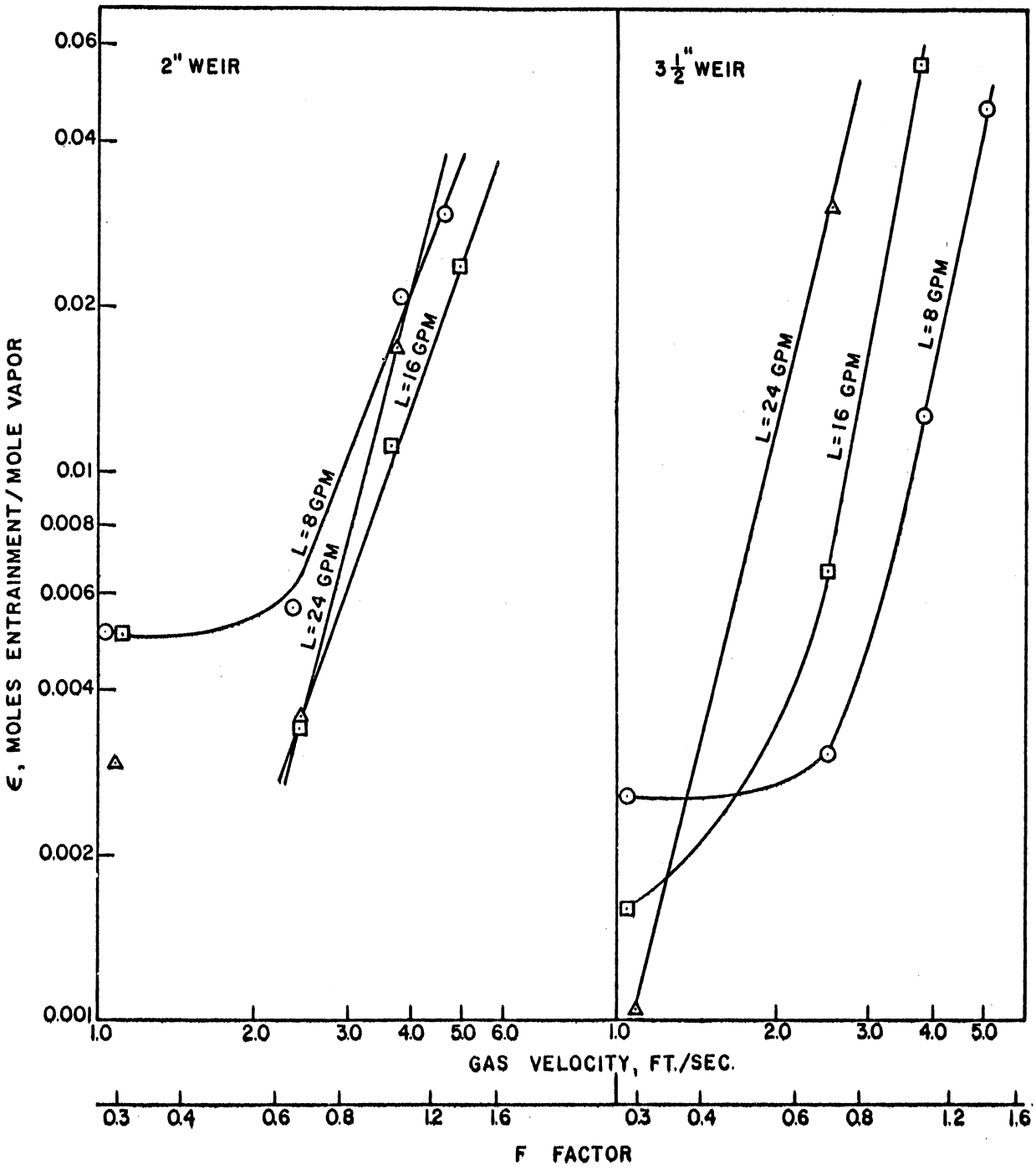

Figure 28. Entrainment with Perforated Tray, Ammonia-Air-Water System

greatly affect the calculated efficiency as the vapor leaving the test tray was usually close to the saturation point.

The data shown in Figures 27 and 28 must be regarded as qualitative rather than quantitative because the efficiency of the dry tray as an entrainment collector is not known. It is estimated that most of the droplets with a diameter greater than 75 microns are collected. Since the drop size distribution is not known, it is not possible to determine the collection efficiency. In addition, since the gas leaving the test tray is not completely saturated, there will be some mass transfer from the entrained liquid to the gas stream.

Liquid Weepage Through the Tray - The amount of liquid that weeps through an operating tray was measured by Talvalkar.[62] He used the one tray unit of Crozier[25] which has the same dimensions as the column used by the author. Talvalkar measured the leakage for two tray designs. One was the valve tray used by the author, and the other was a perforated tray similar to the one used by the author except the perforations had a diameter of one inch instead of 7/8-inch.

He found that the weepage was a function of vapor velocity, weir height, and liquid rate. For the air-water system he found the weeping limit to be as shown in Table VII, where the weeping limit is defined as the point where the liquid leakage is one per cent of the liquid fed to the tray. Thus, at vapor velocities above this limit any effect of weepage is negligible.

The weeping limits given in Table VII are in the range reported by Arnold et al.[8] and Hunt et al.[34], for perforated plates with hole diameters up to one-half inch. The primary factor that affects weeping is the gas velocity through the holes and the weeping limit ranges from

TABLE VII

WEEPING LIMIT** OF VALVE AND PERFORATED TRAYS*

Tray	Weir Height Inches	Liquid Rate gal/min	Superficial Vapor Velocity ft/sec	Hole Vapor Velocity ft/sec
Valve	3-1/2	8	1.64	-
		16	1.46	-
		24	1.35	-
		28.8	1.30	-
Perforated	1-1/2	8	2.98	37.4
		16	2.71	34.0
		24	2.55	32.0
		28.8	2.49	31.2
Perforated	3-1/2	8	3.28	41.1
		16	3.01	37.7
		24	2.85	35.7
		28.8	2.77	34.7

* Data of Talvalkar[62]

** Defined as the point where liquid weepage is one per cent of the liquid fed to tray.

30 to 40 ft/sec. Minor variations in the above range are caused by differences in hole spacing, plate thickness, liquid seal, and liquid flow rate.

Mass Transfer Results - Humidification

The humidification runs were carried out with the air-water system using the valve tray. The range of operating variables was as follows:

1. 1-1/2-inch weir height; Liquid rate 8.0, 16.0, and 24.0 gpm
2. 3-1/2-inch weir height; Liquid rate 8.0 gpm

The vapor velocity was varied from 1.0 to 5.3 ft/sec.

The Murphree vapor efficiencies for the humidification runs are plotted in Figure 29. Several items can be noticed. First, the efficiency increases as the liquid rate is increased; second, the efficiency is increased by an increase in the height of the overflow weir; third, for the 1-1/2-inch weir as the vapor velocity increases the efficiency decreases until a minimum point is reached, after which a further increase in vapor velocity causes an increase in the efficiency; and, fourth, for the 3-1/2-inch weir the efficiency is essentially constant over the range of variables studied.

Mass Transfer Results - Absorption

Absorption was studied by absorbing ammonia in water from an ammonia-air stream. Both the valve tray and perforated tray were used. The range of operating variables was as follows:

1. Valve Tray: Weir height 2 and 3-1/2 inches; Liquid Rate 8.0, 16.0, 24.0, and 32.0 gpm.

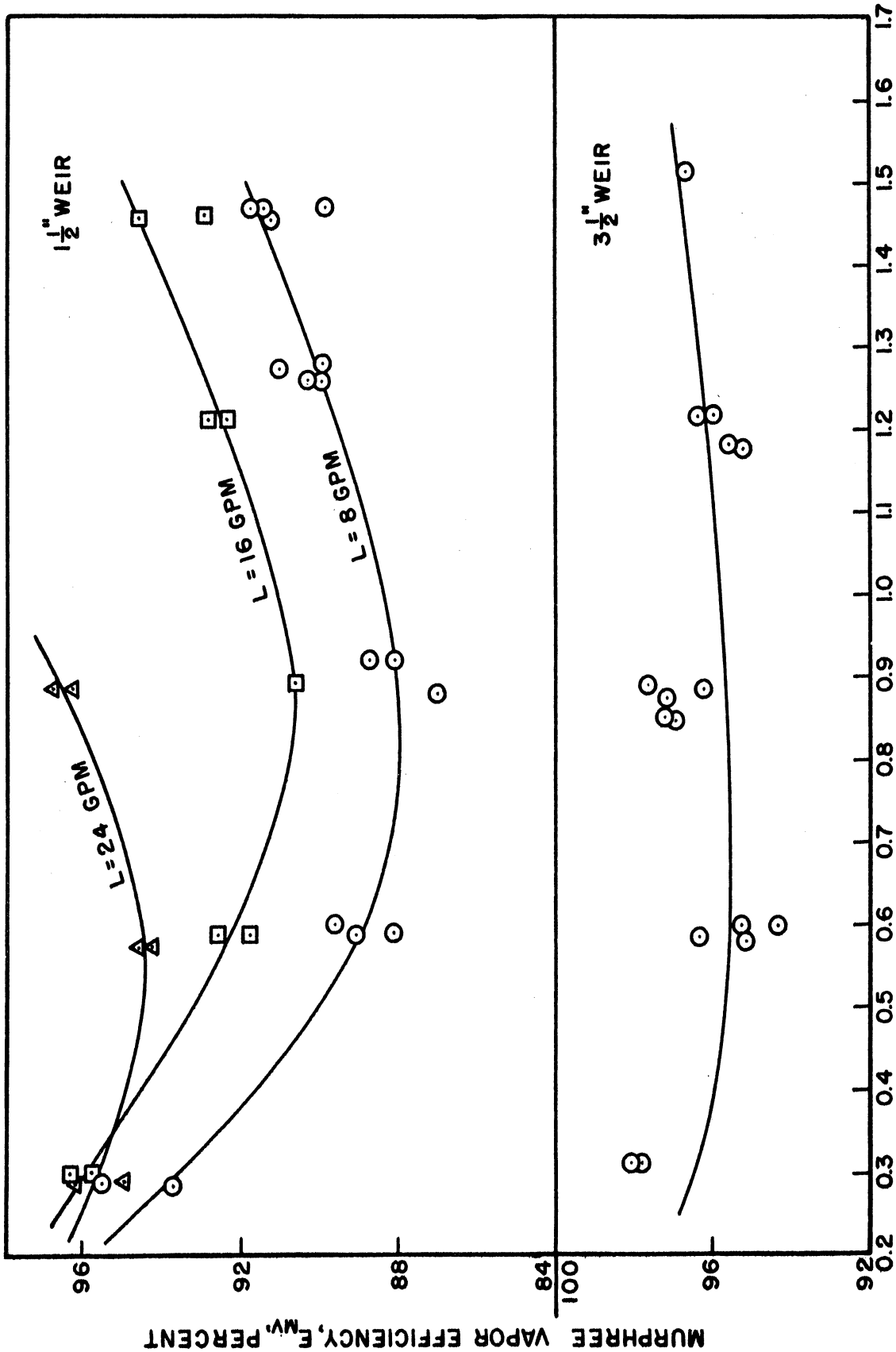

Figure 29. Murphree Vapor Efficiency for Humidification with Valve Tray, Air-Water System

2. Perforated Tray: Weir Height 2 and 3-1/2 inches; Liquid Rate 8.0, 16.0, and 24.0 gpm.

The vapor velocity was varied from 1.0 to 5.0 ft/sec. The amount of ammonia in the entering gas stream was constant for most runs so the concentration depended on the vapor flow rate and varied from 2.2 to 11.9 mole per cent. This resulted in an exit vapor concentration from the tray that was usually less than one mole per cent. At this level the partial pressure of the ammonia in the exit vapor stream was low enough that the Henry's Law constant was a function of temperature only and not of the composition of the liquid on the tray.

The experimentally determined Murphree liquid and vapor efficiencies for ammonia absorption are presented in Figures 30 through 33. For a given vapor rate, the efficiencies were higher for the runs with a 3-1/2-inch weir than with those with a 2-inch weir for both the valve and perforated trays. The perforated tray showed lower efficiencies at the lowest gas rate (about one ft/sec). In this region the liquid is cycling back and forth on the test tray. Consequently, part of the vapor passes through the tray without contacting the liquid to any degree. This accounts for the lower efficiencies obtained. The broken lines in Figures 32 and 33 indicate what the efficiencies might be if there were no liquid cycling and are based in general on the curves drawn through the data for the valve tray. The cycling is probably due to the large hole diameter and may not occur with smaller holes even though the tray may be weeping.

As in the humidification studies, the Murphree vapor efficiency increased with liquid rate. Also for both trays the data taken

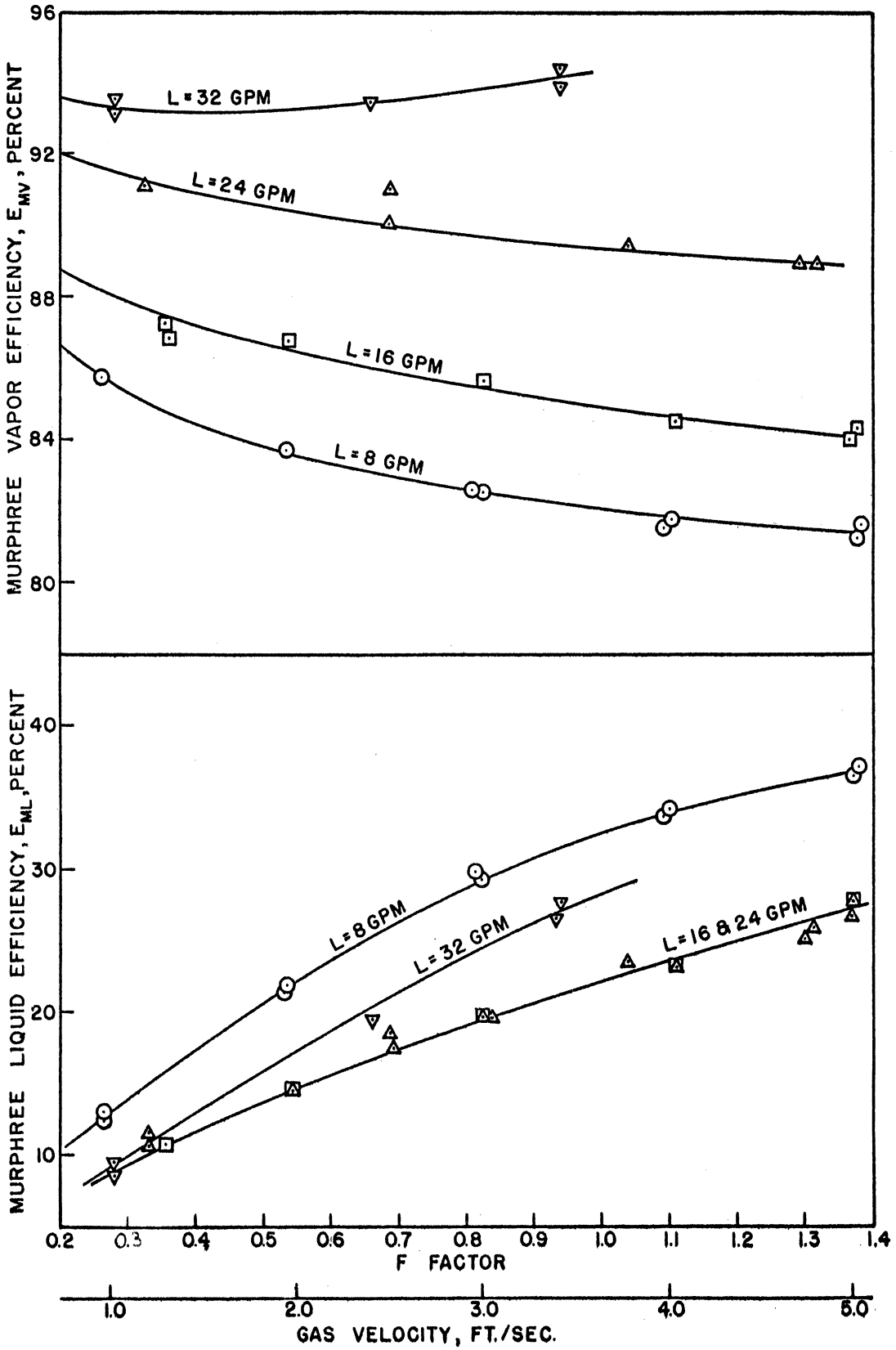

Figure 30. Murphree Efficiencies for Ammonia Absorption with Valve Tray, Weir Height 2-inches

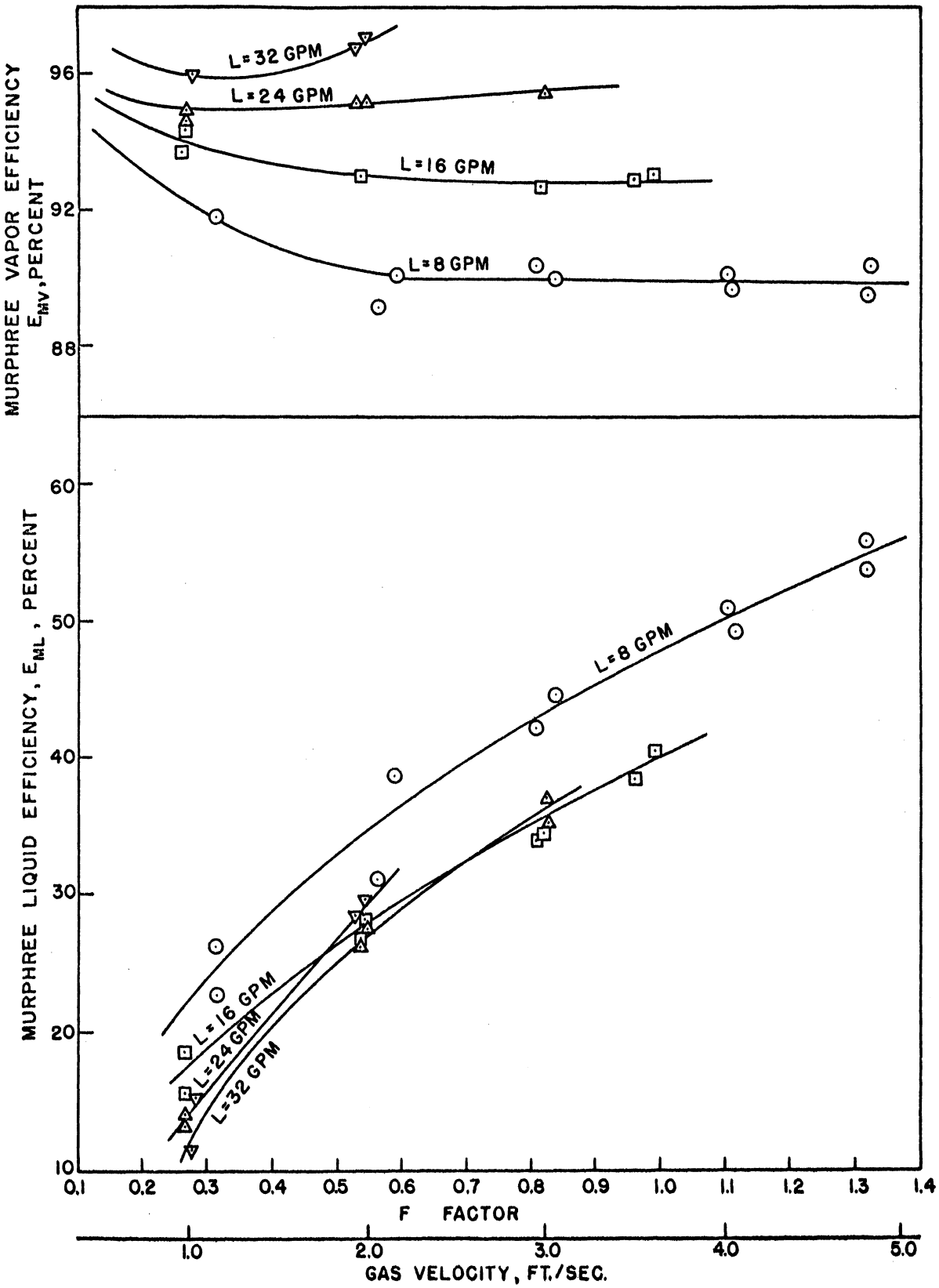

Figure 31. Murphree Efficiencies for Ammonia Absorption with Valve Tray, Weir Height 3-1/2-inches

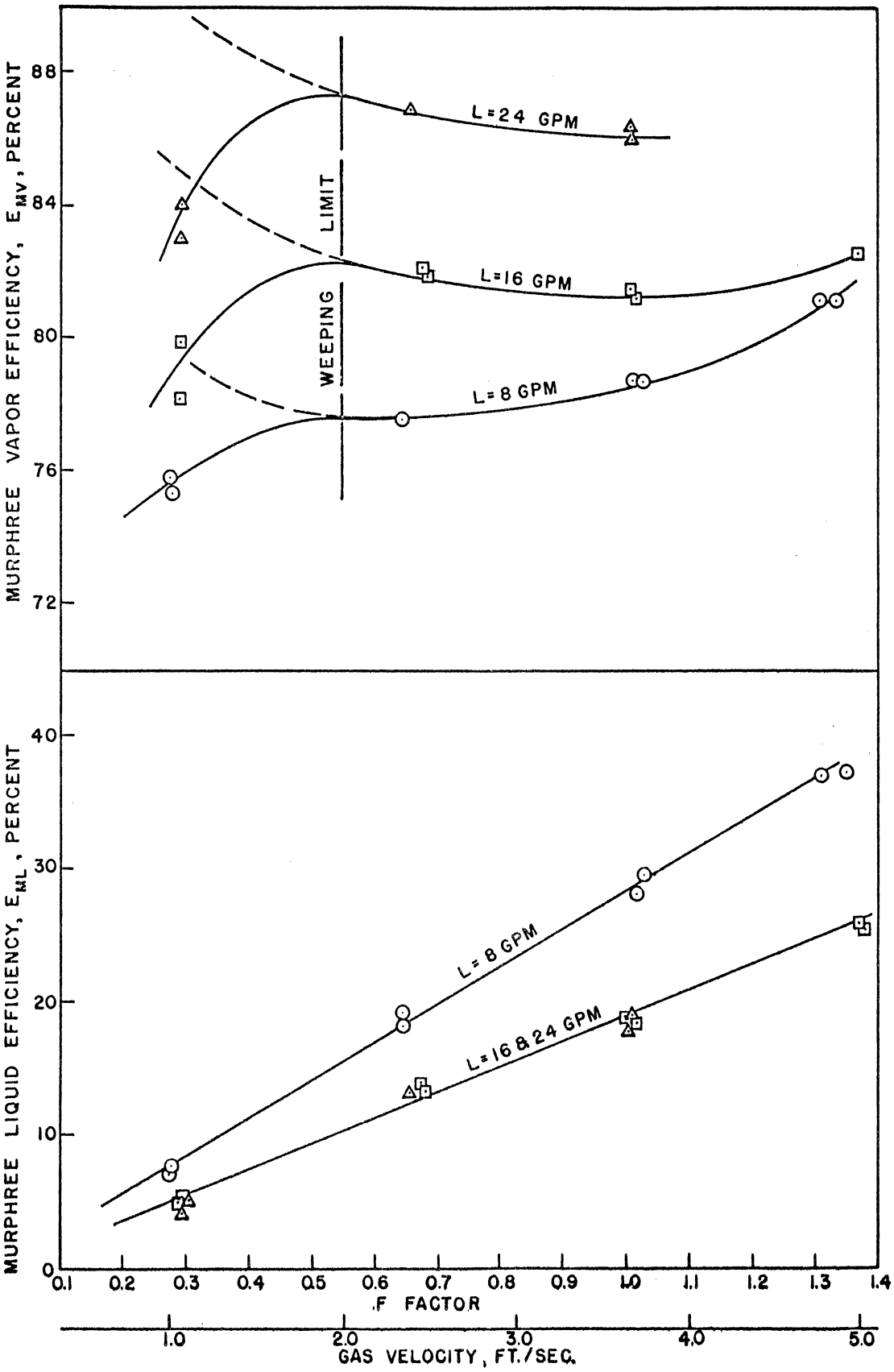

Figure 32. Murphree Efficiencies for Ammonia Absorption with Perforated Tray, Weir Height 2-inches

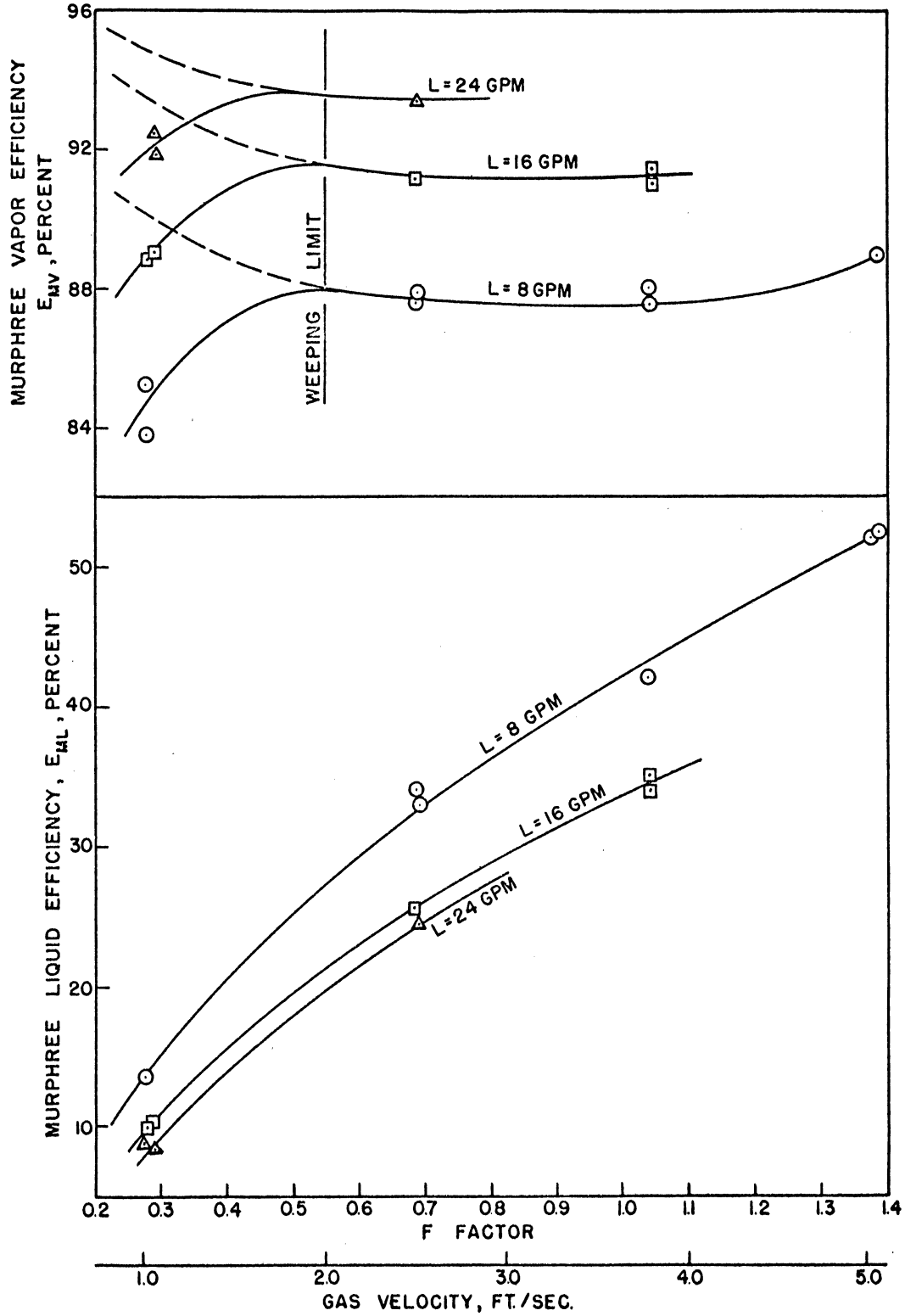

Figure 33. Murphree Efficiency for Ammonia Absorption with Perforated Tray, Weir Height 3-1/2-inches

with the 3-1/2-inch weir showed the Murphree vapor efficiency to be almost independent of vapor rate if the tray operation is stable. With the valve tray, the 2-inch weir height data showed a gradual decrease of Murphree vapor efficiency as the vapor rate was increased with the exception of the set taken at a liquid rate of 32 gpm. The latter set showed the efficiency to be essentially constant. The 2-inch weir height data for the perforated tray showed an increase of Murphree vapor efficiency with vapor rate for the set with a liquid rate of 8 gpm. With the higher liquid rates the efficiency was essentially constant.

Concentration Profiles - For all ammonia absorption runs, samples were taken of the liquid entering and leaving the tray and at four points on the tray floor. Typical concentration profiles are shown in Figures 34 and 35, and the complete data are tabulated in the Appendix. In plotting the data, the experimental values were normalized to give an entrance concentration of zero and an outlet concentration of unity so that runs of different concentration levels could be compared. The data show that the liquid on the tray is neither completely mixed nor conforms to the plug flow model. For plug flow the theoretical concentration profile can be calculated by the following equation[44]

$$x_n = \frac{[(y_n)_o - y_{n-1}]\exp(E_{OG}\lambda w)}{m\,E_{OG}} + \frac{y_{n-1}}{m} \qquad (72)$$

where

w = fractional distance across tray.

By expanding the exponential term in series it can be seen that in the case where $(E_{OG}\lambda)^2/2!$ is small when compared with $(1 + E_{OG}\lambda)$ the concentration profile is essentially linear. As the maximum value of λ in the

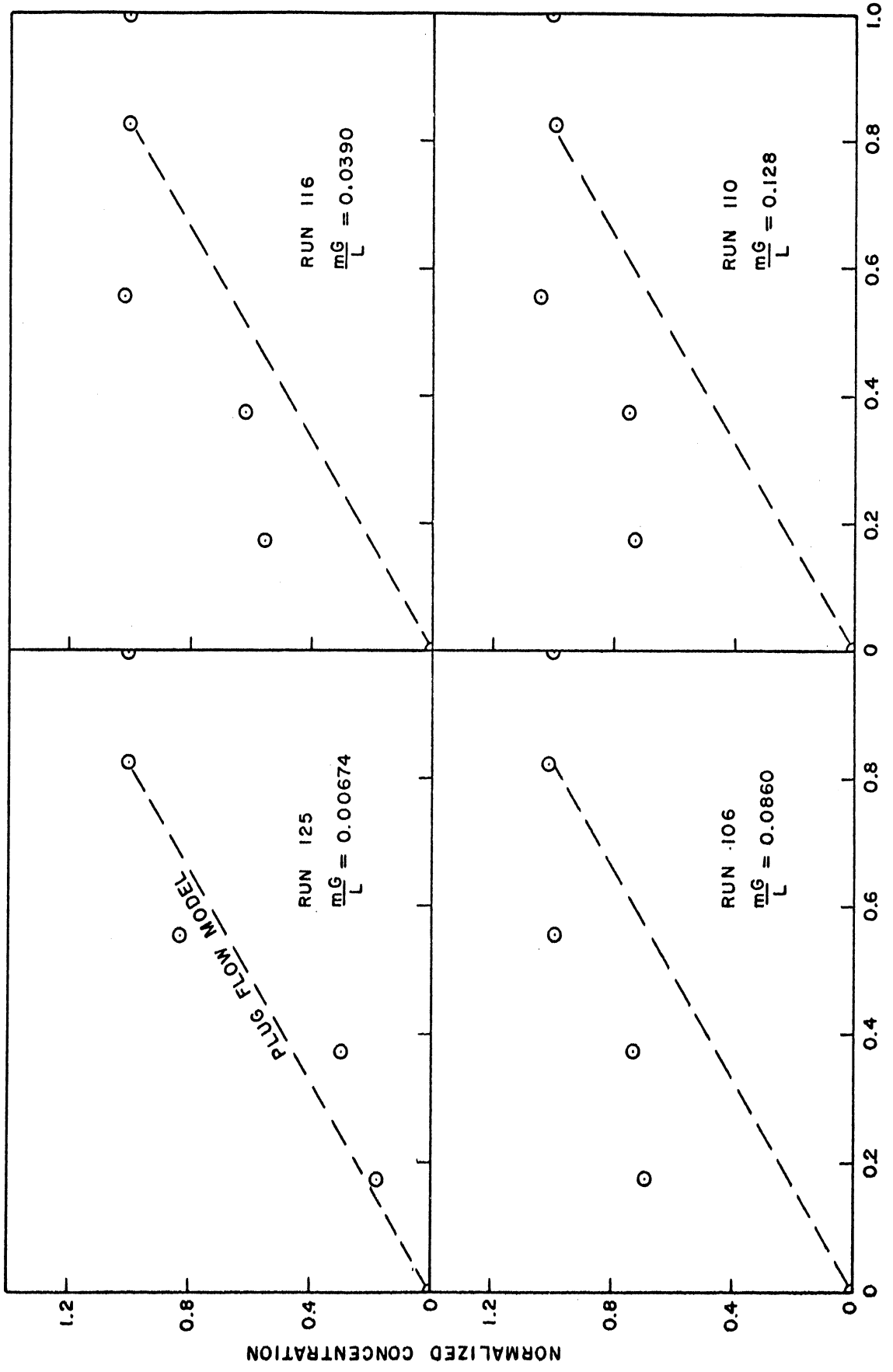

Figure 34. Concentration Profiles for Ammonia Absorption with Valve Tray

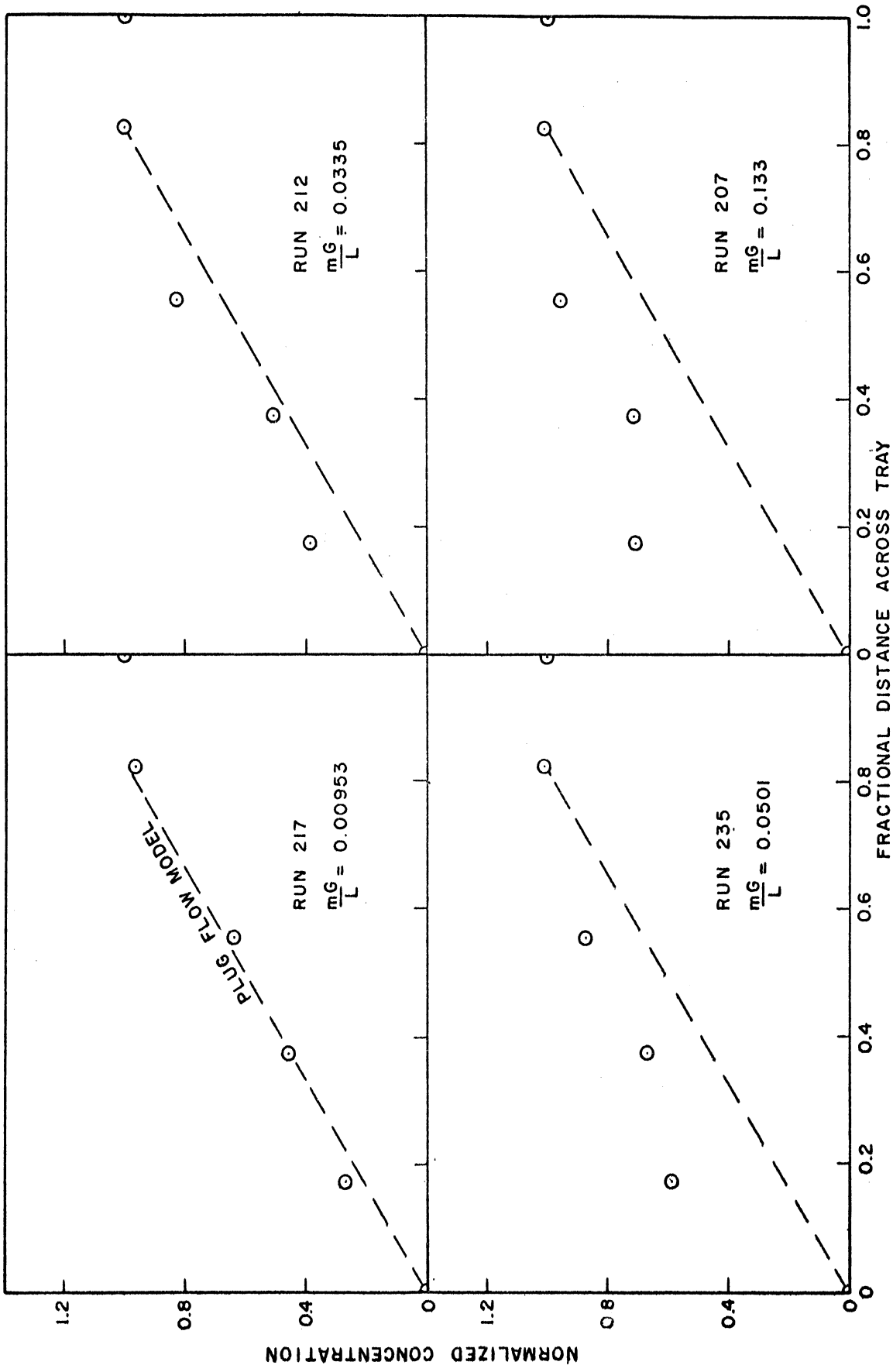

Figure 35. Concentration Profiles for Ammonia Absorption with Perforated Tray

present study is 0.133, and E_{OG} has an average value of about 0.90, the concentration profile should be linear if plug flow exists. The dotted lines in Figures 34 and 35 show the plug flow concentration profile if the active tray is considered to end at the last sampling point on the tray floor. It can be seen that plug flow is approximated when the ratio of gas to liquid is low, but at higher ratios the plug flow model is not valid. In fact, there appear to be two pools of completely mixed liquid.

Liquid Mixing - Warzel's mixing parameter was calculated using the liquid sample obtained from position B of Figure 14 as x_e with Equation (14).

$$C = \frac{x_n - x_{n+1}}{x_n - x_e} \qquad (14)$$

The results are presented in Figures 36 and 37. Warzel's ammonia absorption data[66] for a bubble cap tray with a liquid rate of 9.16 gpm is shown for comparison. The values obtained for C are smaller for the valve and perforated tray than for the bubble cap tray, indicating that there is less mixing on the former trays than on the bubble cap tray. This is to be expected as the bubble caps on the tray present an obstruction to the liquid flow. The mixing was slightly greater on the perforated tray than on the valve tray. At first glance, this might seem to be contradictory, as the valves do present some obstruction to liquid flow. However, the vapor emerging from under the disk of the valve has an appreciable velocity component in the horizontal direction whereas the vapor issuing from the perforations has only a vertical component. This vertical component of velocity tends to carry the liquid with the vapor. This is confirmed by the fact that the perforated tray has a greater froth

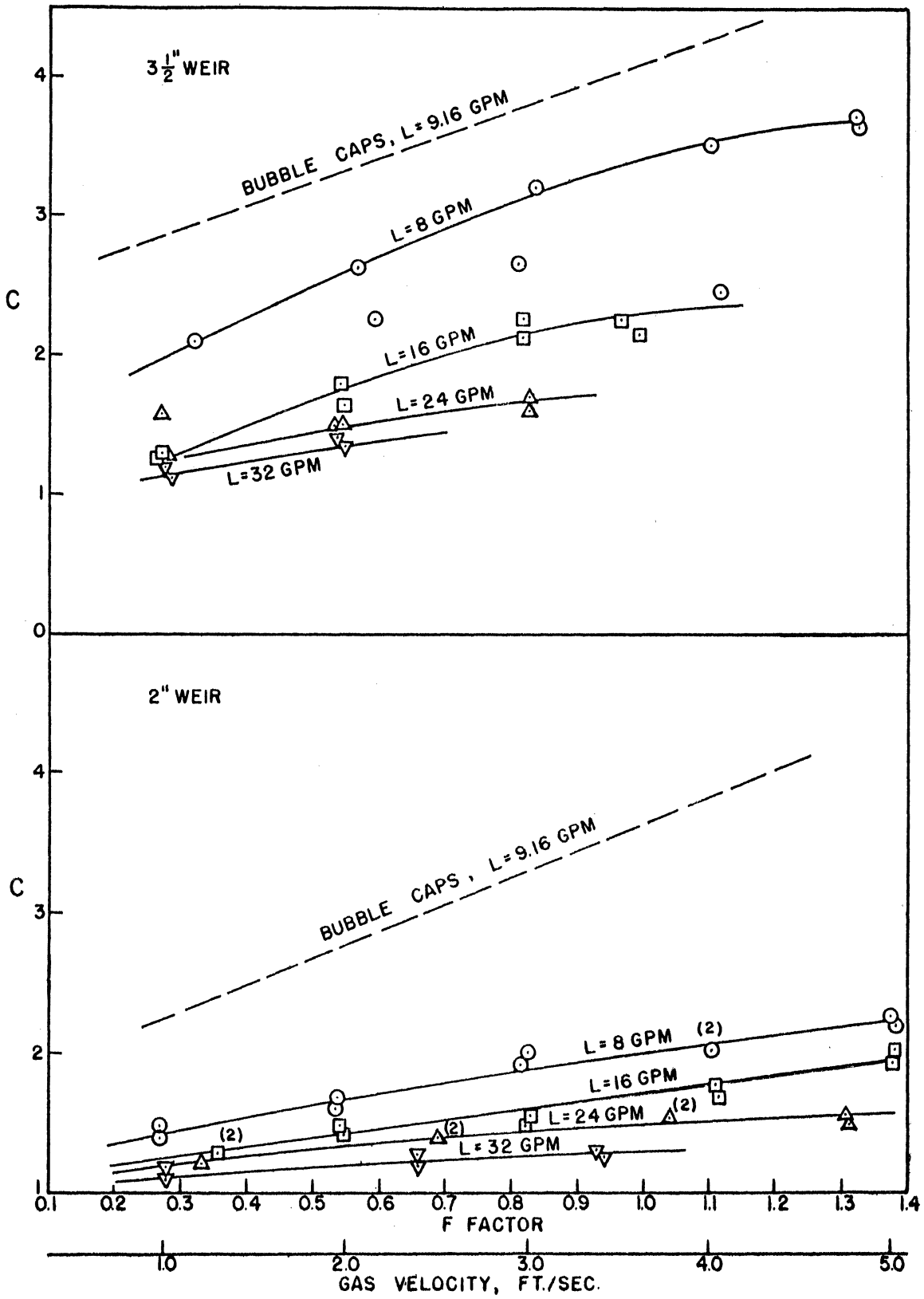

Figure 36. Mixing Parameter C for Valve Tray

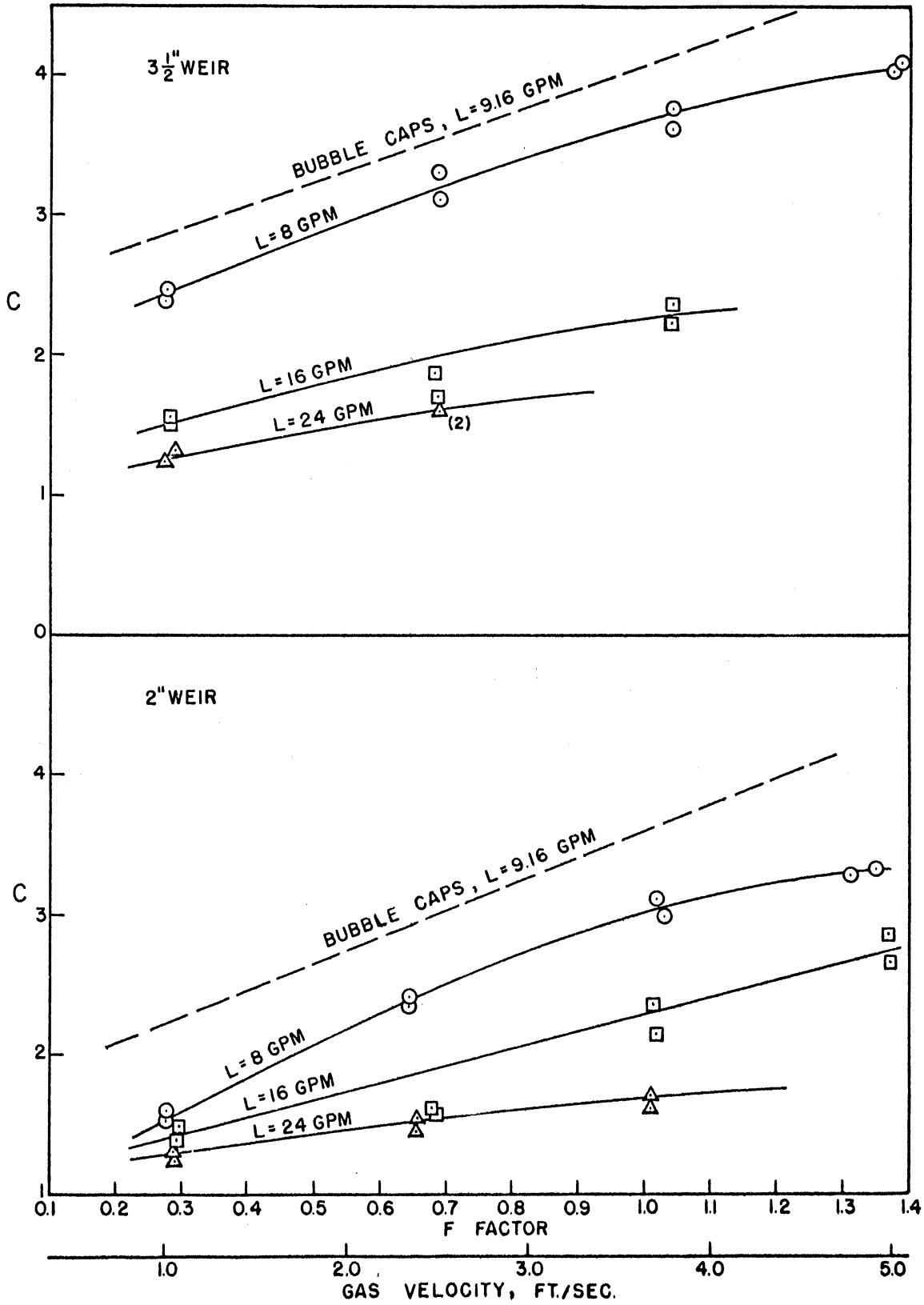

Figure 37. Mixing Parameter C for Perforated Tray

height than the valve tray at comparable operating conditions. The liquid carried up by the vapor returns to the tray and promotes mixing.

Gas Phase Transfer Units

In order to base the correlation of the data on the individual gas film resistance, it was necessary to calculate N_G, the number of individual gas phase transfer units. In general, this can be done most easily by obtaining N_{OG}, the number of overall gas phase transfer units, and correcting for liquid phase resistance to obtain N_G. The procedure used in this investigation depended on the particular system and the methods used were as follows.

Humidification - In the air-water system there is no resistance to mass transfer in the liquid phase. Also, since the liquid is of uniform composition and the vapor is assumed to be completely mixed, the point vapor efficiency E_{OG} will be the same as the Murphree vapor efficiency E_{MV}. Thus, the number of individual gas phase transfer units is the same as the number of overall gas phase transfer units, and can be calculated by Equation (59) if liquid phase resistance is absent.

$$N_G = N_{OG} = \frac{1}{2} \ell n\left(\frac{1-y_1}{1-y_o}\right) - \ell n(1-E_{OG}) \qquad (59)$$

This equation takes into account the change in gas rate on the plate and the effect of unidirectional mass transfer. It was found that for the humidification runs, the value of the first term was negligible compared to the second term and was omitted in the calculations. Values of N_G for each run are tabulated in the Appendix, and are also presented in Figure 38.

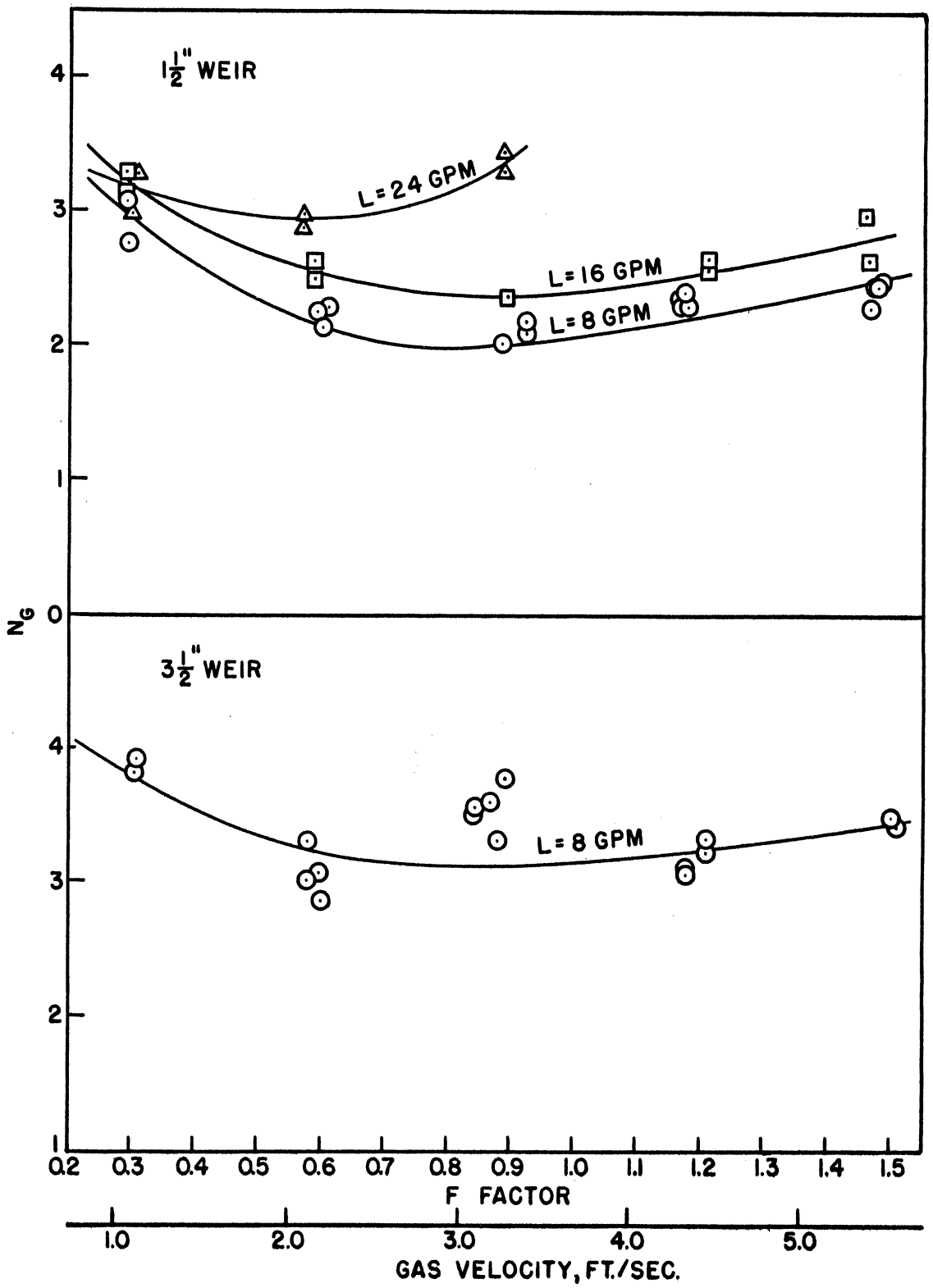

Figure 38. Values of N_G for Humidification with Valve Tray, Air-Water System

Absorption - In the ammonia-air-water system, unless the liquid on the tray is completely mixed, E_{OG} and E_{MV} will not be identical. The relation between the two depends on the degree of mixing and the value of mG/L. If plug flow exists, then E_{OG} can be calculated by Equation (11)

$$E_{OG} = \frac{1}{\lambda} \ell n(\lambda E_{MV}+1) \qquad (11)$$

If the liquid is partially mixed, a different relationship will hold. Using Warzel's[66] parameter, C, to describe the mixing, E_{OG} can be calculated by Equation (13)

$$E_{OG} = \frac{C}{\lambda} \ell n(\frac{\lambda}{C}E_{MV}+1) \qquad (13)$$

A comparison of E_{OG} with E_{MV} has been made for eight runs covering the range of operating conditions for both trays, and is presented in Table VIII. It can be seen that the difference between E_{OG} and E_{MV} is greater when the value of mG/L is large, especially for the case of plug flow. As the concentration profile data showed that plug flow did not exist except at the lowest values of mG/L, the partial mixing model represents a more accurate relationship between E_{OG} and E_{MV}. By comparing the values of E_{OG} and E_{MV} for the mixing model, it is apparent that the difference between the values is very small, even at the higher values of mG/L, and that the value of E_{OG} is intermediate between E_{MV} and E_{OG} calculated for plug flow. Accordingly, the experimentally values of E_{MV} can be used as E_{OG} without incurring appreciable error, and this procedure was followed in the calculations. An error analysis is presented in the Appendix and shows that a one percent error in E_{OG} will result in less than a five per cent error in N_G in most cases.

TABLE VIII

COMPARISON OF E_{OG} WITH E_{MV} FOR AMMONIA ABSORPTION

Run(3)	$\frac{mG}{L}$	C	Observed E_{MV}	Mixing Model(1) E_{OG}	Plug Flow(2) E_{OG}
125	0.00674	1.22	0.960	0.959	0.953
116	0.0390	2.26	0.928	0.916	0.912
106	0.0860	3.23	0.901	0.890	0.868
110	0.128	3.71	0.898	0.884	0.850
217	0.00953	1.37	0.831	0.830	0.826
212	0.0335	1.64	0.822	0.815	0.810
235	0.0501	2.40	0.913	0.904	0.892
207	0.133	3.37	0.812	0.798	0.771

(1) Calculated from E_{MV} by Equation (13)

(2) Calculated from E_{MV} by Equation (11)

(3) 100 Series-Valve Tray, 200 Series-Perforated Tray

Once E_{OG} has been determined, N_{OG} can be evaluated by Equation (59)

$$N_{OG} = \frac{1}{2} \ell n\left(\frac{1-y_1}{1-y_o}\right) - \ell n(1-E_{OG}) \qquad (59)$$

Since liquid phase resistance exists, N_{OG} is not equal to N_G as was true for the humidification system.

In order to relate N_{OG} to N_G, the liquid phase resistance must be known. N_L, the number of individual liquid phase transfer units, was calculated by using Equation (71).

$$N_L = 55.4\ D_L^{1/2} F^{0.575} t_L \qquad (71)$$

Although this equation was developed from experiments with bubble cap trays, it was used for the valve and perforated tray for two reasons. The Murphree vapor efficiencies obtained with bubble cap trays were very close to those obtained with the valve and perforated trays so it might be expected that a correlation for bubble cap trays would be a good approximation to what occurs in the trays used in this investigation. In addition, since the liquid phase resistance is relatively small in the ammonia-air-water system, an error in the calculated N_L will cause only a slight error in the value of N_G.

Using the values of N_{OG} and N_L as determined by the above procedure, N_G was calculated by Equation (52).

$$\frac{1}{N_G} = \frac{1}{N_{OG}} - \frac{\lambda(1-x)_f}{N_L(1-y)_f} \qquad (52)$$

A few typical values obtained are listed in Table IX, while the values for the individual runs are presented in the Appendix, and in Figures 39 and 40.

TABLE IX

TYPICAL VALUES OF CALCULATED DATA FOR GAS PHASE TRANSFER UNITS

Run	$\frac{mG}{L}$	E_{MV}	N_{OG}	N_L	N_G
125	0.00674	0.960	3.28	0.976	3.36
116	0.0390	0.928	2.67	2.51	2.79
106	0.0860	0.901	2.34	3.94	2.48
110	0.128	0.898	2.30	4.78	2.45
217	0.00953	0.831	1.81	0.739	1.86
212	0.0335	0.822	1.76	1.53	1.83
235	0.0501	0.913	2.45	2.93	2.56
207	0.133	0.812	1.69	3.05	1.82

Correlation of the Data

As the physical properties of the air-water and ammonia-air-water systems were almost identical, it was not practical to develop a new correlation based on these properties; and this was not the intent of the present work. Rather, the purpose was to compare the results of the valve and perforated trays with the previous correlations for bubble cap trays and determine if the bubble cap correlations were valid for other tray designs and, if not, what changes need be made.

Based on the expression for N_G given in Equation (38)

$$N_G = k'_G a t_G = k'_G a \frac{Z_f - Z_c}{u} \tag{38}$$

it seemed probable that a correlation for N_G, or alternatively $k'_G a$, should

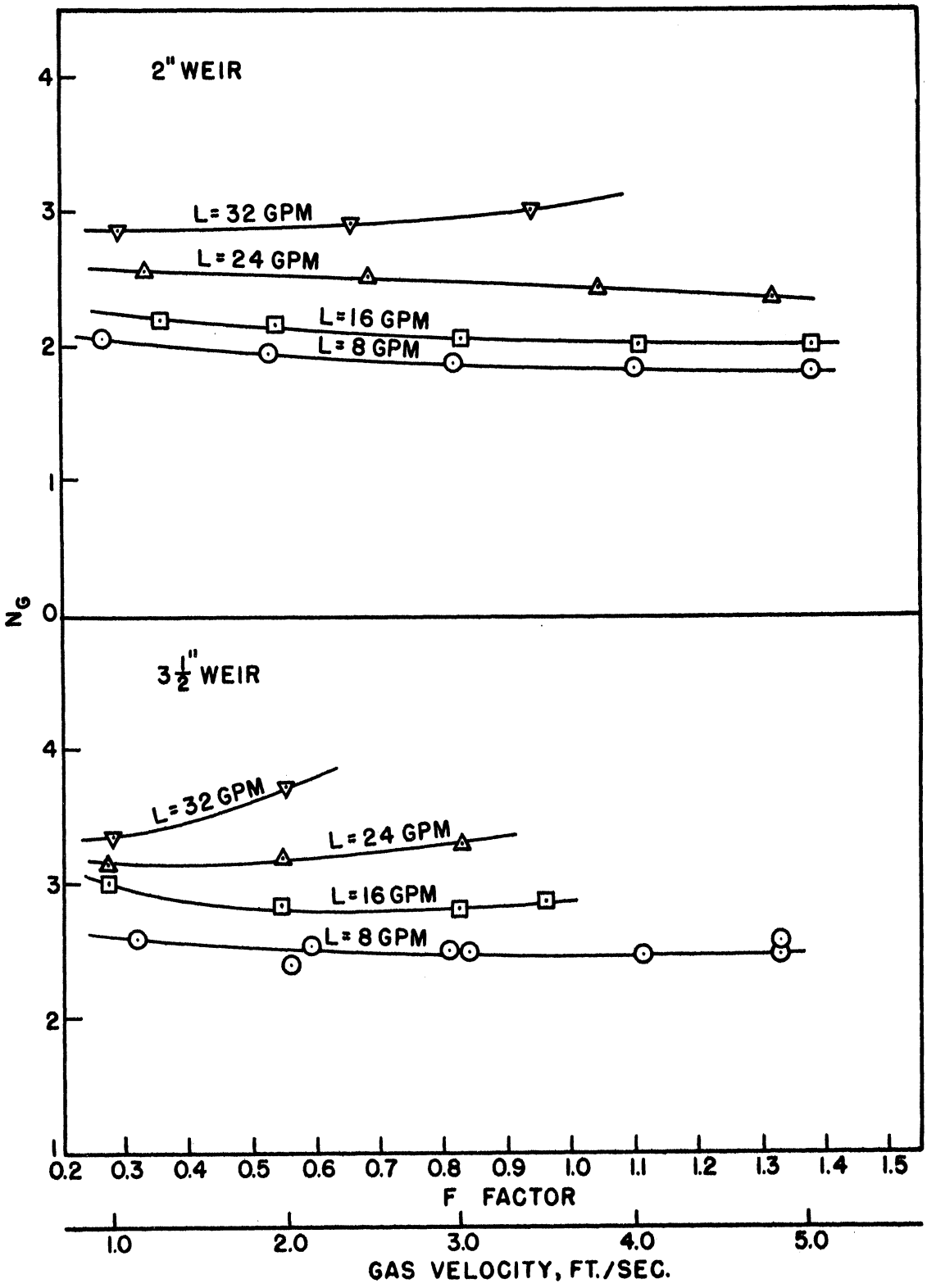

Figure 39. Values of N_G for Ammonia Absorption with Valve Tray

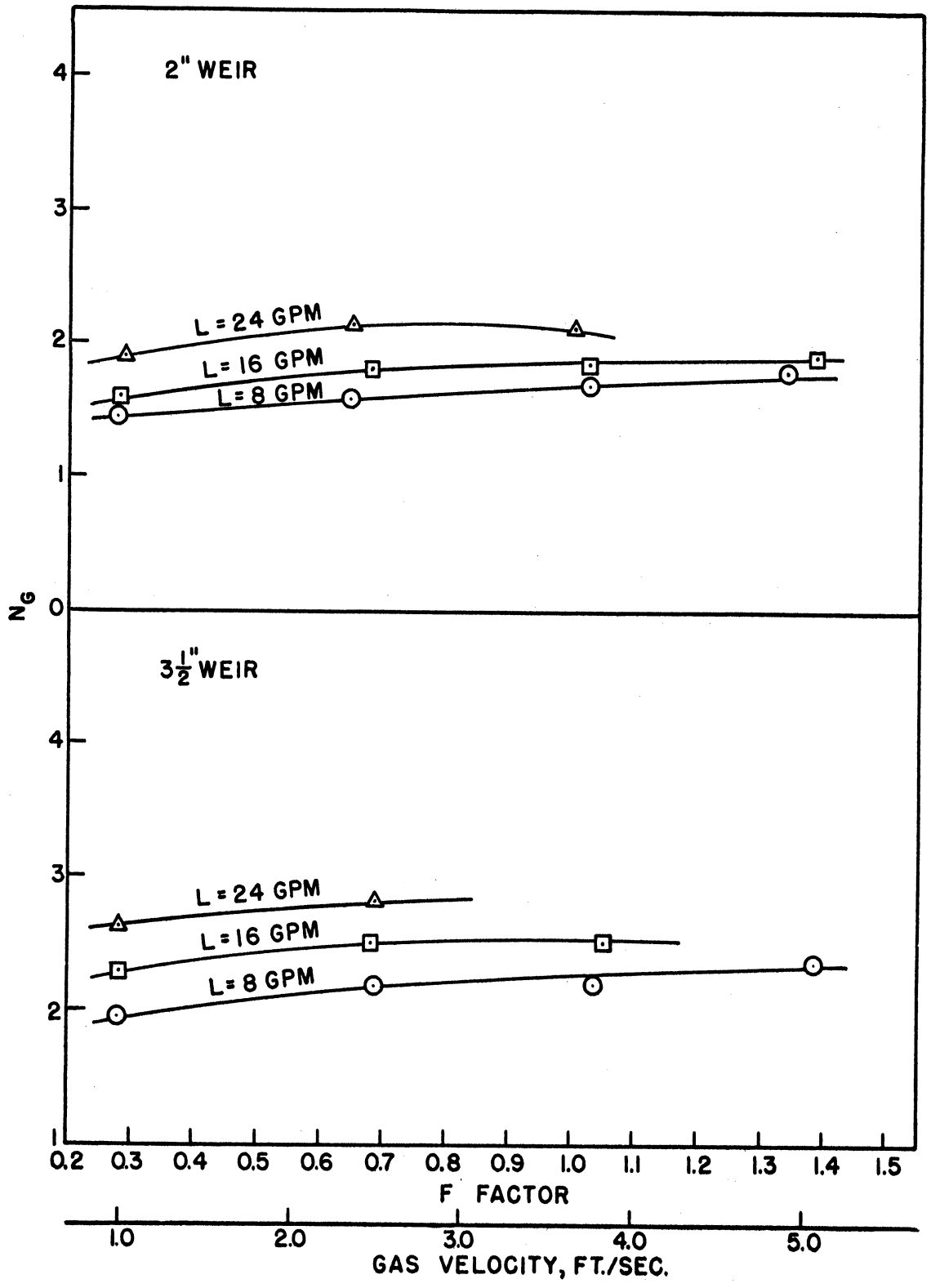

Figure 40. Values of N_G for Ammonia Absorption with Perforated Tray

contain the variables gas holdup and gas velocity. This same reasoning was used by Gerster[4] and Begley[11]. In working with the data, the author found that the weir height also had a significant effect on N_G and might be included as a correlating variable. Accordingly, the form of the correlation chosen was

$$N_G = A(Z_f - Z_c)^b \, u^c \, Z_w^d \qquad (73)$$

This equation is identical in form to that used by Begley except for the addition of the weir height.

The actual correlation was done on the IBM 650 digital computer using the multiple regression program developed by Norman.[47] The program was so written so that the correlation coefficients could be obtained for order n, the number of independent variables, or for lesser orders 1, 2, ..., (n-1). This permitted the correlation of the data either with or without using weir height as a variable. The first part of the program computed the regression coefficients for a least square fit to a linear equation, and accordingly the data input was in logarithmic form. The standard deviation of the dependent variable, $\ell n \, N_G$ in this case, was also obtained. The second part of the program read the correlation coefficients and the data, predicted values of the dependent variable, and computed the deviation of the experimental value from the predicted value.

The results obtained are summarized in Table X. It can be seen from the table that the use of weir height as an independent variable improves the correlation. With the absorption data, the average deviation is only about one-half as large as when weir height is not used. With the humidification data, the improvement is not as noticeable, but

TABLE X

SUMMARY OF CORRELATIONS FOR N_G

$$N_G = A(Z_f - Z_c)^b \, u^c \, Z_w^d$$

Tray Type	A	b	c	d	Average Absolute Deviation	Maximum Absolute Deviation
		Humidification: Air-Water System				
Valve	5.84	0.475	-0.381	0.183	6.1%	20.4%
Valve	8.73	0.656	-0.478	--	8.1%	24.1%
		Absorption: Ammonia-Air-Water System				
Valve	4.97	0.621	-0.458	0.287	4.0%	10.9%
Perforated	3.72	0.650	-0.459	0.407	3.9%	22.0%
Valve	7.76	0.729	-0.545	--	7.5%	19.3%
Perforated	8.48	0.916	-0.689	--	10.0%	38.6%

where

N_G = Gas phase transfer units, dimensionless

$Z_f - Z_c$ = Gas holdup, feet

u = Gas velocity, feet/second

Z_w = Weir height, inches

this may be partially due to the fact that only about one-third of the data were taken at the 3-1/2-inch weir height and, then, only at a single liquid rate. The absorption runs were divided about evenly between the 2-inch and 3-1/2-inch weir heights.

Figures 41, 42, and 43 show the comparison between the experimental values of N_G and the values calculated using the correlations. It can be seen that the agreement between the values is quite good with only a few data points having a deviation greater than 10 per cent. In Figures 44, 45, and 46, the data is plotted to show the effect of gas velocity on the correlation.

Table X shows that the coefficients in the correlation for N_G using the valve tray for humidification, differ slightly from those for ammonia absorption. It might be expected that the coefficients would be the same for both systems as the transport properties are similar. However, the gas diffusivity for air-water is about 10 per cent higher than for air-ammonia at 25°C.[51] In addition, the gas stream in the humidification runs was heated to maintain adiabatic conditions, and therefore the average gas temperature was higher than for the absorption runs. The gas diffusivity would also be higher. The exponents on gas holdup and gas velocity in the correlations are partly self-compensating, i.e., the exponents for ammonia absorption are both larger than for humidification, but the exponent on gas velocity is negative. Thus, the fact that the constant A is larger for humidification than for absorption can be explained by the difference in gas diffusivity. This has been shown also by Begley[11] who used gas diffusivity to correlate the values of A obtained from a large number of systems.

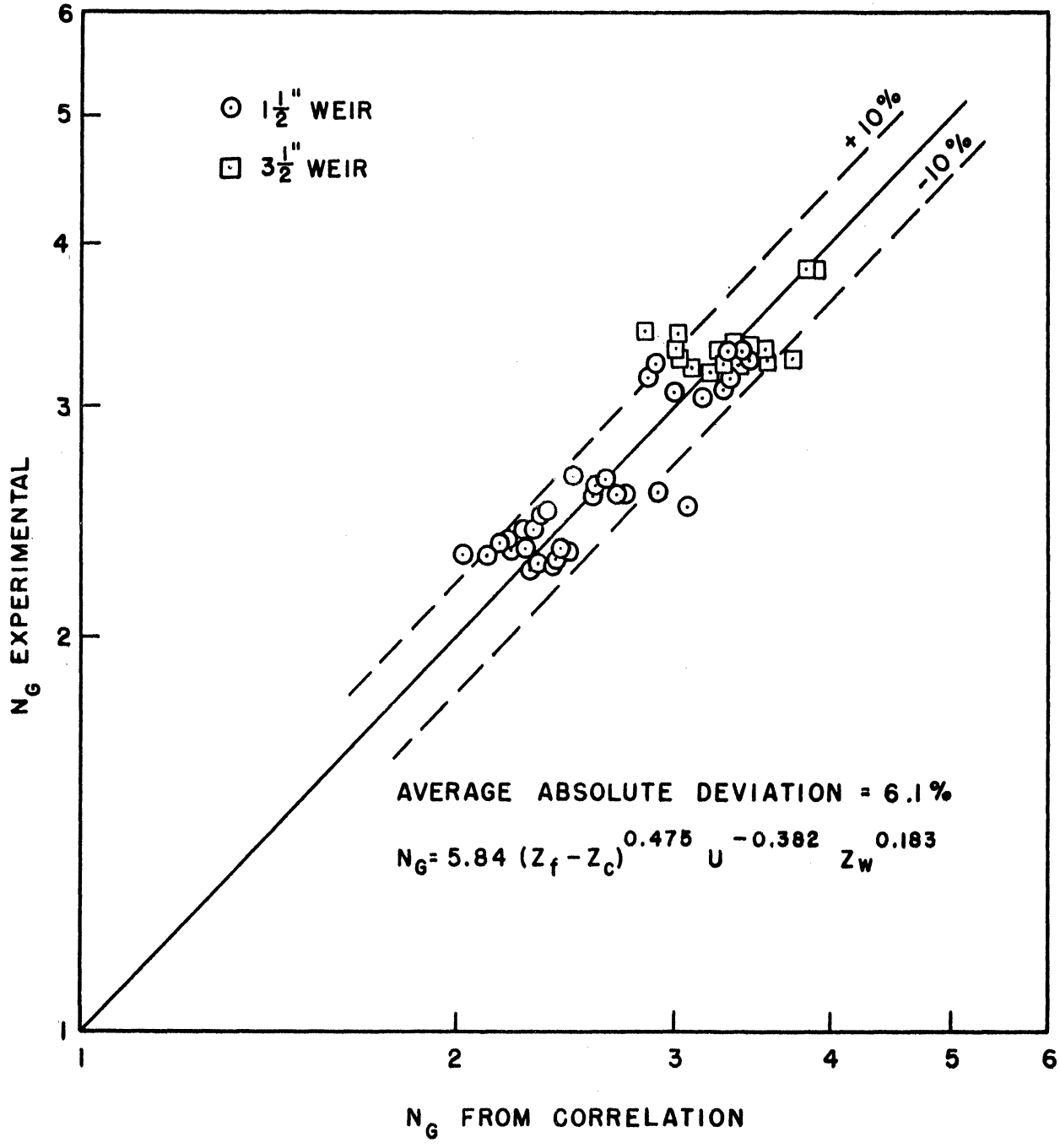

Figure 41. Comparison of Experimental and Predicted Values of N_G for Humidification of Air with Value Tray

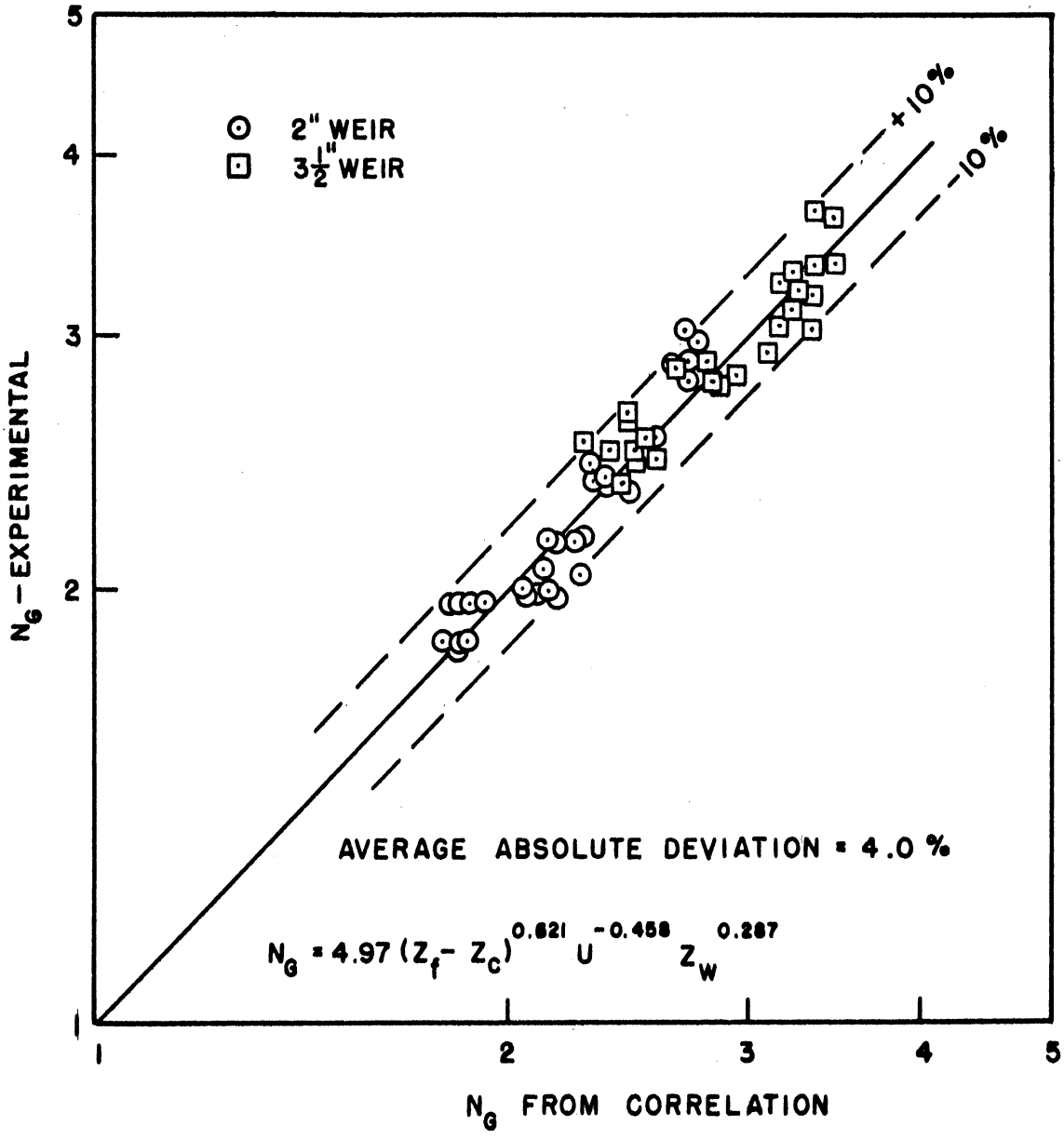

Figure 42. Comparison of Experimental and Predicted Values of N_G for Ammonia Absorption with Valve Tray

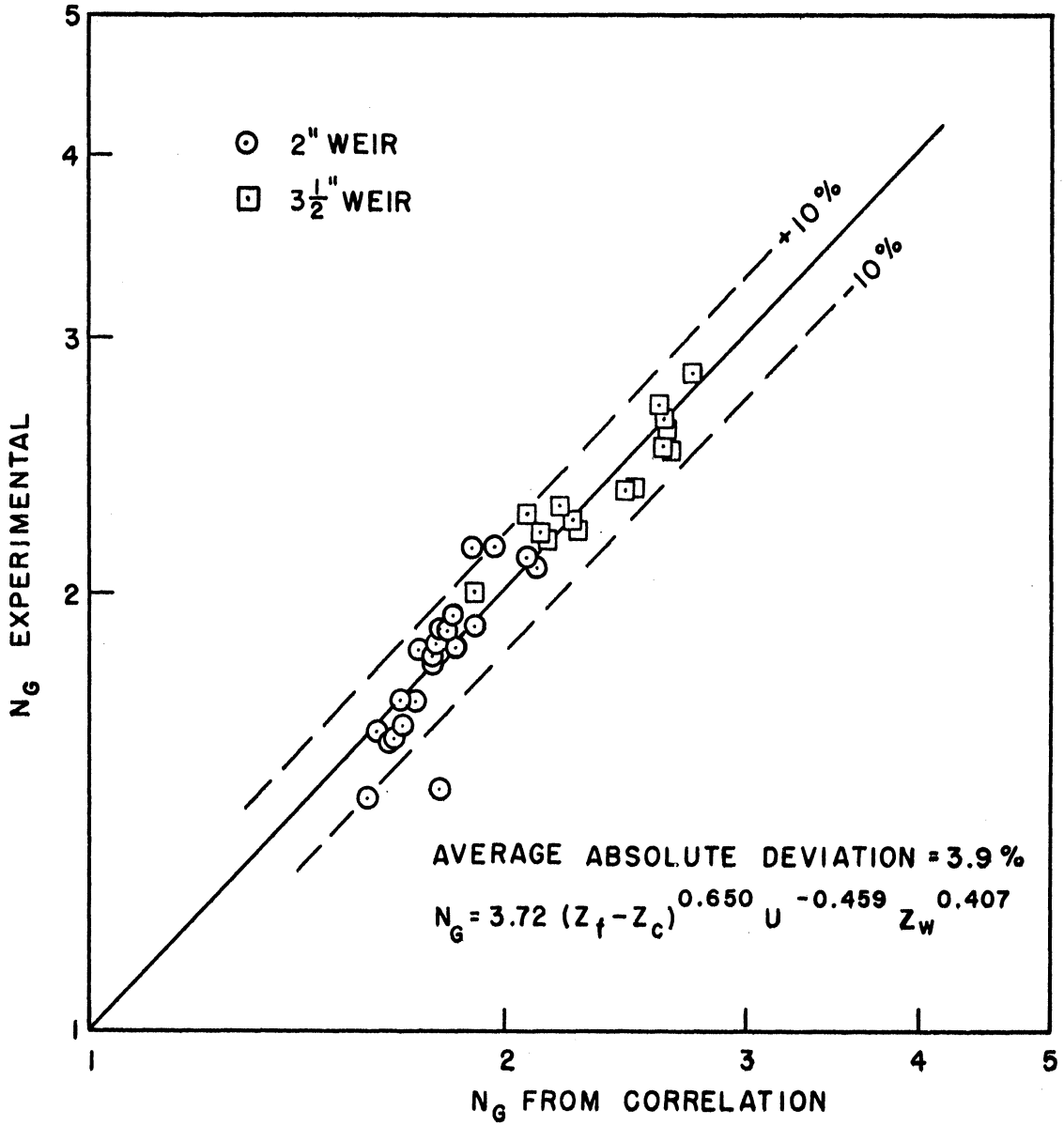

Figure 43. Comparison of Experimental and Predicted Values of N_G for Ammonia Absorption with Perforated Tray

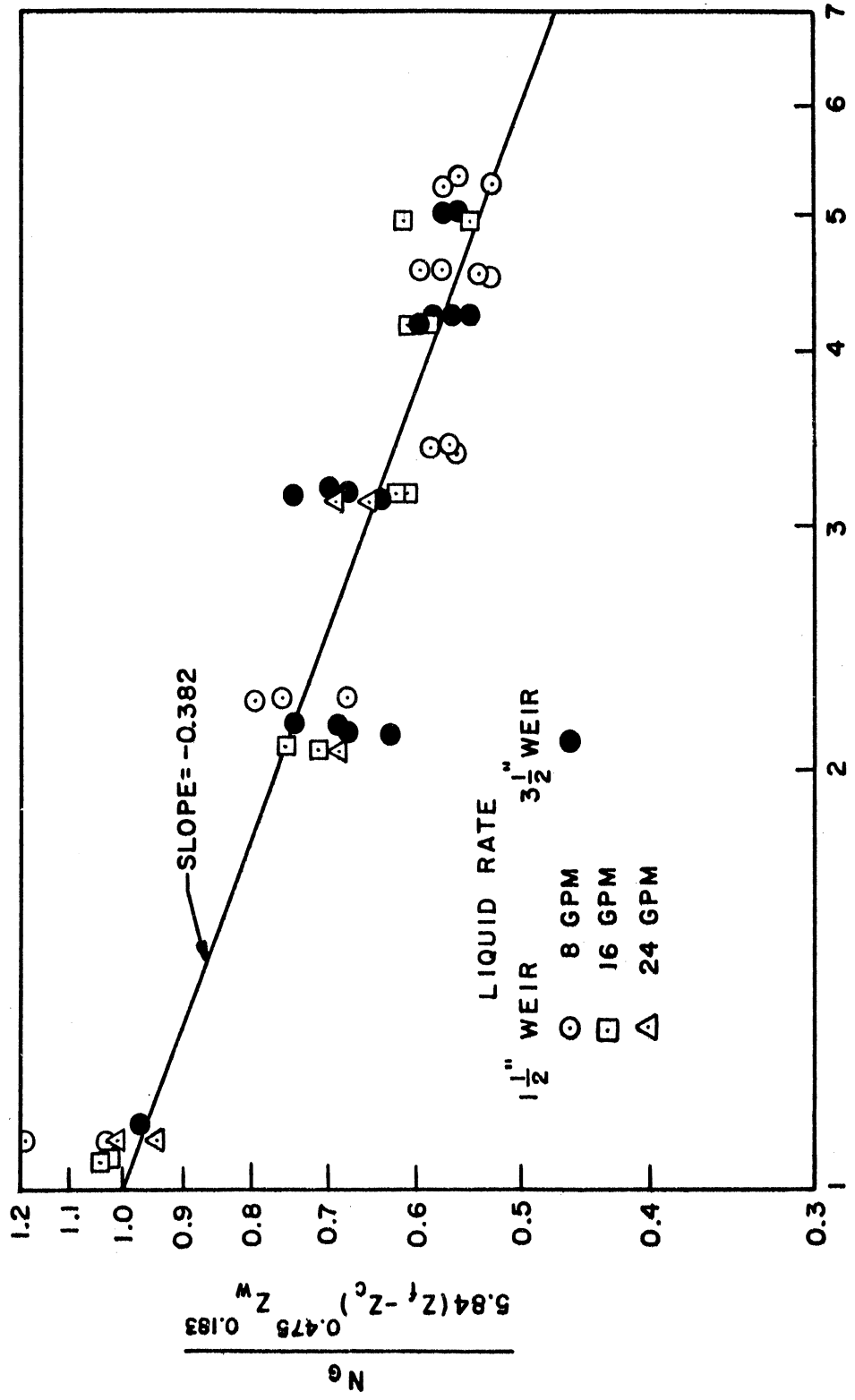

Figure 44. Effect of Gas Velocity on Correlation of N_G for Humidification with Valve Tray

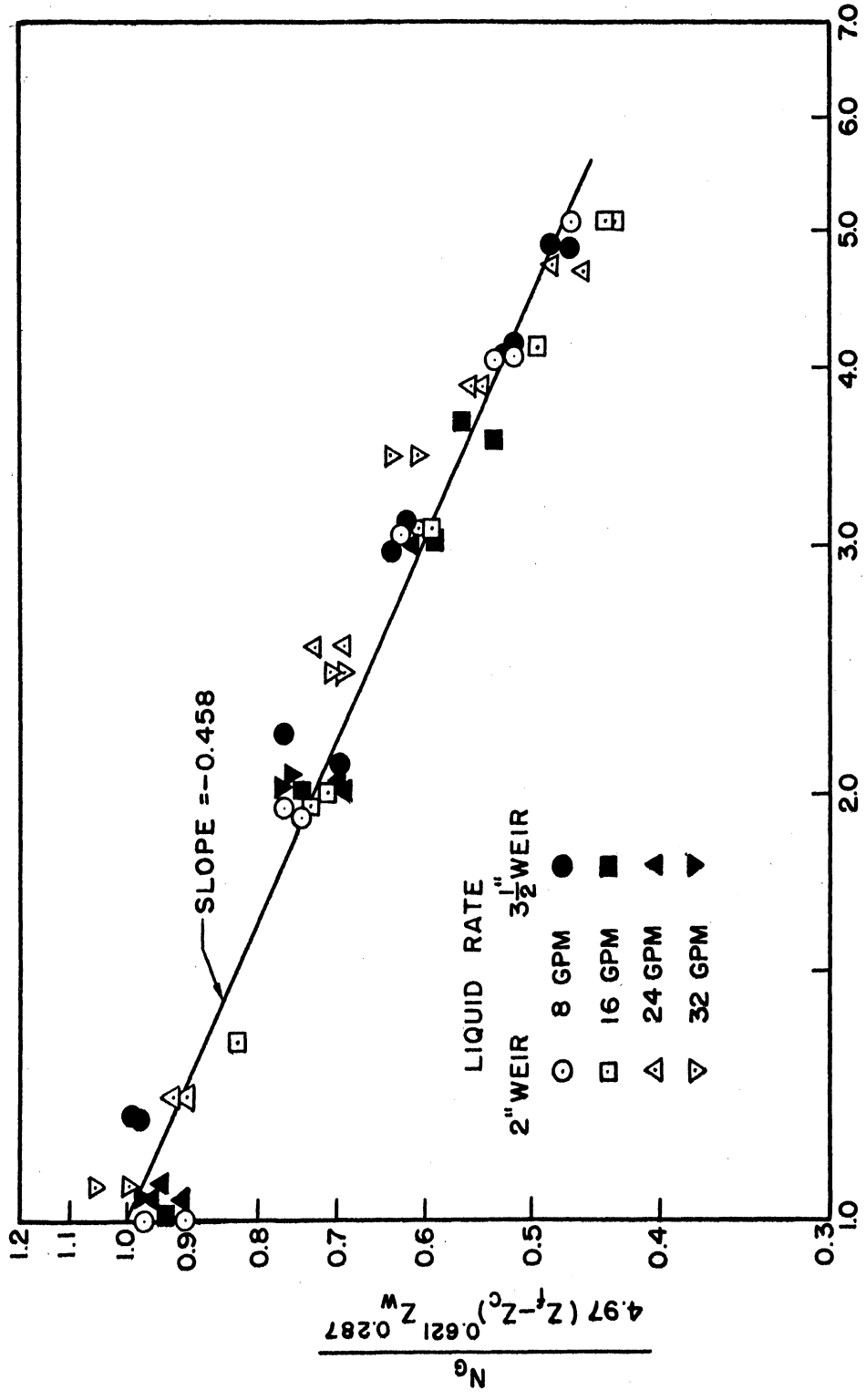

Figure 45. Effect of Gas Velocity on Correlation of N_G for Ammonia Absorption with Valve Tray

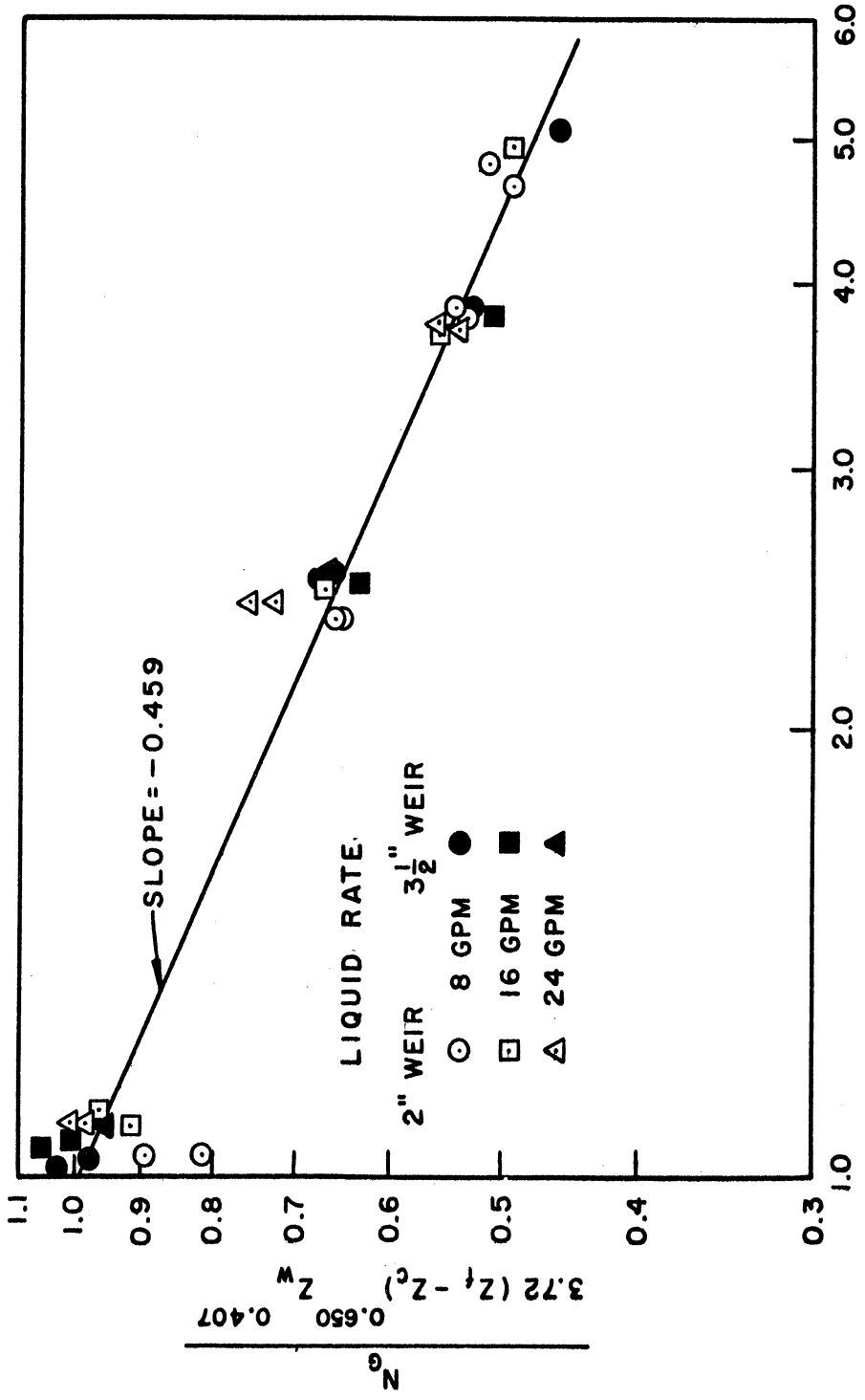

Figure 46. Effect of Gas Velocity on Correlation of N_G for Ammonia Absorption with Perforated Tray

Comparison with Results of Previous Investigators

The data that can be most readily compared with that obtained in the present investigation is that of Warzel[66] and Ashby[9] who, using bubble cap trays, studied ammonia absorption and humidification in the same column used by the author.

Begley[11] used the above data in addition to his own to obtain the correlation previously given. He correlated N_G in terms of gas holdup and gas velocity for each system, and then related the value of the coefficients to the physical properties of the systems.

Figures 47 and 48 show the comparison between the author's data and Begley's correlation of Warzel's ammonia absorption and desorption data. The correlation was obtained by a least square fit of the data in a manner similar to that used by the author. The correlation fits the valve tray data fairly well for the data taken at a weir height of 3-1/2 inches, but gives values of N_G about 10 per cent high for the 2-inch weir data. The perforated tray data do not agree too well with the bubble cap correlation. The latter predicts values of N_G about 10 per cent too high for the 3-1/2-inch weir data and about 30 per cent too high for the 2-inch weir data.

Figure 49 shows the comparison between the author's humidification data and Begley's correlation of Ashby's data. As with the ammonia data, the comparison of the 3-1/2-inch weir data is not bad, but the 1-1/2-inch weir data fall about 15 per cent below the values predicted by the bubble cap correlation.

As the deviation is almost constant for a given weir height, there arises the possibility of using a correction factor to relate

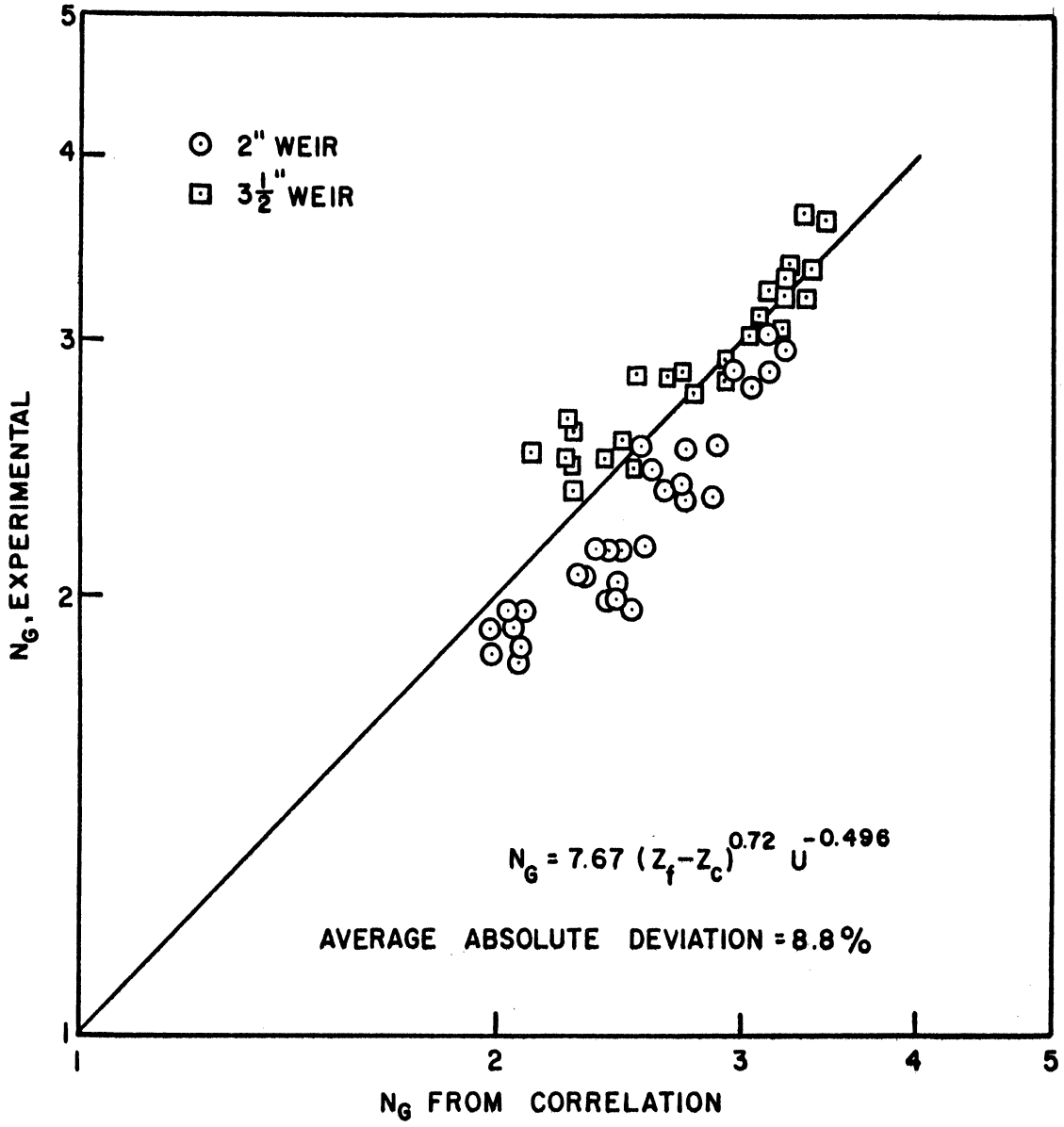

Figure 47. Comparison of Ammonia Absorption Data with Valve Tray with Correlation for Bubble Cap Tray

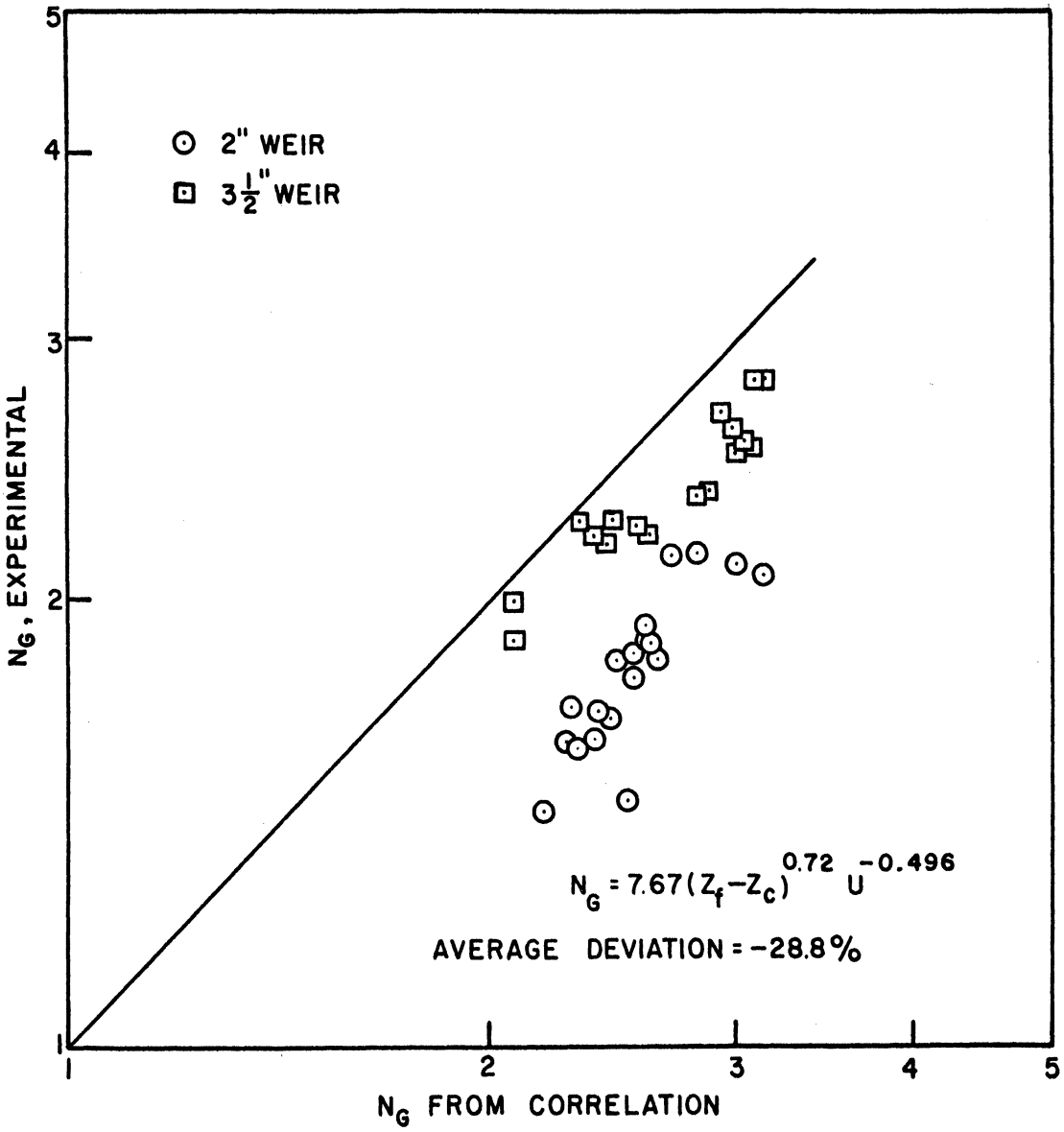

Figure 48. Comparison of Ammonia Absorption Data with Perforated Tray with Correlation for Bubble Cap Tray

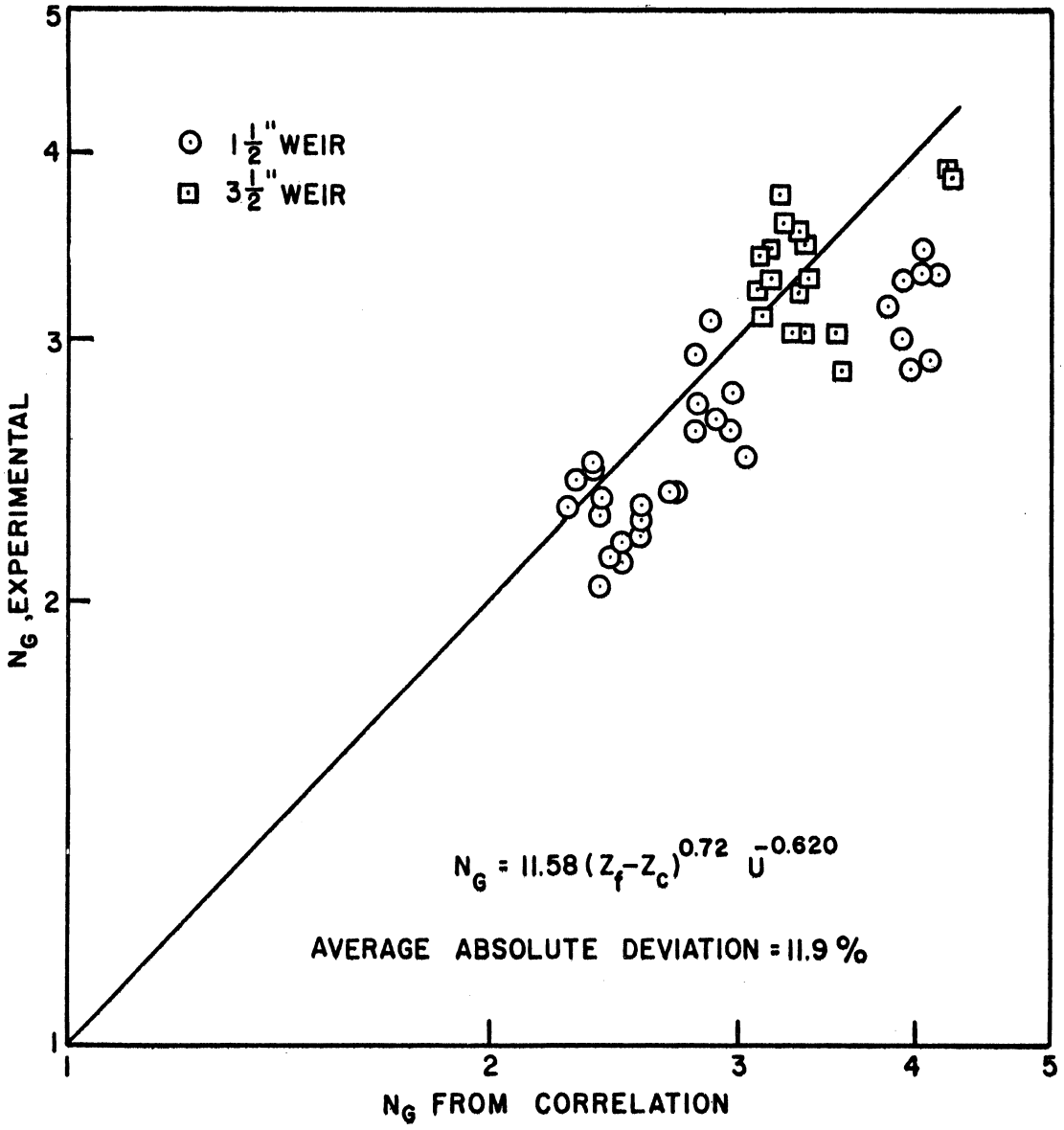

Figure 49. Comparison of Humidification Data with Valve Tray with Correlation for Bubble Cap Tray

the performance of other trays to that of bubble caps. The correction factor would be a function of the design and possibly other variables such as weir height, although the latter might be accounted for in the correlation of bubble cap data. Based on the author's data and Begley's correlations, typical correction factors are listed in Table XI.

TABLE XI

FACTORS TO RELATE PERFORMANCE OF VARIOUS TRAYS

Tray Design	Weir Height	Multiplication Factor to be Applied to N_G's for Bubble Cap Trays
Valve	3-1/2	1.0
	2	0.9
	1-1/2	0.85
Perforated (7/8" holes)	3-1/2	0.9
	2	0.7

The correction factor admittedly is a simplification of the situation and does not preclude the correlation of performance data from the various types of trays. However, it does give a method of estimating the performance of a particular tray design if some data is available.

Figure 50 shows the comparison of the data obtained by West et al.[67], with the correlations for humidification with valve and bubble cap trays. The data were obtained with a 3-1/4 x 3-9/16-inch tray containing eighty-three 1/8-inch perforations spaced on 3/8-inch equilateral triangular centers. The active tray area was 0.077 square foot

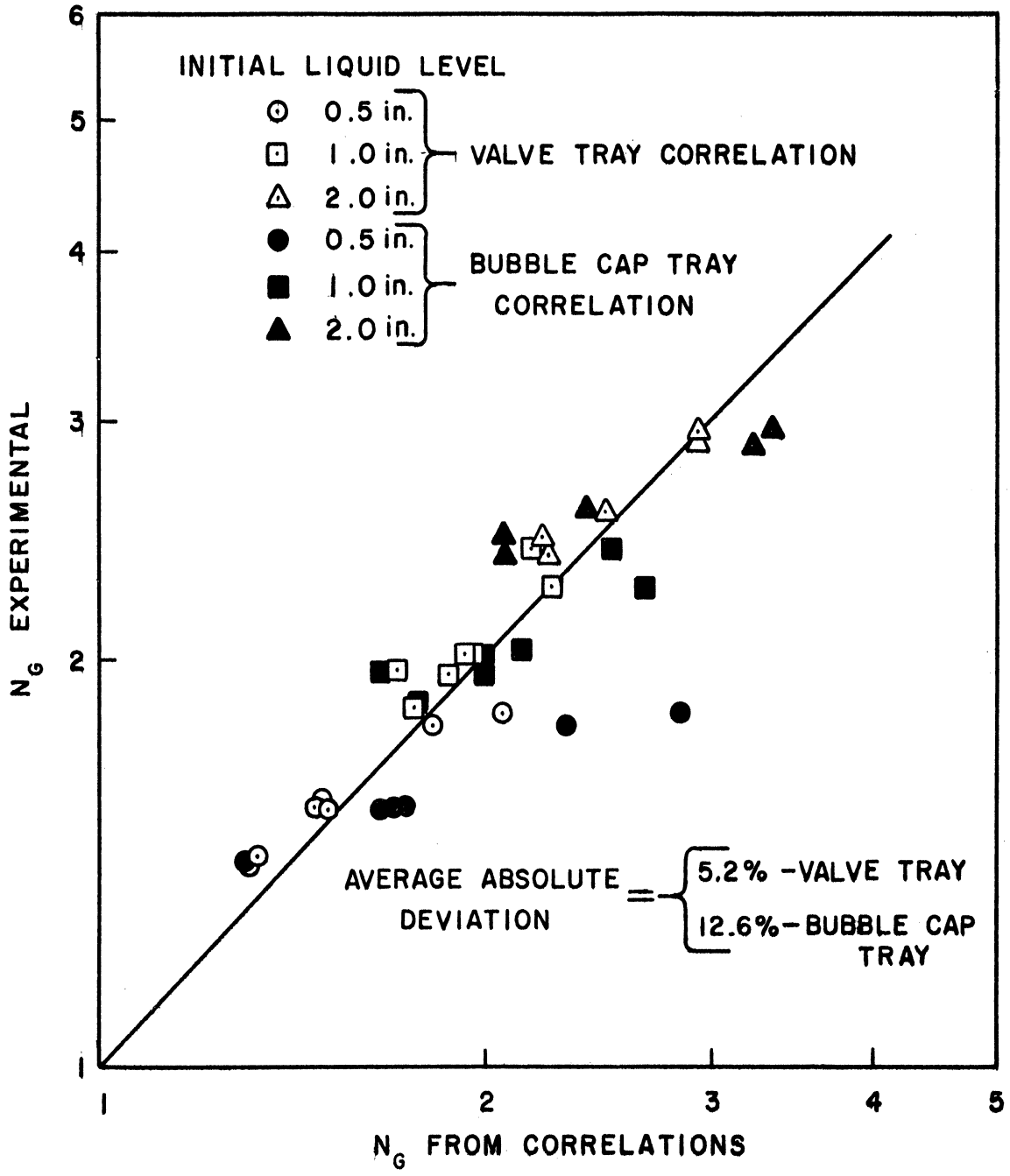

Figure 50. Comparison of Humidification Data of West, Gilbert, and Shimizu[67] with Correlations for Valve Trays and Bubble Cap Trays

and the free area was 9.2 per cent. Their data show better agreement with the valve tray correlation than with the bubble cap correlation. It is suspected that the use of weir height as a correlating variable may be a prime reason for the closer agreement.

Figure 51 shows the comparison of the data of Gerster et al.[1], with the valve tray correlation for ammonia absorption. The data were taken in a 24-inch diameter column containing forty-one 1-1/2-inch bubble caps on 2-1/2-inch square spacing. The bubble cap design is the same as that used by Warzel[66], Ashby[9], and Begley[11]. The data agree fairly well with the correlation at the lower weir heights, but at the higher weir heights the correlation predicts values of N_G 10 to 20 per cent higher than those obtained experimentally. The deviations at the higher weir heights might be expected as a 3-1/2-inch weir was the highest used by the author.

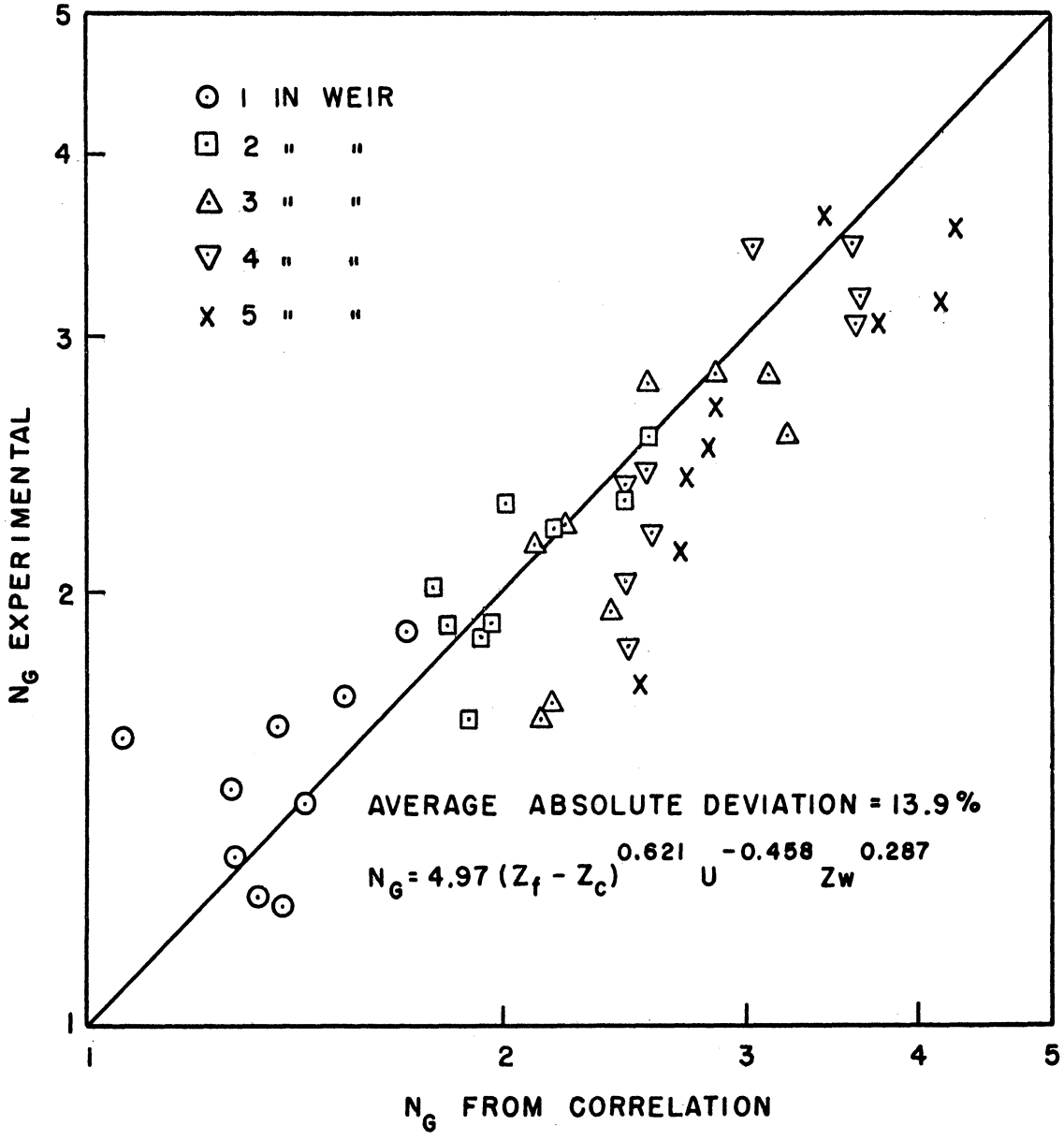

Figure 51. Comparison of Ammonia Absorption Data of Gerster et al.[1] with Correlation for Valve Tray

CONCLUSIONS

The following conclusions can be drawn with regard to the performance of valve and perforated trays in humidification and ammonia absorption.

1. The Murphree vapor efficiency increases with an increase of weir height and an increase of liquid rate.

2. At a weir height of 3-1/2 inches, the Murphree vapor efficiency for a given liquid rate is almost independent of vapor rate if the tray is in the stable operating range.

3. At weir heights of 1-1/2 and 2 inches, the Murphree vapor efficiency decreases as vapor rate is first increased. As the vapor rate is further increased, the efficiency remains constant or increases slightly.

4. The number of individual gas phase transfer units can be correlated by the following equations

Humidification, Valve Tray

$$N_G = 5.84(Z_f-Z_c)^{0.475}\ u^{-0.382}\ Z_w^{0.183} \qquad (74)$$

Ammonia Absorption, Valve Tray

$$N_G = 4.97(Z_f-Z_c)^{0.621}\ u^{-0.458}\ Z_w^{0.287} \qquad (75)$$

Ammonia Absorption, Perforated Tray

$$N_G = 3.72(Z_f-Z_c)^{0.650}\ u^{-0.459}\ Z_w^{0.407} \qquad (76)$$

5. The inclusion of weir height as an independent variable improves the correlation over that obtained using the same form but omitting weir height.

6. Operation of a perforated tray in the region when the amount of liquid weepage is considerable results in lower efficiencies than obtained when operating in the stable region.

7. Performance of the valve and perforated trays can be estimated from present correlations for bubble cap trays. The estimation can be improved by application of a correction factor that is a function of the tray design and the weir height.

8. The weeping limit of the perforated tray is dependent primarily on the vapor velocity through the holes, and the latter values are in the range of 30 - 40 ft/sec. These values have been reported previously for smaller holes, so the weeping limit appears to be essentially independent of hole diameter.

9. Liquid mixing with the perforated tray is greater than with the valve tray, but for either tray is not as large as produced by bubble cap trays.

10. The entrainment produced by the perforated tray is greater than that from the valve tray. This occurs because the vapor rising from the perforated tray has a much larger vertical velocity component than is present on the valve tray.

APPENDIX A

ORIGINAL AND CALCULATED DATA

TABLE XII

HUMIDIFICATION OF AIR WITH WATER USING VALVE TRAY WITH 1-1/2-INCH WEIR

RUN NUMBER	1	2	3	4	5	6	7	8	9	10	11	12	13	14
WATER RATE														
Gallons per minute	8.0	8.0	8.0	8.0	8.0	8.0	8.0	8.0	8.0	8.0	8.0	8.0	8.0	8.0
Lb moles per minute	3.70	3.70	3.70	3.70	3.70	3.70	3.70	3.70	3.70	3.70	3.70	3.70	3.70	3.70
Temperature °F, Tray Inlet	90.50	90.23	91.58	90.03	89.80	89.96	88.99	89.28	90.14	89.98	88.99	88.86	90.01	89.98
Temperature °F, Tray Outlet	90.50	90.07	91.38	90.18	89.80	89.92	89.58	89.73	90.64	90.50	89.44	89.33	90.50	90.52
VAPOR FLOW THROUGH TRAY (Avg. Conditions)														
Lb moles per minute x 10^2	19.49	19.63	19.67	29.43	29.78	29.78	40.31	40.31	40.01	40.00	46.32	46.32	46.14	46.16
Velocity, ft per sec.	2.25	2.26	2.26	3.34	3.43	3.42	4.58	4.58	4.53	4.53	5.28	5.29	5.35	5.35
F Factor, $u\rho_G^{1/2}$	0.58	0.59	0.59	0.87	0.89	0.89	1.20	1.20	1.18	1.18	1.38	1.38	1.38	1.38
EQUILIBRIUM CONDITIONS ON TRAY														
Liquid Temperature, °F	90.50	90.15	91.48	90.11	89.80	89.94	89.29	89.50	90.39	90.24	89.22	89.10	90.26	90.25
Pressure, in Hg	30.22	30.45	30.50	30.63	30.90	30.90	31.51	31.51	31.61	31.61	31.26	31.16	30.90	30.91
Vapor Pressure, in Hg	1.4441	1.4215	1.4853	1.4260	1.4127	1.4189	1.3903	1.3991	1.4391	1.4333	1.3881	1.3819	1.4342	1.4333
VAPOR COMPOSITION, MOLE PER CENT														
y_o	1.995	1.343	1.325	2.499	1.198	1.112	1.024	1.016	1.230	1.195	1.052	1.015	1.196	1.184
y_1	4.476	4.324	4.449	4.376	4.168	4.202	4.073	4.137	4.210	4.203	4.097	4.147	4.332	4.339
y_1^*	4.779	4.639	4.870	4.656	4.572	4.592	4.412	4.440	4.553	4.534	4.440	4.435	4.641	4.637
MURPHREE VAPOR EFFICIENCY, PER CENT	89.1	90.4	88.1	87.0	88.0	88.8	90.0	91.1	89.7	90.1	89.9	91.6	91.0	91.4
N_G	2.22	2.35	2.13	2.04	2.12	2.19	2.30	2.42	2.27	2.31	2.29	2.48	2.41	2.45
$k_G'a$, sec^{-1}	20.19	23.36	20.66	21.38	21.57	22.08	27.17	27.43	22.87	23.12	25.66	28.32	28.38	27.71
HYDRAULIC DATA														
Pressure drop, in water	2.50	2.40	2.40	3.25	3.30	3.30	5.07	5.00	4.90	4.75	6.00	6.00	6.06	5.80
Froth height, in	4.6	4.4	4.5	5.5	5.5	5.5	6.1	6.3	6.7	6.8	7.1	7.0	6.8	7.1
Clear liquid height, in														
Position B	1.90	1.95	1.95	2.00	2.00	2.00	2.00	2.05	2.00	2.05	2.00	2.00	1.95	1.90
C	1.60	1.65	1.65	1.70	1.35	1.25	1.35	1.30	1.10	1.10	1.40	1.40	1.20	1.45
D	1.65	1.70	1.75	1.65	1.55	1.60	1.55	1.60	1.50	1.65	1.50	1.50	1.50	1.40
E	1.80	1.90	1.90	1.90	1.90	1.95	1.95	1.95	1.90	1.95	1.90	1.90	1.85	1.75
Gas contact time, sec.	0.110	0.101	0.103	0.096	0.0984	0.0992	0.0847	0.0883	0.0993	0.0999	0.0892	0.0874	0.0849	0.0884

TABLE XII (CONT'D)

RUN NUMBER	15	16	17	18	19	20	21	22	23	24	25	26	27	28	29	30	31	32
WATER RATE																		
Gallons per minute	8.0	8 0	16.0	16.0	16.0	16.0	16.0	16.0	16.0	16.0	16.0	16.0	24.0	24.0	24.0	24.0	24.0	24.0
Lb moles per minute	3.70	3.70	7.40	7.40	7.40	7.40	7.40	7.40	7.40	7.40	7.40	7.40	11.10	11.10	11.10	11.10	11.10	11.10
Temperature °F, Tray Inlet	86.00	86.00	77.00	77.14	76.98	76.91	76.91	76.87	77.14	77.14	77.23	77.52	77.00	77.00	77.18	77.36	77.04	76 91
Temperature °F, Tray Outlet	86.18	86.23	77.13	77.25	77.02	77.00	76.98	76.93	77.18	77.12	77.36	77.59	77.14	77.09	77.31	77.54	77.11	77 18
VAPOR FLOW THROUGH TRAY (Avg. Conditions)																		
Lb moles per minute x 10^2	9.80	9.78	9.81	9.81	19.70	19.68	29.69	29.68	39.93	39.89	47.52	47.53	19.56	19.56	29.75	29.75	9 96	9 96
Velocity, ft per sec.	1.09	1.09	1.05	1.05	2.09	2.08	3.17	3.17	4.19	4.19	4.97	4.97	2.06	2.06	3.11	3 11	1.08	1 08
F Factor, $u\rho_G^{1/2}$	0.29	0.29	0.28	0.28	0.56	0.56	0.85	0.85	1.14	1.14	1.35	1.35	0.56	0.56	0 85	0 85	0.29	0.29
EQUILIBRIUM CONDITIONS ON TRAY																		
Liquid Temperature, °F	86.09	86.12	77.07	77.20	77.00	76.96	76.95	76.90	77.16	77.13	77.29	77.56	77 07	77.05	77 24	77.45	77.07	77.04
Pressure, in Hg	31.07	31.07	31.41	31.41	31.63	31.62	31.39	31.39	31.81	31.77	32.24	32.24	31 96	31.96	32.13	32.13	30.46	30.46
Vapor Pressure, in Hg	1.2563	1.2571	0.9374	0.9409	0 9532	0.9340	0.9337	0 9318	0.9402	0.9387	0.9443	0.9528	0.9374	0.9368	0.9421	0.9493	0.9365	0.9337
VAPOR COMPOSITION, MOLE PER CENT																		
y_o	2.050	2.056	1.156	1.161	1.258	1.308	0.958	0.951	0.868	0.867	0.756	0.758	1.014	1.012	0.963	0.958	1.750	1.682
y_1	3.953	3.920	2.908	2.927	2.831	2.818	2.783	2.778	2.815	2.799	2.775	2.838	2.824	2.826	2.860	2.892	3.009	3.016
y_1^*	4.043	4.046	2.984	2.996	2.957	2.954	2.975	2.968	2.956	2.955	2.929	2.955	2.933	2.931	2.932	2.955	3.076	3.065
MURPHREE VAPOR EFFICIENCY, PER CENT	95.5	93 7	95.8	96.3	92.6	91.7	90.5	90.6	93.3	92.6	92.9	94.6	94.3	94.5	96.3	96.8	95.0	96.4
N_G	3.10	2.76	3.17	3.29	2.60	2.49	2.36	2.36	2.70	2.60	2.65	2.93	2.87	2.90	3.31	3.46	3.00	3.33
$k'_G a$, sec^{-1}	21.68	18.33	14.81	14.83	19.03	17.70	20.95	20.74	23.51	22.73	22.62	26.26	13.96	13.58	16.05	17.28	13.69	14.51
HYDRAULIC DATA																		
Pressure drop, in water	2.23	2.23	2.66	2.66	2.84	2.85	3.75	3.93	5.35	5.52	6.93	7.05	3.84	3.70	6.35	6.60	3.20	3 17
Froth height, in	3.8	3.9	5.0	5.1	5.5	5.6	6.4	6.5	8.2	8.1	9.3	8.9	7.9	8.1	11.0	10.8	5.5	5.6
Clear liquid height, in																		
Position B	1.95	1.95	2.40	2.40	2.50	2.50	2.70	2.70	3.10	3.00	2.95	2.90	3 30	3.30	4.00	4.00	2.90	2.90
C	1.90	1.90	2.25	2.25	1.95	1.95	2.00	2.05	2.35	2.30	2.35	2.30	2.75	2.75	3.20	3.25	2.55	2.55
D	1.95	1.95	2.35	2.35	2.20	2.20	2.25	2.30	2.50	2.40	2.30	2.20	2.90	2.90	3.40	3.40	2.75	2.70
E	2 10	2.05	2.45	2.45	2.35	2.35	2.50	2.55	2.80	2.70	2.60	2.55	3.10	3.10	3.70	3.70	2.80	2 80
Gas contact time, sec.	0.143	0.150	0.214	0.222	0.138	0.141	0.112	0.114	0.115	0.114	0.117	0.112	0.206	0.214	0.206	0.200	0.219	0.229

TABLE XIII

HUMIDIFICATION OF AIR WITH WATER USING VALVE TRAY WITH 3 1/2 INCH WEIR

RUN NUMBER	33	34	35	36	37	38	39	40	41	42	43	44	45	46	47	48	49
WATER RATE																	
Gallons per minute	8.0	8.0	8.0	8.0	8.0	8.0	8.0	8.0	8.0	8.0	8.0	8.0	8.0	8.0	8.0	8.0	8.0
Lb moles per minute	3.70	3.70	3.70	3.70	3.70	3.70	3.70	3.70	3.70	3.70	3.70	3.70	3.70	3.70	3.70	3.70	3.70
Temperature °F, Tray Inlet	75.96	75.81	77.11	77.02	75.29	75.34	77.14	76.82	75.20	76.84	76.78	76.98	77.09	75.38	75.25	74.98	75.06
Temperature °F, Tray Outlet	76.14	76.05	77.34	77.14	75.56	75.56	77.38	77.04	75.38	77.00	76.98	77.03	77.18	75.60	75.49	75.22	75.34
VAPOR FLOW THROUGH TRAY (Avg. conditions)																	
Lb moles per minute x 10^2	10.34	10.34	19.86	19.86	19.96	19.94	29.10	29.08	29.35	29.67	29.56	39.46	39.43	39.79	39.78	49.43	49.42
Velocity, ft per sec.	1.12	1.12	2.12	2.12	2.16	2.15	3.18	3.17	3.20	3.16	3.15	4.24	4.24	4.18	4.18	5.01	5.02
F Factor, $up_G^{1/2}$	0.30	0.30	0.57	0.57	0.58	0.58	0.85	0.85	0.85	0.85	0.85	1.14	1.14	1.14	1.14	1.39	1.39
EQUILIBRIUM CONDITIONS ON TRAY																	
Liquid Temperature, °F	76.05	75.93	77.22	77.08	75.42	75.45	77.26	76.93	74.29	76.92	76.88	77.02	77.13	75.49	75.38	75.10	75.20
Pressure, in Hg	31.18	31.20	31.72	31.72	31.21	31.21	30.65	30.65	30.94	31.61	31.61	31.37	31.36	32.00	32.00	33.09	33.07
Vapor pressure, in Hg	0.9061	0.9028	0.9421	0.9374	0.8874	0.8883	0.9424	0.9331	0.8836	0.9340	0.9312	0.9358	0.9393	0.8895	0.8862	0.8788	0.8809
VAPOR COMPOSITION, MOLE PER CENT																	
y_o	0.826	0.811	0.665	0.656	0.798	0.772	1.405	1.262	0.565	0.750	0.744	0.609	0.573	0.553	0.541	0.543	0.533
y_1	2.862	2.851	2.861	2.822	2.768	2.746	3.028	2.990	2.793	2.903	2.861	2.878	2.880	2.690	2.687	2.587	2.594
y_1^*	2.906	2.894	2.970	2.955	2.843	2.846	3.075	3.044	2.856	2.955	2.946	2.983	2.995	2.779	2.769	2.656	2.664
MURPHREE VAPOR EFFICIENCY, PER CENT	97.9	97.9	95.2	94.2	96.3	95.2	97.2	97.0	97.3	97.7	96.2	95.6	95.3	96.0	96.3	96.7	96.7
N_G	3.85	3.89	3.05	2.85	3.30	3.03	3.58	3.50	3.60	3.76	3.26	3.12	3.05	3.21	3.30	3.42	3.42
$k_G'a$, sec^{-1}	15.65	15.81	17.71	16.37	20.45	18.73	23.93	23.15	24.85	25.92	21.71	23.66	22.48	24.58	24.54	26.29	25.72
HYDRAULIC DATA																	
Pressure drop, in water	3.90	3.90	3.80	3.80	3.60	3.57	4.34	4.30	4.81	4.45	4.35	5.48	5.66	6.38	6.30	7.39	8.00
Froth height, in	6.5	6.5	7.1	7.1	6.8	6.8	8.2	8.3	8.1	8.1	8.3	9.3	9.5	9.5	9.7	10.6	10.7
Clear liquid height, in																	
Position B	3.40	3.40	3.10	3.10	3.10	3.05	3.00	3.00	3.10	3.15	3.15	3.15	3.15	3.55	3.55	3.25	3.15
C	3.20	3.20	2.75	2.70	2.65	2.60	2.60	2.65	2.65	2.65	2.70	2.70	2.70	3.15	3.10	2.95	2.85
D	3.20	3.20	2.70	2.65	2.60	2.65	2.40	2.45	2.45	2.55	2.55	2.50	2.50	2.75	2.80	2.60	2.55
E	3.35	3.35	3.10	3.05	3.05	3.00	3.00	3.00	3.00	3.05	3.05	3.10	3.10	3.35	3.35	3.10	3.10
Gas contact time, sec.	0.246	0.246	0.172	0.174	0.161	0.162	0.150	0.151	0.145	0.145	0.150	0.131	0.136	0.131	0.135	0.130	0.133

TABLE XIV

AMMONIA ABSORPTION FROM AIR BY WATER USING VALVE TRAY WITH 2-INCH WEIR

RUN NUMBER	129	130	131	132	133	134	135	136	137	138	139	140	141	142	143	144	145
WATER RATE																	
Gallons per minute	8.0	8.0	8.0	8.0	8.0	8.0	8.0	8.0	8.0	8.0	16.0	16.0	16.0	16.0	16.0	16.0	16.0
Lb moles per minute	3.70	3.70	3.70	3.70	3.70	3.70	3.70	3.70	3.70	3.70	7.40	7.40	7.40	7.40	7.40	7.40	7.40
Temperature °F, Tray Inlet	76.5	76.5	77.2	76.8	76.8	77.2	76.8	76.8	77.2	76.6	77.2	76.8	77.0	77.2	76.8	77.0	77.0
Temperature °F, Tray Outlet	78.2	77.9	79.9	79.5	79.5	79.9	79.0	79.2	78.4	77.9	78.6	78.4	78.3	78.6	78.1	78.4	78.6
AMMONIA FLOW																	
Lb moles per minute x 10^2	1.17	1.17	1.93	1.93	2.07	2.07	1.91	1.91	2.02	2.02	2.07	2.06	2.02	2.00	1.91	1.89	1.90
AIR FLOW																	
Temperature °F at blower suction																	
Dry bulb	81.0	81.0	90.0	90.0	87.5	87.5	85.2	85.2	82.0	82.0	87.5	87.5	84.0	84.0	80.1	80.1	83.1
Wet bulb	59.0	59.0	66.0	66.0	70.0	70.0	69.8	69.8	59.0	59.0	64.5	64.5	61.0	61.0	58.7	58.7	65.5
AIR-AMMONIA FLOW THROUGH TRAY (Avg. conditions)																	
Lb moles per minute x 10^2	9.65	9.64	19.54	19.52	28.97	28.69	38.94	38.82	49.77	49.40	49.02	49.09	39.15	39.07	29.41	29.53	19.39
Velocity, ft. per sec	0.99	0.99	1.95	1.93	3.07	3.04	4.08	4.07	5.04	5.00	5.05	5.05	4.12	4.11	3.05	3.06	2.00
F Factor, $u\rho_G^{1/2}$	0.27	0.27	0.54	0.53	0.82	0.81	1.10	1.10	1.39	1.38	1.38	1.38	1.11	1.11	0.83	0.83	0.54
EQUILIBRIUM CONDITIONS ON TRAY																	
Temperature, °F	78.2	77.9	79.9	79.5	79.5	79.9	79.0	79.2	78.4	77.9	78.6	78.4	78.3	78.6	78.1	78.4	78.6
Pressure, in Hg	30.92	30.92	32.03	32.20	30.17	30.15	30.45	30.43	31.43	31.43	30.96	30.96	30.26	30.26	30.73	30.73	30.97
Henry's Law Constant, In Hg/mole fraction	31.20	30.77	32.60	32.27	32.27	32.60	31.77	31.93	31.27	30.77	31.44	31.27	31.12	31.43	30.93	31.27	31.43
LIQUID COMPOSITION, MOLE FRACTION x 10^4																	
x_2	0	0	0	0	0	0	0	0	0	0	0	0	0	0	0	0	0
x_1	24.78	25.83	41.65	41.48	43.66	43.85	39.61	38.90	39.70	40.49	22.42	23.04	22.06	21.82	21.45	21.08	21.13
x_1^*	193.3	198.8	190.8	193.3	149.1	147.5	116.5	115.2	107.3	110.2	83.13	82.96	95.02	93.98	109.5	107.5	144.7
VAPOR COMPOSITION, MOLE FRACTION x 10^4																	
y_0	1200	1203	972.1	973.3	701.8	697.9	480.2	482.3	402.6	403.0	410.0	409.9	506.9	505.7	639.4	636.3	965.8
y_1	195.0	197.8	194.2	193.7	159.5	159.4	121.5	120.9	106.8	107.9	84.42	83.79	97.72	97.61	110.2	109.4	146.9
y_1^*	25.00	25.71	42.39	41.57	46.70	47.41	41.32	40.82	39.49	39.64	22.77	23.27	22.69	22.66	21.59	21.45	21.44
MURPHREE EFFICIENCY, PER CENT																	
Vapor, E_{MV}	85.5	85.4	83.7	83.7	82.8	82.8	81.7	81.9	81.5	81.2	84.1	84.3	84.5	84.5	85.7	85.7	86.7
Liquid, E_{ML}	12.8	13.0	21.8	21.5	29.3	29.7	34.0	33.8	37.0	36.7	27.0	27.8	23.2	23.2	19.6	19.6	14.6
NUMBER OF TRANSFER UNITS																	
N_{OG}	1.99	1.98	1.85	1.85	1.79	1.79	1.72	1.73	1.70	1.69	1.85	1.87	1.89	1.88	1.97	1.97	2.06
N_L	1.53	1.58	2.10	2.09	2.49	2.60	2.91	3.32	3.15	3.18	2.06	2.08	1.88	1.86	1.68	1.69	1.38
N_G	2.06	2.05	1.95	1.95	1.91	1.90	1.84	1.83	1.84	1.82	1.98	1.99	2.00	2.00	2.07	2.07	2.15
GAS PHASE MASS TRANSFER COEFFICIENT																	
k_G^1a, sec^{-1}	11.06	9.96	15.21	14.61	16.91	17.56	17.42	18.66	18.62	18.64	15.55	16.17	15.62	15.79	15.53	15.63	13.39
LIQUID CONCENTRATION PROFILE, MOLE FRACTION x 10^4																	
x_A	0	0	0	0	0	0	0	0	0	0	0	0	0	0	0	0	0
x_B	7.551	9.141	16.66	15.44	20.97	20.23	19.52	19.02	21.80	22.52	11.06	11.28	9.582	8.979	7.068	7.389	6.119
x_C	13.50	14.44	19.84	19.85	22.67	22.59	20.13	19.51	24.83	24.18	11.81	12.03	10.58	10.63	9.005	8.800	8.081
x_D	21.64	22.89	40.74	40.58	44.78	44.71	39.25	39.50	42.80	42.88	23.62	24.04	22.50	22.58	20.86	19.97	19.93
x_E	27.54	29.20	41.45	41.39	42.22	42.47	38.86	37.80	40.18	40.39	22.54	22.42	22.23	22.20	21.37	21.15	21.79
x_F	24.79	25.83	41.65	41.48	43.66	43.85	39.61	38.90	39.70	40.49	22.42	23.04	22.06	21.82	21.45	21.08	21.13
x_G	28.36	27.11	43.67	44.14	44.43	44.07	39.22	37.54	41.11	41.01	22.83	22.97	22.71	22.55	22.15	22.05	22.33
x_H	29.33	27.31	43.33	43.96	45.71	44.80	39.77	38.71	41.17	41.29	22.97	23.27	23.04	22.79	22.50	22.20	22.96
HYDRAULIC DATA																	
Pressure drop, in water	2.75	2.75	2.85	2.94	3.57	3.55	4.50	4.58	5.80	6.15	6.80	6.95	5.40	5.50	4.40	4.40	3.70
Froth height, in	4.5	4.8	5.1	5.2	6.1	6.0	7.1	7.0	7.8	7.7	10.1	9.9	8.8	8.7	7.5	7.5	6.6
Clear liquid height, in																	
Position B	2.45	2.50	2.40	2.35	2.35	2.30	2.35	2.40	2.30	2.30	3.25	3.30	3.30	3.25	3.15	3.20	3.20
C	2.30	2.35	2.10	2.10	1.95	2.05	1.95	2.20	1.95	1.95	2.45	2.50	2.40	2.40	2.45	2.50	2.60
D	2.25	2.35	2.10	2.10	1.95	2.05	1.90	2.20	1.70	1.75	2.35	2.35	2.55	2.50	2.80	2.75	2.90
E	2.40	2.40	2.35	2.30	2.25	2.30	2.20	2.35	2.25	2.20	3.00	3.05	3.00	3.00	3.10	3.00	3.10
Gas contact time, sec.	0.187	0.206	0.128	0.134	0.113	0.108	0.106	0.0983	0.0987	0.0975	0.127	0.123	0.128	0.126	0.133	0.133	0.161
Liquid contact time, sec.	6.54	6.77	6.04	6.04	5.61	5.89	5.53	6.32	5.25	5.32	3.45	3.49	3.56	3.52	3.77	3.77	3.95
Mixing Parameter C	1.44	1.55	1.67	1.59	1.92	1.86	1.97	1.96	2.22	2.25	1.97	1.96	1.77	1.70	1.49	1.54	1.41
$m G/L = \lambda$	0.0263	0.0259	0.0537	0.0529	0.0837	0.0839	0.1098	0.1101	0.1338	0.1307	0.0673	0.0670	0.0544	0.0548	0.0400	0.0406	0.0266
ENTRAINMENT, MOLES LIQUID/MOLE VAPOR x 10^3	--	--	--	--	1.05	--	3.88	--	5.43	--	6.98	--	5.22	--	4.12	--	--

TABLE XIV (CONT'D)

RUN NUMBER	146	147	148	149	150	151	152	153	154	155	156	157	158	159	160	161	162
WATER RATE																	
Gallons per minute	16.0	16.0	16.0	24.0	24.0	24.0	24.0	24.0	24.0	24.0	24.0	32.0	32.0	32.0	32.0	32.0	32.0
Lb moles per minute	7.40	7.40	7.40	11.10	11.10	11.10	11.10	11.10	11.10	11.10	11.10	14.80	14.80	14.80	14.80	14.80	14.80
Temperature °F, Tray Inlet	77.0	77.4	77.0	77.0	76.8	77.0	77.2	77.5	77.2	76.5	76.5	77.0	77.0	77.0	77.2	76.8	77.0
Temperature °F, Tray Outlet	78.6	78.3	77.9	77.9	77.7	78.1	78.4	78.6	78.3	77.5	77.5	77.7	77.7	77.9	78.1	77.5	77.7
AMMONIA FLOW																	
Lb moles per minute x 10^2	1.90	1.16	1.16	1.17	1.17	1.91	1.87	2.03	2.07	1.77	1.77	1.16	1.15	1.92	1.89	1.72	1.69
AIR FLOW																	
Temperature °F at blower suction																	
Dry bulb	83.1	79.5	79.5	81.0	81.0	75.0	75.0	81.0	81.0	83.0	83.0	82.5	82.5	73.5	73.5	78.0	78.0
Wet bulb	65.5	58.5	58.5	70.5	70.5	63.0	63.0	66.5	66.5	62.0	62.0	72.5	72.5	54.5	54.5	58.0	58.0
AIR-AMMONIA FLOW THROUGH TRAY (Avg. conditions)																	
Lb moles per minute x 10^2	19.29	12.59	12.58	11.85	11.81	24.59	24.57	36.81	36.92	47.83	47.29	9.99	9.96	23.54	23.50	33.71	33.52
Velocity, ft per sec	1.98	1.33	1.33	1.22	1.22	2.54	2.54	3.87	3.88	4.71	4.66	1.06	1.05	2.43	2.43	3.44	3.42
F Factor, $up_G^{1/2}$	0.54	0.36	0.36	0.33	0.33	0.69	0.69	1.04	1.05	1.32	1.30	0.28	0.28	0.66	0.66	0.94	0.94
EQUILIBRIUM CONDITIONS ON TRAY																	
Temperature, °F	78.6	78.3	77.9	77.9	77.7	78.1	78.4	78.6	78.3	77.5	77.5	77.7	77.7	77.9	78.1	77.5	77.7
Pressure, in Hg	30.97	30.13	30.14	30.78	30.78	30.79	30.79	30.30	30.30	32.30	32.25	30.03	30.03	30.78	30.78	31.19	31.17
Henry's Law Constant, In Hg/mole fraction	31.43	31.12	30.77	30.77	30.60	30.94	31.19	31.43	31.11	30.43	30.43	30.60	30.60	30.77	30.93	30.43	30.60
LIQUID COMPOSITION, MOLE FRACTION x 10^4																	
x_2	0	0	0	4.932	4.855	6.861	7.322	7.909	7.832	6.734	6.849	11.09	11.05	17.49	17.47	15.64	15.31
x_1	21.17	12.74	13.02	13.74	13.66	23.02	22.31	23.75	24.35	20.57	20.23	17.71	17.90	29.32	29.26	25.84	25.57
x_1^*	144.2	117.7	121.4	91.17	90.55	94.64	92.33	75.25	78.01	59.98	59.92	84.98	81.96	77.87	76.67	52.52	53.71
VAPOR COMPOSITION, MOLE FRACTION x 10^4																	
y_o	964.4	859.7	859.8	877.8	878.6	817.0	739.4	531.5	544.0	359.4	358.2	1003	1024	774.3	770.3	487.4	482.2
y_1	146.4	121.6	123.9	91.14	90.02	95.10	93.53	78.05	80.09	56.51	56.53	86.59	83.52	77.84	77.04	51.24	52.73
y_1^*	21.48	13.16	13.29	13.73	13.58	23.14	22.60	24.64	25.00	19.38	19.08	18.05	18.24	29.31	29.40	25.21	25.10
MURPHREE EFFICIENCY, PER CENT																	
Vapor, E_{MV}	86.8	87.2	86.9	91.0	91.2	90.9	90.1	89.5	89.4	89.1	89.0	93.0	93.5	93.5	93.6	94.4	94.0
Liquid, E_{ML}	14.7	10.8	10.7	10.2	10.3	18.4	17.6	23.5	23.5	26.0	25.2	9.0	9.7	19.6	19.9	27.6	26.7
NUMBER OF TRANSFER UNITS																	
N_{OG}	2.07	2.09	2.07	2.45	2.47	2.44	2.35	2.27	2.27	2.23	2.22	2.71	2.78	2.77	2.78	2.90	2.83
N_L	1.36	1.15	1.06	0.88	0.88	1.34	1.34	1.66	1.67	1.85	1.90	0.72	0.72	1.23	1.24	1.55	1.55
N_G	2.16	2.17	2.15	2.53	2.55	2.55	2.45	2.39	2.38	2.35	2.33	2.79	2.86	2.88	2.89	3.03	2.95
GAS PHASE MASS TRANSFER COEFFICIENT																	
$k'_G a$, sec^{-1}	13.61	11.18	11.34	11.29	10.59	15.78	14.86	15.42	15.94	14.95	15.76	10.28	10.99	13.07	13.01	15.42	14.43
LIQUID CONCENTRATION PROFILE, MOLE FRACTION x 10^4																	
x_A	0	0	0	4.932	4.855	6.861	7.321	7.909	7.832	6.734	6.849	11.09	11.05	17.49	17.47	15.64	15.31
x_B	6.799	2.771	2.809	6.465	6.414	11.54	11.67	13.48	13.66	11.31	11.73	11.84	12.10	19.49	20.02	17.80	17.62
x_C	7.812	4.118	3.964	7.538	7.372	13.24	13.40	14.73	13.63	12.29	13.34	12.82	12.80	21.75	21.55	18.99	18.90
x_D	19.54	11.53	11.97	11.52	11.46	21.55	21.04	22.87	23.57	18.32	19.71	16.52	16.30	28.88	28.76	25.40	25.09
x_E	21.88	12.78	13.26	13.76	13.74	23.64	22.33	23.74	24.39	20.29	20.51	17.59	17.91	29.39	29.29	26.13	25.63
x_F	21.17	12.74	13.02	13.74	13.66	23.02	22.31	23.75	24.35	20.57	20.23	17.71	17.90	29.32	29.26	25.84	25.57
x_G	22.51	13.37	13.20	14.11	13.90	23.02	22.85	23.73	24.48	20.88	20.67	17.77	17.99	29.55	29.35	26.15	25.75
x_H	22.78	14.34	14.34	15.06	15.09	23.59	23.09	24.17	24.80	21.07	21.01	18.78	18.85	29.72	29.71	26.46	26.10
HYDRAULIC DATA																	
Pressure drop, in water	3.75	3.44	3.25	4.10	4.10	4.85	4.85	6.10	5.90	7.10	7.20	4.80	4.70	5.60	5.75	6.70	6.80
Froth height, in	6.5	6.0	5.7	6.8	7.0	8.4	8.5	10.6	10.4	12.2	11.7	7.6	7.5	10.8	10.9	12.6	12.9
Clear liquid height, in																	
Position B	3.15	3.10	2.90	3.80	3.70	4.00	4.10	4.15	4.20	4.30	4.30	4.50	4.50	5.10	5.10	5.40	5.60
C	2.60	2.80	2.55	3.40	3.35	3.35	3.35	3.30	3.30	3.25	3.35	4.10	4.10	4.35	4.35	4.60	4.50
D	2.85	3.00	2.80	3.60	3.60	3.60	3.60	3.50	3.60	3.40	3.40	4.20	4.30	4.40	4.50	4.40	4.50
E	3.10	3.05	3.00	3.75	3.70	3.90	3.75	4.00	4.00	3.75	3.80	4.40	4.50	4.70	4.70	4.70	4.80
Gas contact time, sec.	0.159	0.194	0.190	0.225	0.241	0.161	0.165	0.155	0.149	0.157	0.148	0.272	0.261	0.220	0.222	0.196	0.205
Liquid contact time, sec.	3.92	4.17	3.85	3.35	3.33	3.33	3.33	3.26	3.31	3.19	3.28	2.98	3.02	3.14	3.18	3.23	3.23
Mixing Parameter C	1.47	1.28	1.28	1.21	1.22	1.41	1.41	1.54	1.54	1.49	1.57	1.13	1.18	1.20	1.28	1.27	1.29
$mG/L = \lambda$	0.0265	0.0176	0.0174	0.0108	0.0106	0.0223	0.0224	0.0344	0.0341	0.0406	0.0402	0.00688	0.00686	0.0159	0.0160	0.0222	0.0222
ENTRAINMENT, MOLES LIQUID/MOLE VAPOR x 10^3	--	--	--	--	--	--	3.11	--	13.8	--	28.7	--	--	7.41	--	--	102.5

TABLE XV

AMMONIA ABSORPTION FROM AIR BY WATER USING VALVE TRAY WITH 3-1/2-INCH WEIR

RUN NUMBER	101	102	103	104	105	106	107	108	109	110	111	112	113	114
WATER RATE														
Gallons per minute	8.0	8.0	8.0	8.0	8.0	8.0	8.0	8.0	8.0	8.0	16.0	16.0	16.0	16.0
Lb moles per minute	3.70	3.70	3.70	3.70	3.70	3.70	3.70	3.70	3.70	3.70	7.40	7.40	7.40	7.40
Temperature °F, Tray Inlet	76.5	75.9	76.1	78.2	75.4	78.4	77.2	77.0	77.4	77.2	75.7	76.8	77.0	76.6
Temperature °F, Tray Outlet	79.0	77.4	77.9	79.7	77.4	79.9	78.6	78.3	78.4	78.3	76.6	77.9	78.4	78.1
AMMONIA FLOW														
Lb moles per minute x 10^2	0.503	0.501	1.76	1.75	2.11	2.09	2.11	2.11	2.13	2.13	1.16	1.17	2.08	2.08
AIR FLOW														
Temperature °F at blower suction														
Dry bulb	80.0	83.0	83.0	83.0	82.0	80.0	88.0	87.0	82.0	82.0	83.0	81.5	82.0	82.0
Wet bulb	61.5	58.0	55.0	56.0	57.0	57.0	60.0	61.0	57.0	57.0	58.0	56.5	63.0	63.0
AIR-AMMONIA FLOW THROUGH TRAY (Avg. conditions)														
Lb moles per minute x 10^2	11.17	11.16	20.01	20.77	28.97	29.51	39.23	39.58	47.07	46.98	9.52	9.62	19.31	19.24
Velocity, ft per sec	1.17	1.18	2.10	2.21	2.97	3.12	4.06	4.10	4.86	4.85	1.00	1.00	2.01	2.00
F Factor, $u\rho_G^{1/2}$	0.32	0.32	0.56	0.59	0.81	0.84	1.11	1.12	1.33	1.32	0.27	0.27	0.54	0.54
EQUILIBRIUM CONDITIONS ON TRAY														
Temperature, °F	79.0	77.4	77.9	79.7	77.4	79.9	78.6	78.3	78.4	78.3	76.6	77.9	78.4	78.1
Pressure, in Hg	30.35	30.13	30.38	30.05	31.02	30.23	30.77	30.75	30.81	30.83	30.33	30.74	30.63	30.61
Henry's Law Constant, In Hg/mole fraction	31.77	30.27	30.77	32.43	30.27	32.60	31.44	31.10	31.27	31.10	29.64	30.77	31.27	30.94
LIQUID COMPOSITION, MOLE FRACTION x 10^4														
x_2	0	0	0	0	0	0	0	0	0	0	15.01	15.16	0	0
x_1	10.80	13.27	40.05	42.49	47.95	47.81	47.06	46.34	46.96	46.21	27.61	29.34	26.90	25.63
x_1^*	47.07	50.28	128.4	109.0	113.5	107.3	92.32	93.87	84.12	85.91	95.96	91.43	94.29	94.34
VAPOR COMPOSITION, MOLE FRACTION x 10^4														
y_o	465.0	483.9	881.9	818.3	711.1	699.6	519.7	516.9	446.8	437.9	1100	1156	1035	1035
y_1	49.27	50.52	130.0	117.7	110.8	115.7	94.33	94.94	85.38	86.66	93.77	91.52	96.26	95.36
y_1^*	11.31	13.33	40.57	45.86	46.79	51.56	48.08	46.86	47.66	46.62	26.98	29.37	27.47	25.91
MURPHREE EFFICIENCY, PER CENT														
Vapor, E_{MV}	91.6	92.1	89.4	90.7	90.4	90.1	90.2	89.8	90.5	89.8	93.8	94.5	93.2	93.1
Liquid, E_{ML}	23.0	26.4	31.2	39.0	42.2	44.5	51.0	49.4	55.8	53.8	15.6	18.6	28.5	27.2
NUMBER OF TRANSFER UNITS														
N_{OG}	2.50	2.56	2.28	2.41	2.37	2.34	2.34	2.30	2.38	2.30	2.83	2.95	2.73	2.73
N_L	2.40	2.55	3.32	3.40	3.92	3.94	4.46	4.49	4.83	4.78	1.36	1.42	2.05	2.04
N_G	2.59	2.64	2.38	2.53	2.49	2.48	2.49	2.44	2.54	2.45	2.91	3.04	2.84	2.83
GAS PHASE MASS TRANSFER COEFFICIENT														
$k_G'a$, sec^{-1}	14.90	15.25	16.26	19.25	19.30	19.50	19.43	19.22	20.28	18.92	11.05	11.10	16.60	15.36
LIQUID CONCENTRATION PROFILE, MOLE FRACTION x 10^4														
x_A	0	0	0	0	0	0	0	0	0	0	15.01	15.15	0	0
x_B	8.744	6.943	24.77	23.73	29.96	33.03	33.63	27.44	34.10	33.75	17.62	18.29	10.75	11.53
x_C	11.32	8.819	27.07	25.58	32.98	34.76	36.35	35.27	35.65	34.48	20.78	20.36	14.20	14.10
x_D	11.67	12.10	39.62	42.78	48.58	47.27	48.26	48.28	48.52	47.94	26.54	26.77	26.16	25.78
x_E	12.45	12.36	38.93	38.61	48.45	48.12	46.82	46.05	46.53	45.64	28.12	29.08	27.06	25.32
x_F	10.81	13.27	40.05	42.49	47.95	47.81	47.06	46.34	46.96	46.21	27.61	29.34	26.91	25.63
x_G	8.719	13.15	40.87	41.42	48.77	48.43	47.13	46.21	46.76	45.84	28.06	29.34	24.38	25.79
x_H	13.30	12.50	43.18	41.32	47.78	47.91	47.45	46.67	46.87	45.99	29.73	29.83	25.11	25.71
HYDRAULIC DATA														
Pressure drop, in water	3.80	3.96	4.16	3.90	4.80	4.90	5.90	5.95	7.00	7.00	4.75	4.85	5.10	5.20
Froth height, in	5.7	5.9	6.9	6.7	7.7	7.8	9.2	9.2	10.2	10.4	7.2	7.5	8.2	8.5
Clear liquid height, in														
Position B	3.50	3.70	3.55	3.55	3.65	3.60	3.70	3.70	3.60	3.70	4.30	4.55	4.50	4.60
C	3.30	3.45	3.20	3.20	3.05	3.00	3.00	3.00	3.00	3.00	4.00	4.25	4.00	4.00
D	3.20	3.45	3.25	3.25	3.15	3.10	2.90	2.90	2.75	2.70	4.10	4.20	4.15	4.15
E	3.35	3.50	3.40	3.40	3.50	3.40	3.50	3.50	3.45	3.50	4.25	4.30	4.35	4.40
Gas contact time, sec.	0.174	0.173	0.146	0.131	0.129	0.127	0.128	0.128	0.125	0.130	0.264	0.274	0.171	0.184
Liquid contact time, sec.	9.34	9.92	9.27	9.27	8.91	8.77	8.48	8.48	8.27	8.19	5.82	6.07	5.86	5.86
Mixing Parameter C	5.24	2.10	2.62	2.26	2.67	3.23	3.50	2.45	3.65	3.71	1.26	1.28	1.66	1.82
$mG/L = \lambda$	0.0316	0.0303	0.0548	0.0606	0.0764	0.0860	0.1083	0.1082	0.1291	0.1281	0.0126	0.0130	0.0266	0.0263
ENTRAINMENT, MOLES LIQUID/MOLE VAPOR x 10^3	--	--	--	1.98	3.73	--	5.50	5.32	9.64	9.57	--	--	1.78	--

TABLE XV (CONT'D)

RUN NUMBER	115	116	117	118	119	120	121	122	123	124	125	126	127	128
WATER RATE														
Gallons per minute	16.0	16.0	16.0	16.0	24.0	24.0	24.0	24.0	24.0	24.0	32.0	32.0	32.0	32.0
Lb moles per minute	7.40	7.40	7.40	7.40	11.1	11.1	11.1	11.1	11.1	11.1	14.8	14.8	14.8	14.8
Temperature °F, Tray Inlet	76.5	76.4	77.0	76.6	77.0	76.7	77.9	77.4	77.0	77.2	77.0	77.7	76.6	76.5
Temperature °F, Tray Outlet	77.9	77.7	78.3	78.1	77.7	77.5	79.2	78.6	77.9	78.1	77.7	78.3	77.5	77.4
AMMONIA FLOW														
Lb moles per minute x 10^2	2.13	2.13	2.07	2.07	1.15	1.14	2.04	2.04	1.85	1.84	1.15	1.15	1.90	1.89
AIR FLOW														
Temperature °F at blower suction														
Dry bulb	87.0	87.0	87.0	85.0	80.0	80.0	82.5	82.5	80.0	80.0	85.0	85.0	79.0	79.0
Wet bulb	62.0	62.0	62.0	60.0	64.5	64.5	65.0	65.0	60.0	60.0	63.0	63.0	58.0	58.0
AIR-AMMONIA FLOW THROUGH TRAY (Avg. conditions)														
Lb moles per minute x 10^2	29.15	29.09	34.29	34.92	9.47	9.44	19.40	19.05	30.12	30.04	9.727	9.913	19.44	19.08
Velocity, ft per sec	3.01	3.00	3.53	3.68	1.02	1.01	2.04	2.00	2.98	2.98	1.04	1.06	2.01	1.97
F Factor, $u\rho_G^{1/2}$	0.82	0.82	0.96	0.99	0.27	0.27	0.55	0.54	0.83	0.83	0.28	0.28	0.55	0.54
EQUILIBRIUM CONDITIONS ON TRAY														
Temperature, °F	77.9	77.7	78.3	78.1	77.7	77.5	79.2	78.6	77.9	78.1	77.7	78.3	77.5	77.4
Pressure, in Hg	30.86	30.85	30.94	30.32	29.64	29.64	30.38	30.38	32.15	32.10	29.86	29.85	30.75	30.75
Henry's Law Constant, In Hg/mole fraction	30.77	30.60	31.11	30.93	30.60	30.44	31.94	31.44	30.77	30.94	30.60	31.10	30.43	30.26
LIQUID COMPOSITION, MOLE FRACTION x 10^4														
x_2	0	0	0	0	4.816	4.854	8.607	8.381	7.607	7.568	9.120	8.980	12.12	12.53
x_1	25.39	25.37	25.29	24.91	13.65	13.46	25.74	25.52	22.86	22.63	15.82	16.24	23.58	24.37
x_1^*	73.92	74.26	65.63	61.46	71.20	66.11	70.29	71.96	48.79	49.62	55.76	56.21	50.62	54.38
VAPOR COMPOSITION, MOLE FRACTION x 10^4														
y_o	697.8	700.9	602.2	572.5	1114	1086	1015	1036	599.0	604.0	1046	1070	916.9	952.4
y_1	73.70	73.66	65.99	62.69	73.51	67.90	73.90	74.47	46.70	47.83	57.14	58.56	50.09	53.52
y_1^*	25.32	25.16	25.43	25.42	14.09	13.82	27.07	26.41	21.88	21.81	16.21	16.92	23.33	23.98
MURPHREE EFFICIENCY, PER CENT														
Vapor, E_{MV}	92.8	92.8	93.0	93.2	94.6	95.0	95.3	95.2	95.7	95.5	96.0	96.0	97.0	96.8
Liquid, E_{ML}	34.4	34.2	38.5	40.5	13.3	14.0	27.8	27.0	37.0	35.8	14.4	15.4	29.8	28.3
NUMBER OF TRANSFER UNITS														
N_{OG}	2.66	2.67	2.68	2.71	2.97	3.04	3.10	3.10	3.18	3.14	3.28	3.29	3.55	3.50
N_L	2.51	2.51	2.76	2.79	1.08	1.11	1.67	1.67	2.05	2.06	0.98	0.97	1.45	1.43
N_G	2.79	2.79	2.81	2.85	3.05	3.12	3.22	3.21	3.31	3.27	3.36	3.37	3.68	3.61
GAS PHASE MASS TRANSFER COEFFICIENT														
k_G^1a, sec^{-1}	16.34	16.06	16.01	17.99	10.34	11.07	13.43	12.82	15.59	15.86	11.36	10.76	14.67	13.64
LIQUID CONCENTRATION PROFILE, MOLE FRACTION x 10^4														
x_A	0	0	0	0	4.816	4.854	8.607	8.381	7.607	7.568	9.121	8.979	12.12	12.53
x_B	13.41	14.12	14.12	13.27	8.081	6.893	14.39	13.99	13.83	13.39	10.31	9.967	15.35	16.03
x_C	15.51	15.51	16.41	15.35	9.470	7.981	17.11	16.48	16.46	16.27	11.07	11.19	17.32	17.73
x_D	25.62	25.93	25.78	25.33	10.51	10.73	25.82	25.52	22.82	22.40	14.70	14.61	21.83	22.78
x_E	25.28	25.32	25.21	24.84	13.97	13.52	25.64	25.63	22.67	22.65	15.82	15.82	24.18	24.50
x_F	25.39	25.37	25.29	24.92	13.65	13.46	25.74	25.52	22.86	22.63	15.82	16.24	23.58	24.37
x_G	25.63	25.63	25.24	24.91	14.07	13.77	25.69	25.71	22.94	22.79	16.15	16.01	23.91	24.64
x_H	25.82	25.82	25.79	25.29	14.87	14.94	26.13	26.20	23.36	23.26	16.69	16.82	24.77	25.13
HYDRAULIC DATA														
Pressure drop, in water	5.86	5.88	6.45	6.30	5.42	5.30	5.90	6.05	6.95	7.75	6.18	6.15	6.65	6.83
Froth height, in	10.1	10.2	11.4	10.9	8.4	8.4	10.8	11.0	12.4	12.2	9.4	9.6	11.8	12.0
Clear liquid height, in														
Position B	4.60	4.60	4.65	4.65	4.90	5.10	5.50	5.45	5.50	5.50	6.00	5.90	6.30	6.20
C	3.90	3.90	3.90	3.90	4.60	4.95	4.90	4.90	4.70	4.75	5.75	5.60	5.70	5.65
D	4.00	4.00	4.00	3.95	5.00	5.00	5.00	5.10	4.90	4.90	5.70	5.65	5.80	5.80
E	4.40	4.40	4.50	4.40	4.90	5.05	5.30	5.35	5.20	5.20	5.90	5.80	6.00	5.90
Gas contact time, sec.	0.170	0.174	0.176	0.159	0.295	0.282	0.239	0.250	0.212	0.206	0.296	0.313	0.251	0.265
Liquid contact time, sec.	5.68	5.68	5.68	5.64	4.60	4.77	4.74	4.79	4.60	4.62	4.11	4.04	4.13	4.11
Mixing Parameter C	2.12	2.26	2.26	2.14	1.59	1.31	1.51	1.49	1.69	1.63	1.22	1.16	1.39	1.42
$m_G/L = \lambda$	0.0393	0.0390	0.0466	0.0481	0.00881	0.00873	0.0184	0.0178	0.0260	0.0261	0.00674	0.00698	0.0130	0.0127
ENTRAINMENT, MOLES LIQUID/MOLE VAPOR x 10^3	11.93	--	15.16	--	--	--	4.03	--	70.2	--	--	--	20.4	--

TABLE XVI

AMMONIA ABSORPTION FROM AIR BY WATER USING PERFORATED TRAY WITH 2-INCH WEIR

RUN NUMBER	201	202	203	204	205	206	207	208	209	210	211	212	213	214	215	216	217	218	219	220	220	222
WATER RATE																						
Gallons per minute	8.0	8.0	8.0	8.0	8.0	8.0	8.0	8.0	16.0	16.0	16.0	16.0	16.0	16.0	16.0	16.0	24.0	24.0	24.0	24.0	24.0	24.0
Lb moles per minute	3.70	3.70	3.70	3.70	3.70	3.70	3.70	3.70	7.40	7.40	7.40	7.40	7.40	7.40	7.40	7.40	11.10	11.10	11.10	11.10	11.10	11.10
Temperature °F, Tray Inlet	76.9	76.8	76.6	76.9	77.1	76.6	76.7	77.2	76.9	77.0	77.4	77.0	77.0	77.0	77.0	77.3	77.0	77.5	76.8	77.0	77.1	77.0
Temperature °F, Tray Outlet	78.4	78.3	79.9	80.1	79.9	79.3	80.2	81.0	78.1	78.3	79.2	79.0	79.0	79.3	79.2	79.7	78.1	78.6	78.4	78.6	78.6	78.6
AMMONIA FLOW																						
Lb moles per minute x 10^2	1.16	1.16	1.95	1.95	1.95	1.92	2.00	1.99	1.14	1.15	1.78	1.77	1.99	1.98	2.12	2.11	1.15	1.15	1.75	1.68	1.66	1.53
AIR FLOW																						
Temperature °F at blower suction																						
Dry bulb	80.0	80.0	93.1	93.1	92.5	92.5	85.5	85.5	88.5	88.5	88.0	88.0	94.5	94.5	90.7	90.7	88.5	88.5	86.0	86.0	95.0	95.0
Wet bulb	69.0	69.0	73.0	73.0	70.5	70.5	73.5	73.5	72.0	72.0	67.5	67.5	76.5	76.5	75.5	75.5	71.5	71.5	73.0	73.0	78.5	78.5
AIR-AMMONIA FLOW THROUGH TRAY (Avg. conditions)																						
Lb moles per minute x 10^2	9.96	9.94	23.20	23.17	36.18	35.88	49.56	48.55	10.27	10.24	24.33	24.23	36.77	36.47	49.84	49.73	10.31	10.28	22.97	22.96	35.86	35.84
Velocity, ft per sec	1.03	1.03	2.38	2.38	3.84	3.80	4.79	4.64	1.08	1.12	2.50	2.49	3.68	3.65	4.96	4.95	1.09	1.09	2.44	2.44	3.72	3.72
F Factor, $u\rho_G^{1/2}$	0.28	0.28	0.65	0.65	1.03	1.02	1.35	1.31	0.29	0.30	0.68	0.68	1.02	1.01	1.38	1.37	0.29	0.29	0.65	0.65	1.01	1.01
EQUILIBRIUM CONDITIONS ON TRAY																						
Temperature, °F	78.4	78.3	79.9	80.1	79.9	79.3	80.2	81.0	78.1	78.3	79.2	79.0	79.0	79.3	79.2	79.7	78.1	78.6	78.4	78.6	78.6	78.6
Pressure, in Hg	30.75	30.77	31.16	31.16	30.12	30.12	33.05	33.47	30.16	30.16	31.03	31.03	31.88	31.86	32.05	32.05	30.14	30.14	29.93	29.97	30.73	30.73
Henry's Law Constant, In Hg/mole fraction	31.27	31.11	32.60	32.76	32.60	32.10	32.93	33.60	30.93	31.12	31.93	31.77	31.77	32.10	32.10	32.43	30.93	31.43	31.27	31.43	31.43	31.43
LIQUID COMPOSITION, MOLE FRACTION x 10^4																						
x_2	0	0	0	0	0	0	0	0	0	0	0	0	0	0	0	0	4.587	4.523	6.580	6.478	6.069	5.596
x_1	15.93	14.86	37.11	38.73	39.63	37.54	39.56	39.27	7.564	8.075	18.83	18.74	20.97	20.92	22.41	22.26	10.63	10.27	19.68	19.17	18.55	17.36
x_1^*	209.6	209.7	203.0	201.9	134.4	134.1	106.6	105.7	163.1	157.6	142.0	140.0	115.1	112.7	87.96	86.31	138.2	135.4	106.6	103.0	75.66	68.56
VAPOR COMPOSITION, MOLE FRACTION x 10^4																						
y_o	815.4	793.3	813.7	815.3	532.6	526.7	395.2	397.3	738.7	806.8	717.4	715.2	521.3	518.7	400.0	394.8	786.4	833.0	717.1	697.3	437.4	405.6
y_1	213.1	212.0	212.4	212.2	145.5	142.9	106.2	106.1	167.2	168.2	146.1	142.9	114.7	113.6	88.10	87.33	141.8	141.2	111.4	108.0	77.38	70.12
y_1^*	16.20	15.02	38.83	40.72	42.89	40.01	39.42	39.42	7.757	8.618	19.38	19.19	20.89	21.07	22.45	22.52	10.91	10.71	20.56	20.10	18.97	17.76
MURPHREE EFFICIENCY, PER CENT																						
Vapor, E_{MV}	75.4	74.7	77.6	77.9	79.1	78.9	81.2	81.4	78.2	80.0	81.8	82.2	81.2	81.4	82.6	82.6	83.1	84.1	87.0	87.0	86.0	86.5
Liquid, E_{ML}	7.6	7.1	18.3	19.2	29.5	28.0	37.1	37.2	4.6	5.1	13.3	13.4	18.2	18.6	25.5	25.8	4.5	4.4	13.1	13.1	17.9	18.7
NUMBER OF TRANSFER UNITS																						
N_{OG}	1.43	1.41	1.53	1.54	1.58	1.57	1.69	1.70	1.55	1.64	1.74	1.76	1.70	1.70	1.76	1.76	1.81	1.88	2.07	2.07	1.99	2.02
N_L	1.44	1.40	2.33	2.25	2.76	2.67	3.05	3.09	0.88	0.91	1.46	1.53	1.66	1.72	2.10	2.06	0.74	0.77	1.23	1.23	1.48	1.51
N_G	1.48	1.45	1.60	1.62	1.69	1.68	1.82	1.83	1.59	1.69	1.81	1.83	1.79	1.79	1.87	1.88	1.86	1.92	2.15	2.15	2.08	2.11
GAS PHASE MASS TRANSFER COEFFICIENT																						
$k'_G a$, sec^{-1}	7.02	8.31	11.42	10.78	12.96	12.46	14.37	13.00	8.65	9.36	11.45	11.35	12.53	12.49	13.85	13.94	8.83	8.96	11.47	12.14	11.20	11.72
LIQUID CONCENTRATION PROFILE, MOLE FRACTION x 10^4																						
x_A	0	0	0	0	0	0	0	0	0	0	0	0	0	0	0	0	4.587	4.523	6.580	6.478	6.069	5.596
x_B	6.120	5.737	21.72	21.29	25.24	24.88	27.83	26.94	2.262	2.670	6.849	7.283	11.26	12.13	13.81	14.32	6.222	5.903	10.83	11.03	11.02	10.50
x_C	7.960	7.781	23.37	23.46	25.07	25.85	27.99	27.34	3.948	4.293	9.212	9.468	12.94	13.51	14.44	14.76	7.360	7.142	12.82	12.83	13.20	12.30
x_D	11.58	13.34	35.25	34.26	35.90	35.44	37.71	37.34	6.478	6.465	15.52	15.52	16.48	17.90	17.72	16.87	9.046	9.263	17.20	15.97	14.90	14.30
x_E	16.61	16.76	37.54	36.36	37.90	36.70	39.83	38.81	8.113	7.973	18.64	18.83	20.71	21.04	22.10	22.00	10.46	10.50	19.77	19.03	18.59	17.35
x_F	15.93	14.86	37.12	38.73	39.63	37.54	39.56	39.27	7.564	8.075	18.83	18.74	20.97	20.92	22.41	22.26	10.63	10.27	19.68	19.17	18.55	17.36
x_G	18.08	15.81	40.55	38.79	39.04	38.04	40.28	39.55	8.842	8.944	19.56	19.68	21.53	21.43	22.79	22.50	11.24	11.38	20.32	19.49	18.34	17.48
x_H	26.67	26.32	41.12	40.34	39.65	38.43	40.52	40.18	14.09	14.12	20.09	20.15	21.89	21.80	22.86	22.73	14.37	14.08	20.78	20.09	18.81	17.81
HYDRAULIC DATA																						
Pressure drop, in water	2.35	2.40	3.20	3.20	4.50	4.40	6.10	6.00	3.00	3.00	3.90	3.90	4.90	4.90	6.60	6.70	3.60	3.60	4.85	4.80	5.70	5.70
Froth height, in	4.7	4.2	6.1	6.3	7.9	8.0	9.1	9.7	4.9	5.0	7.3	7.5	8.6	8.7	10.5	10.4	5.9	6.1	8.8	8.5	11.4	11.2
Clear liquid height, in																						
Position B	2.10	2.10	2.25	2.30	2.20	2.10	2.10	2.05	2.70	2.75	3.00	3.00	2.80	2.80	2.90	2.90	3.30	3.35	3.70	3.75	3.90	4.00
C	2.10	2.00	2.00	1.95	1.80	1.70	1.60	1.70	2.40	2.60	2.30	2.55	2.10	2.10	2.10	2.00	3.00	3.20	3.10	3.30	2.90	3.10
D	2.10	2.00	2.20	2.10	2.00	2.00	2.00	2.00	2.60	2.55	2.80	2.80	2.50	2.70	2.80	2.80	3.30	3.40	3.50	3.30	3.30	3.20
E	2.15	2.15	2.35	2.30	2.20	2.35	2.35	2.30	2.70	2.70	2.90	2.90	2.80	2.90	3.10	3.05	3.40	3.35	3.70	3.80	3.70	3.70
Gas contact time, sec.	0.210	0.174	0.140	0.150	0.130	0.135	0.127	0.141	0.184	0.181	0.158	0.161	0.143	0.144	0.135	0.135	0.210	0.215	0.187	0.177	0.186	0.180
Liquid contact time, sec.	6.04	5.89	6.04	5.82	5.46	5.32	5.18	5.32	3.59	3.70	3.67	3.85	3.31	3.45	3.52	3.45	3.02	3.16	3.16	3.16	2.97	3.02
Mixing Parameter C	1.62	1.63	2.41	2.22	2.75	2.97	3.37	3.18	1.43	1.49	1.57	1.64	2.16	2.38	2.61	2.81	1.37	1.32	1.48	1.56	1.66	1.72
$mG/L = \lambda$	0.0274	0.0272	0.0656	0.0658	0.1058	0.1034	0.1334	0.1317	0.0142	0.0148	0.0338	0.0335	0.0495	0.0496	0.0675	0.0680	0.00953	0.00965	0.0216	0.0217	0.0330	0.0330
ENTRAINMENT, MOLES LIQUID/MOLE VAPOR x 10^3	--	5.13	5.65	--	--	20.8	--	29.5	--	5.07	--	3.47	11.35	--	24.0	--	2.94	--	3.56	--	--	17.13

TABLE XVII

AMMONIA ABSORPTION FROM AIR BY WATER USING PERFORATED TRAY WITH 3-1/2-INCH WEIR

RUN NUMBER	223	224	225	226	227	228	229	230	231	232	233	234	235	236	237	238	239	240
WATER RATE																		
Gallons per minute	8.0	8.0	8.0	8.0	8.0	8.0	8.0	8.0	16.0	16.0	16.0	16.0	16.0	16.0	24.0	24.0	24.0	24.0
Lb moles per minute	3.70	3.70	3.70	3.70	3.70	3.70	3.70	3.70	7.40	7.40	7.40	7.40	7.40	7.40	11.10	11.10	11.10	11.10
Temperature °F, Tray Inlet	77.0	77.2	77.0	77.2	77.0	76.9	77.1	77.2	76.9	76.8	76.7	76.8	77.2	77.2	76.8	77.0	76.8	76.8
Temperature °F, Tray Outlet	78.8	78.8	79.2	79.3	78.8	78.6	78.1	78.1	78.1	78.1	77.9	77.9	78.1	77.9	77.7	77.9	77.9	78.1
AMMONIA FLOW																		
Lb moles per minute x 10^2	1.16	1.15	1.44	1.37	1.27	1.18	1.29	1.17	1.16	1.15	1.26	1.17	1.31	1.18	1.18	1.17	1.29	1.22
AIR FLOW																		
Temperature °F at blower suction																		
Dry bulb	90.0	90.0	90.0	90.0	77.5	77.5	73.5	73.5	86.0	86.0	77.5	77.5	76.0	76.0	76.5	76.5	86.4	86.4
Wet bulb	77.8	77.8	73.5	73.5	69.5	69.5	62.0	62.0	72.0	72.0	67.5	67.5	61.5	61.5	65.0	65.0	74.5	74.5
AIR-AMMONIA FLOW THROUGH TRAY (Avg. conditions)																		
Lb moles per minute x 10^2	9.84	9.80	24.49	24.45	36.94	36.89	49.42	49.09	10.06	10.02	24.23	24.18	37.16	37.12	10.49	9.93	24.51	24.48
Velocity, ft. per sec	1.03	1.02	2.55	2.54	3.83	3.82	5.06	5.04	1.06	1.05	2.52	2.52	3.82	3.82	1.08	1.02	2.55	2.55
F Factor, $u\rho_G^{1/2}$	0.28	0.28	0.69	0.69	1.04	1.04	1.39	1.38	0.28	0.28	0.68	0.68	1.05	1.04	0.29	0.28	0.69	0.69
EQUILIBRIUM CONDITIONS ON TRAY																		
Temperature, °F	78.8	78.8	79.2	79.3	78.8	78.6	78.1	78.1	78.1	78.1	77.9	77.9	78.1	77.9	77.7	77.9	77.9	78.1
Pressure, in Hg	30.60	30.60	30.67	30.67	30.76	30.76	31.00	31.04	30.33	30.33	30.56	30.57	30.98	30.97	30.92	30.99	30.53	30.54
Henry's Law Constant, In Hg/mole fraction	31.62	31.62	31.93	32.10	31.62	31.43	30.93	30.93	30.93	30.93	30.77	30.77	30.93	30.77	30.60	30.77	30.77	30.93
LIQUID COMPOSITION, MOLE FRACTION x 10^4																		
x_2	0	0	0	0	0	0	0	0	0	0	0	0	0	0	5.025	5.097	5.240	5.054
x_1	17.88	18.06	32.02	30.74	27.32	25.41	27.58	24.98	10.51	10.19	14.96	13.71	15.20	13.87	11.99	12.42	15.72	14.73
x_1^*	132.6	133.7	96.55	90.16	84.82	80.54	52.51	47.70	101.0	101.4	58.15	53.86	43.23	40.68	86.92	87.28	47.68	44.65
VAPOR COMPOSITION, MOLE FRACTION x 10^4																		
y_o	747.4	829.6	569.4	542.4	335.1	322.0	252.6	229.1	847.8	836.5	502.3	468.9	336.1	307.8	922.8	1003	502.4	472.7
y_1	137.0	138.1	100.5	94.36	66.63	61.86	52.39	47.53	103.0	103.4	58.55	54.21	43.16	40.42	86.02	86.66	48.05	45.22
y_1^*	18.48	18.66	33.34	32.18	28.08	25.96	27.52	24.89	10.72	10.39	15.06	13.80	15.18	13.78	11.86	12.33	15.84	14.92
MURPHREE EFFICIENCY, PER CENT																		
Vapor, E_{MV}	83.7	85.3	87.5	87.8	87.4	87.9	89.0	88.9	89.0	88.7	91.1	91.1	91.3	90.9	91.9	92.5	93.4	93.4
Liquid, E_{ML}	13.5	13.5	33.2	34.1	42.2	42.0	52.5	52.4	10.4	10.1	25.7	24.5	35.2	34.1	8.5	8.9	24.7	24.4
NUMBER OF TRANSFER UNITS																		
N_{OG}	1.85	1.95	2.10	2.13	2.09	2.13	2.21	2.21	2.24	2.22	2.44	2.44	2.45	2.42	2.55	2.64	2.74	2.74
N_L	2.25	2.25	3.63	3.66	4.31	4.31	4.57	4.64	1.37	1.40	2.33	2.38	2.93	2.78	1.08	1.12	1.85	1.83
N_G	1.89	2.00	2.19	2.22	2.20	2.24	2.37	2.36	2.30	2.28	2.53	2.53	2.56	2.53	2.61	2.70	2.83	2.83
GAS PHASE MASS TRANSFER COEFFICIENT																		
$k'_G a$, sec^{-1}	11.64	12.26	14.41	14.98	15.20	15.69	15.77	15.50	11.43	12.22	12.46	12.43	14.16	13.61	9.96	10.32	12.97	13.05
LIQUID CONCENTRATION PROFILE, MOLE FRACTION x 10^4																		
x_A	0	0	0	0	0	0	0	0	0	0	0	0	0	0	5.025	5.097	5.240	5.054
x_B	10.49	10.49	22.24	21.40	19.87	19.35	20.80	18.71	3.546	3.704	6.116	6.417	8.872	7.753	6.762	6.475	9.217	8.801
x_C	12.55	12.59	23.67	23.09	21.13	20.01	21.75	19.17	5.226	5.240	8.241	7.983	10.16	9.088	7.666	7.710	10.71	10.34
x_D	16.70	15.52	31.06	29.47	25.74	24.64	25.57	23.24	8.772	8.557	12.68	12.53	13.92	11.63	10.71	9.834	13.24	13.19
x_E	17.69	17.97	32.70	30.69	27.31	25.25	27.51	24.85	10.32	10.34	14.97	13.71	15.39	13.93	12.02	11.96	15.76	14.80
x_F	17.88	18.06	32.02	30.74	27.32	25.41	27.58	24.98	10.51	10.19	14.96	13.71	15.20	13.87	11.99	12.42	15.72	14.73
x_G	17.86	17.89	31.40	31.13	27.13	25.87	27.55	24.95	10.77	10.80	14.89	13.80	15.05	13.87	12.00	11.87	15.82	14.64
x_H	28.22	28.28	32.64	31.49	27.41	26.00	27.74	25.48	14.59	14.36	15.42	14.10	15.46	14.04	15.52	14.64	16.11	14.92
HYDRAULIC DATA																		
Pressure drop, in water	3.55	3.60	4.50	4.40	5.45	5.40	7.70	7.30	4.40	4.45	5.25	5.30	7.85	7.90	5.20	5.20	6.20	6.10
Froth height, in	5.3	5.3	7.8	7.7	9.6	9.5	11.8	11.9	6.5	6.4	10.2	10.3	12.3	12.3	8.0	8.1	11.5	11.4
Clear liquid height, in																		
Position B	3.40	3.40	3.50	3.60	3.30	3.30	3.30	3.20	4.20	4.20	4.50	4.50	4.50	4.50	4.90	4.90	5.30	5.30
C	3.30	3.30	3.00	3.15	2.70	3.00	2.50	2.60	3.80	4.10	3.80	4.00	3.70	3.50	4.40	4.90	4.60	4.80
D	3.30	3.30	3.30	3.20	3.20	2.90	2.80	2.80	4.10	4.00	4.30	4.30	4.30	4.10	4.80	4.90	5.00	4.70
E	3.40	3.30	3.50	3.50	3.40	3.40	3.20	3.20	4.20	4.20	4.50	4.40	4.50	4.30	4.90	4.90	5.10	5.10
Gas contact time, sec.	0.163	0.163	0.152	0.148	0.145	0.143	0.150	0.152	0.201	0.186	0.203	0.204	0.181	0.186	0.262	0.262	0.219	0.217
Liquid contact time, sec.	9.49	9.49	9.06	9.13	8.48	8.48	7.62	7.76	5.68	5.82	5.82	5.97	5.75	5.46	4.41	4.70	4.60	4.55
Mixing Parameter C	2.40	2.39	3.28	3.29	3.67	4.19	4.07	3.98	1.51	1.57	1.69	1.88	2.40	2.27	1.33	1.23	1.61	1.63
$mG/L = \lambda$	0.0275	0.0274	0.0689	0.0692	0.1026	0.1019	0.1333	0.1322	0.0139	0.0138	0.0330	0.0329	0.0501	0.0498	0.00935	0.00888	0.0223	0.0223
ENTRAINMENT, MOLES LIQUID/MOLE VAPOR x 10^3	--	2.56	3.04	--	12.82	--	4.64	--	1.62	--	6.68	--	56.8	--	1.05	--	30.8	--

TABLE XVIII

HYDRAULIC STUDIES WITH VALVE TRAY USING 2 INCH WEIR

Liquid Rate	Vapor Rate		Pressure Drop	Froth Height	Clear Liquid Height, in			
gal/min	u, ft/sec	F Factor	in H_2O	in	B	C	D	E
8.0	1.03	0.28	2.80	5.0	2.20	2.10	2.10	2.20
12.8	1.03	0.28	3.10	5.6	2.50	2.35	2.40	2.55
19.2	1.03	0.28	3.26	6.0	2.80	2.55	2.70	2.80
22.4	1.00	0.27	3.60	6.6	3.10	2.75	3.00	3.10
30.4	1.00	0.27	4.40	7.8	4.00	3.80	3.90	4.00
8.0	2.01	0.56	2.80	5.5	2.30	1.90	1.95	2.10
12.8	2.01	0.56	3.01	6.4	2.60	2.10	2.30	2.50
19.2	2.01	0.56	3.80	7.4	3.30	2.75	2.95	3.15
22.4	2.01	0.56	4.45	9.0	4.05	3.50	3.60	3.80
30.4	1.98	0.55	5.65	11.5	5.20	4.50	4.50	4.80
8.0	3.08	0.84	3.40	6.1	2.15	1.75	1.65	2.05
12.8	3.05	0.83	3.80	7.5	2.70	2.10	2.20	2.50
19.2	3.05	0.83	4.70	9.6	3.60	2.90	3.10	3.30
22.4	3.02	0.82	5.40	11.2	4.30	3.50	3.70	4.00
30.4	3.05	0.83	6.60	--	5.70	4.90	4.80	5.10
8.0	4.06	1.12	4.65	7.3	2.20	1.75	1.60	2.00
12.8	4.06	1.12	5.00	8.4	2.70	2.10	2.15	2.50
19.2	4.06	1.12	5.80	11.5	3.75	2.90	3.00	3.30
22.4	4.03	1.11	6.35	--	4.40	3.50	3.60	4.00
30.4	4.00	1.10	7.55	--	6.10	5.00	4.80	4.80
8.0	4.95	1.37	6.10	8.0	2.15	1.75	1.60	2.00
12.8	4.97	1.37	6.55	9.7	2.70	2.15	2.00	2.30
19.2	4.95	1.37	7.20	12.3	3.50	2.70	2.75	3.00
22.4	4.93	1.36	7.75	--	4.70	3.80	3.80	4.30
30.4	4.90	1.35	9.10	--	5.70	4.50	4.30	4.30

TABLE XIX

HYDRAULIC STUDIES WITH VALVE TRAY USING 3 1/2 INCH WEIR

Liquid Rate	Vapor Rate		Pressure Drop	Froth Height	Clear Liquid Height, in			
gal/min	u, ft/sec	F Factor	in H_2O	in	B	C	D	E
8.0	0.79	0.21	3.78	6.4	3.60	3.35	3.30	3.40
12.8	0.79	0.21	4.46	7.6	4.00	3.95	3.80	3.95
19.2	0.76	0.21	5.02	8.4	4.50	4.15	4.30	4.35
22.4	0.76	0.21	5.20	9.1	4.85	4.70	4.55	4.90
30.4	0.74	0.20	5.50	10.1	5.50	5.35	5.30	5.30
8.0	1.03	0.28	3.80	6.9	3.50	3.30	3.35	3.40
12.8	1.00	0.27	4.30	8.0	4.00	3.90	3.85	3.90
19.2	1.00	0.27	4.95	9.4	4.70	4.60	4.40	4.50
22.4	0.98	0.26	5.42	9.9	5.15	5.05	4.80	4.90
30.4	0.95	0.26	6.10	10.9	5.85	5.60	5.60	5.65
8.0	2.05	0.56	3.60	7.4	3.05	2.60	2.55	3.00
12.8	2.05	0.56	4.15	9.1	3.80	3.30	3.35	3.65
19.2	2.05	0.56	5.20	11.2	4.80	4.20	4.35	4.50
22.4	2.05	0.56	5.80	12.5	5.45	4.75	4.90	5.10
30.4	2.02	0.55	6.90	13.5	6.50	5.90	6.00	6.10
8.0	3.03	0.83	4.20	8.5	3.05	2.60	2.50	3.10
12.8	3.00	0.83	4.95	10.5	3.75	3.20	3.20	3.70
19.2	2.98	0.82	6.15	12.8	5.00	4.30	4.30	4.60
22.4	3.00	0.83	6.60	--	5.60	4.90	4.90	5.20
30.4	3.00	0.83	8.10	--	6.70	6.00	6.00	6.10
8.0	3.56	0.97	4.85	9.1	3.10	2.55	2.50	3.10
12.8	3.54	0.97	5.65	11.3	4.00	3.35	3.30	3.80
19.2	3.51	0.96	6.60	13.5	5.10	4.40	4.50	4.85
22.4	3.51	0.96	7.00	--	5.55	4.75	4.80	5.15
30.4	3.46	0.95	8.30	--	6.40	5.70	5.70	5.90
8.0	4.43	1.26	6.30	10.7	3.15	2.70	2.40	3.00
12.8	4.43	1.26	6.80	12.6	4.00	3.40	3.30	3.60
19.2	4.38	1.24	8.60	--	5.50	4.80	4.70	5.00

TABLE XX

HYDRAULIC STUDIES WITH PERFORATED TRAY USING 2 INCH WEIR

Liquid Rate	Vapor Rate		Pressure Drop	Froth Height	Clear Liquid Height, in			
gal/min	u, ft/sec	F. Factor	in H_2O	in	B	C	D	E
8.0	1.00	0.28	2.45	4.4	2.20	2.10	2.10	2.30
12.8	1.00	0.28	2.75	4.7	2.40	2.20	2.30	2.40
19.2	1.00	0.28	3.16	5.6	2.80	2.50	2.80	2.90
22.4	1.00	0.28	3.60	6.5	3.30	2.90	3.20	3.30
30.4	1.00	0.28	4.30	7.6	4.00	3.50	3.80	4.00
8.0	2.05	0.56	2.75	5.8	2.10	1.90	2.00	2.10
12.8	2.05	0.56	3.10	6.7	2.50	2.10	2.30	2.50
19.2	2.05	0.56	3.90	8.2	3.30	2.70	3.00	3.20
22.4	2.05	0.56	4.55	9.8	3.90	3.30	3.60	3.80
30.4	2.05	0.56	5.60	12.2	5.00	4.30	4.60	5.00
8.0	3.02	0.83	4.00	6.3	2.10	1.70	1.80	2.00
12.8	3.02	0.83	4.40	7.8	2.50	2.00	2.20	2.40
19.2	3.02	0.83	5.15	9.5	3.40	2.60	3.00	3.10
22.4	3.02	0.83	5.90	12.2	4.90	4.00	4.30	4.60
30.4	3.02	0.83	6.30	--	5.10	4.20	4.30	4.60
8.0	4.13	1.12	4.75	8.0	1.70	1.55	1.75	1.80
12.8	4.13	1.12	5.05	9.0	2.00	1.80	2.10	2.20
19.2	4.13	1.12	5.70	11.1	2.80	2.20	2.50	2.70
22.4	4.13	1.12	6.70	--	5.70	4.60	4.80	5.30
30.4	4.13	1.12	7.20	--	5.40	4.20	4.50	4.80
8.0	5.12	1.40	6.20	9.3	1.80	1.50	1.60	1.70
12.8	5.12	1.40	6.30	10.7	2.60	2.00	2.50	2.70
19.2	5.12	1.40	7.00	--	3.10	2.20	2.50	2.90
22.4	5.12	1.40	8.3	--	4.20	3.00	3.40	4.00
30.4	5.12	1.40	8.1	--	4.20	3.00	3.40	4.00

TABLE XXI

HYDRAULIC STUDIES WITH PERFORATED TRAY USING 3 1/2 INCH WEIR

Liquid Rate	Vapor Rate		Pressure Drop	Froth Height	Clear Liquid Height, in			
gal/min	u, ft/sec	F Factor	in H_2O	in	B	C	D	E
8.0	1.01	0.28	3.70	6.7	3.40	3.10	3.20	3.40
12.8	1.01	0.28	4.35	7.0	3.80	3.40	3.60	3.70
19.2	1.01	0.28	4.70	7.7	4.30	4.00	4.20	4.30
22.4	1.01	0.28	5.10	8.8	4.80	4.40	4.70	4.80
30.4	1.01	0.28	6.00	10.7	5.50	5.00	5.50	5.60
8.0	1.99	0.55	3.60	7.6	3.20	3.00	2.90	3.20
12.8	1.99	0.55	4.25	9.1	3.80	3.20	3.50	3.70
19.2	1.99	0.55	5.50	11.5	5.00	4.40	4.60	4.80
22.4	1.99	0.55	5.80	12.5	5.40	4.70	4.90	5.20
30.4	1.99	0.55	7.00	--	6.10	5.40	5.80	5.90
8.0	3.07	0.84	5.25	8.9	3.20	2.70	2.70	3.00
12.8	3.07	0.84	6.10	11.3	3.50	2.90	3.10	3.50
19.2	3.07	0.84	7.30	--	5.20	4.40	4.70	5.00
22.4	3.07	0.84	7.90	--	5.60	4.60	5.00	5.20
30.4	3.07	0.84	8.80	--	6.20	5.40	5.50	5.80
8.0	4.09	1.10	5.60	10.6	2.90	2.40	2.60	2.80
12.8	4.09	1.10	6.30	13.0	3.40	2.60	3.00	3.20
19.2	4.09	1.10	8.30	--	5.20	4.40	4.40	5.20
8.0	5.02	1.40	7.90	12.0	2.80	2.20	2.60	2.80
12.8	5.02	1.40	8.70	--	3.80	3.00	3.50	3.90

TABLE XXII

DRY TRAY PRESSURE DROP FOR VALVE TRAY

Gas Velocity ft/sec	F Factor	Pressure Drop in H_2O	Number of Valves Fully Open
1.20	0.32	1.40	3
1.40	0.38	1.65	3
1.69	0.45	1.55	4
1.96	0.53	1.96	4
2.21	0.59	1.84	5
2.79	0.75	2.68	5
2.22	0.60	2.06	5
2.45	0.66	2.31	5
2.66	0.71	2.56	5
3.14	0.84	2.92	6
2.91	0.78	2.47	6
2.08	0.56	1.40	6
2.30	0.62	1.30	7
3.34	0.90	2.28	8
3.72	1.00	2.82	8
3.96	1.06	3.22	8
3.82	1.06	2.76	8
4.11	1.10	2.85	9
4.72	1.27	3.73	9
5.03	1.35	4.20	9
5.35	1.44	4.78	9
2.72	0.73	1.28	9
4.68	1.26	3.70	9
4.60	1.23	3.40	9
4.33	1.17	3.05	9
3.98	1.06	2.65	9

TABLE XXIII

DRY TRAY PRESSURE DROP FOR PERFORATED TRAY

Gas Velocity ft/sec	F Factor	Pressure Drop in H_2O
0.77	0.21	0.17
1.01	0.28	0.25
1.25	0.34	0.35
1.52	0.42	0.45
1.77	0.48	0.52
1.98	0.55	0.62
2.51	0.69	0.90
2.99	0.83	1.27
3.55	0.97	1.65
4.00	1.11	2.25
4.43	1.25	2.75
5.00	1.40	3.44

APPENDIX B

SOURCES OF EXPERIMENTAL ERROR

SOURCES OF EXPERIMENTAL ERROR

It is almost impossible to determine the absolute error in the experiments conducted. However, the sources of possible error will be discussed, and their effect on the results will be shown.

The effect of an error on N_G will vary with the efficiency of the tray. For example, an experimental error causing a one-half per cent error in E_{OG} will cause an error in N_G that depends on the value of E_{OG}. This can be seen in Table XXIV. In computing the values in Table XXIV, liquid phase resistance was assumed to be absent.

TABLE XXIV

ERROR IN N_G CAUSED BY A ONE-HALF PER CENT ERROR IN E_{OG}

E_{OG}	Error in N_G, per cent
0.95	3.7
0.90	2.2
0.85	1.9
0.80	1.6
0.75	1.1

The possible errors that will influence the values of N_G may be grouped into four classes: (1) errors in determination of the correct inlet and outlet gas compositions, (2) errors in the determination of the correct equilibrium composition of the gas above the test tray, (3) errors in the correction for liquid phase resistance to mass transfer, and (4) miscellaneous errors.

Table XXV shows the error that would be caused by a one per cent error in y_o, y_1, and y_1^*. The values are based on runs No. 10 and 152 where the plate vapor efficiency was 90.1%.

TABLE XXV

ERROR IN N_G RESULTING FROM ERRORS IN y_o, y_1, OR y_1^*

System	% Error in N_G Resulting from a 1% Error:		
	y_o	y_1	y_1^*
Air-Water	0.2	5.6	5.6
Ammonia-Air-Water	0.4	0.4	0.2

It can be seen from Table XXV that the air-water system is more sensitive to gas composition errors than the ammonia-air-water system. This is to be expected since the difference between inlet and outlet concentration is considerably greater for the system containing ammonia. An error in y_o is almost self-compensating as it appears in both the numerator and the denominator in the expression for plate efficiency. However, since y_o is so much larger than either y_1 or y_1^*, an error in the latter terms is overshadowed by the size of y_o. In the air-water system, this is not the case. The values of y_1 and y_1^* are much closer to y_o so an error in the former terms will cause a larger error in plate efficiency and N_G.

Table XXVI shows the error that would be caused in N_G by a ten per cent error in N_L. In making this table, it was assumed that the value of N_L was equal to that of N_{OG}.

TABLE XXVI

ERROR IN N_G RESULTING FROM ERRORS IN N_L

$\frac{mG}{L}$	% Error in N_G for 10% Error in N_L
0.008	0.1
0.02	0.2
0.08	1.0
0.12	1.5

Thus, a large error in N_L has a relatively small effect on N_G, especially where the liquid phase resistance is smallest.

In the determination of gas compositions, errors can arise from several sources. These depend on the particular sample, and for the equilibrium composition are:

1. Measurement of the average bulk liquid temperature.
2. Assumption that the liquid surface temperature was equal to the bulk temperature.
3. Vapor pressure or solubility data.
4. Influence of impurities.
5. Measurement of the pressure above the test plate.

Ashby[9] discussed these sources for the air-water system and estimated the maximum error in y_1^* to be less than one per cent. For the ammonia-air-water system, items 1 and 2 above can be combined. The liquid flowing across the tray showed a temperature rise of from 1 - 2°F in most cases. This was due to heat of solution of ammonia. Thus, it is very likely that the surface temperature was greater than the bulk liquid

temperature. To compensate for this heating effect the equilibrium temperature was taken to be the temperature of the liquid leaving the tray. It is estimated that the maximum error in y_1^* is less than two per cent for the ammonia-air-water system.

The errors in inlet and outlet gas compositions could be caused by:

1. Weighing the drying tubes or analyzing the bubblers.
2. Failure of the drying tubes or bubblers to remove all of the solute.
3. Inaccuracy of the wet test meters.

Ashby estimated the maximum errors in y_o and y_1 to be less than two per cent for the air-water system. For the ammonia-air-water system the errors should be about the same value.

The error in N_L would be caused by the application of the bubble cap correlation to other types of trays, or possibly by an error in the correlation itself. This is a minor correction as was shown in Table XXVI.

Miscellaneous errors might arise from:

1. Measurement of liquid and gas flow rates.
2. Variation of gas composition with time.
3. Failure to obtain a uniform sample.
4. Entrained liquid in the outlet vapor sample.

The fluid flow rates enter into the expression for N_G only in the ammonia-air-water, and they have only a slight effect. It is believed that the flow rate measurements are accurate enough so that any error caused is negligible.

It was found that even for the duplicate runs the composition of the gas samples varied somewhat. This variance was quite small and had a relatively minor effect as can be seen by comparing the experimental results.

The problem of obtaining a uniform vapor sample is one that arises in experiments on gas-liquid contacting apparatus. It is assumed that the turbulence on the tray is sufficient to completely mix the vapor. As the material balance over the tray closed within five per cent for all runs, it appears that the error caused by a non-uniform sample would be very small.

Entrained liquid in the exit vapor sample would cause a very large error in the air-water system as the vapor is very close to saturation. It would be expected the entrainment would increase with increasing vapor rate. It was found that the reproducibility of the data was as good for high vapor velocities as for the low velocities so it appears that the entrainment was negligible. In the ammonia-air-water system entrainment would not have much effect as the ammonia in the entrained liquid is insignificant compared to the ammonia in the vapor sample.

If all of the errors did exist and were additive, a large error in N_G would result. This could be as high as 25 per cent for the air-water system, and 5 per cent for the ammonia-air-water system. As the exit gas is close to equilibrium conditions in gas phase controlling systems, there is a possibility of a large error as N_G is very sensitive to changes in the exit gas or equilibrium vapor compositions. This is magnified still further if the difference between entrance and exit gas compositions is small.

APPENDIX C

SOLUBILITY AND CALIBRATION DATA

SOLUBILITY AND CALIBRATION DATA

The ammonia solubility data used in this work were obtained from the survey made for the A.I.Ch.E. Tray Efficiency Program.[2] The values listed in the following table are taken from the above survey and are based primarily on the data of Sherwood[57], Breitenbach[16], and Morgan and Maass[45].

TABLE XXVII

AMMONIA SOLUBILITY IN WATER AT LOW PARTIAL PRESSURES*

Temperature °C	Temperature °F	Henry's Law Constant, H, in Hg/Mole Fraction
20	68.0	23.07
22	71.6	25.62
24	75.2	28.46
25	77.0	29.93
26	78.8	31.62
27	80.6	33.25
28	82.4	34.96
29	84.2	36.77
30	86.0	38.66

* For partial pressures of ammonia less than 10 mm Hg and liquid concentrations less than 1.5 mole per cent.

Rotameter Calibrations

Liquid rotameters were calibrated by weighing the water collected for a measured time at several scale readings. The ammonia rotameter was calibrated with a Critical Flow Orifice Prover, and

readings were converted to ammonia rates by

$$Q = Q_c \sqrt{\rho_c/\rho} \tag{77}$$

where

Q = volumetric flow rate at given reading

Q_c = calibrated volumetric flow rate at same reading

ρ_c = density at calibration conditions

ρ = density at flowing conditions

Wet Test Meter Calibrations

The wet test meters were calibrated by passing a known volume of saturated air through one of them and comparing the known volume with the indicated volume. The air was obtained by forcing air from a five-gallon jug with water. The volume of air used was found by weighing the jug before and after testing. The two meters were then placed in series and the readings compared after passing a quantity of saturated air through them. Knowing the calibration of one meter and the ratio of the two, the calibration of the second was readily computed.

TABLE XXVIII

CALIBRATION OF ROTAMETER W70-402A/1[9]

Water at 54°F	
Scale Reading	Water, gpm
20	6.38
40	12.77
60	19.14
80	25.55

TABLE XXIX

CALIBRATION OF ROTAMETER 5601 D 1038B1[25]

Water at 60°F	
Scale Reading	Water, gpm
19.0	6.20
34.5	11.03
48.0	15.50
60.0	18.95
75.0	23.45
90.0	28.40
96.5	30.00

TABLE XXX

CALIBRATION OF ROTAMETER V5-1200/1

Scale Reading	cfm NH_3 at 70°F and 30.00 in Hg
23.3	5.25
38.8	8.75
49.3	11.02
58.5	13.65
69.5	15.83
79.1	18.13
88.8	20.49
89.0	22.69

TABLE XXXI

CALIBRATION OF WET TEST METER H9SS

Actual Volume, ft^3	Indicated Volume, ft^3	Correction Factor
0.5740	0.5872	0.9775
0.5771	0.5886	0.9805
0.6080	0.6237	0.9748
		avg. 0.9776

TABLE XXXII

CALIBRATION OF WET TEST METER J5SS

Reading, ft^3 Meter, H9SS	Reading, ft^3 Meter, J5SS	Ratio	Correction Factor for Meter J5SS
0.4949	0.4907	1.0085	0.9859
0.5037	0.4993	1.0085	0.9859
			avg. 0.9859

APPENDIX D

SAMPLE CALCULATIONS

SAMPLE CALCULATIONS

The data from ammonia absorption run 115 will be used to show the methods used to calculate the results.

1. Vapor Sample Concentrations

a. Inlet Sample

HCl in bubblers = (35.00 ml)(1.0486N) = 36.7010 meq.

NaOH to neutralize = (12.78 ml)(0.3461N) = 4.4232

meq. NH_3 in sample = 32.2778

Humidity of air = 0.01009 mole water/mole dry air

Wet Test Meter conditions

T = 84.0°F

P = 29.28 in Hg

Vapor pressure of water = 1.1750 in Hg

Mole fraction dry air = (29.28-1.1750)/29.28 = 0.9599

Molar density = $(29.28)/(21.85)(544) = 246.3 \times 10^{-5}$ lb moles/ft^3

Measured volume = 0.4025 ft^3

Meter factor = 0.9859

Moles dry air in sample
$= (0.4025)(0.9599)(0.9859)(246.3 \times 10^{-5}) = 93.82 \times 10^{-5}$

Moles water in sample
$= (0.01009)(93.82 \times 10^{-5}) = 0.9466 \times 10^{-5}$

Moles ammonia in sample
$= (32.2778)/(454)(1) = 7.110 \times 10^{-5}$

Total moles in sample $\times 10^5$
$= 93.82 + 0.9466 + 7.110 = 101.8766$

$$y_o = \frac{7.110}{101.8766} = 0.06979 \text{ mole fraction}$$

$$y_{ho} = \frac{0.9466}{101.8766} = 0.00929 \text{ mole fraction}$$

b. Outlet Sample

In the same manner as for the inlet sample are found:

Moles dry air in sample = 93.33×10^{-5}

Moles ammonia in sample = 0.7156×10^{-5}

The outlet gas is assumed to be saturated with water at the temperature on the test tray.

T = 77.9°F

P = 30.86 in Hg

Vapor pressure of water = 0.9635 in Hg

$y_{hl} = (0.9635)/30.86 = 0.03122$ mole fraction

Total moles in sample $\times 10^5$
$= (93.33 + 0.7156)/(1-0.03122) = 97.076$

$y_l = (0.7156)/(97.076) = 0.007371$ mole fraction

2. Liquid Sample Concentrations

a. Blank Correction (Sample A)

HCl in bottle = (5.00 ml) (1.0486 N) = 5.2430 meq.

NaOH to neutralize = (15.05 ml)(0.3461 N) = 5.2088

Correction for alkalinity of tap water = 0.0342 meq.

b. Sample B

HCl in bottle = (5.00)(1.0486) = 5.2430 meq.

NaOH to neutralize = (4.33)(0.3461) = 1.4986

3.7444 meq.

Less correction 0.0342

meq. NH_3 in sample = 3.7102

Volume of sample = 49.80 ml = 2.767 gram moles

$x_B = (3.7102 \times 10^{-3})/(1)(2.767) = 13.41 \times 10^{-4}$ mole fraction

c. Other Liquid Sample Concentrations

Other liquid sample concentrations are calculated in the same manner.

$x_F = 25.39 \times 10^{-4}$ mole fraction

Thus

$$x_2 = 0$$

$$x_e = 13.41 \times 10^{-4}$$

$$x_1 = 25.39 \times 10^{-4}$$

3. Mixing Parameter C

$$C = \frac{x_1 - x_2}{x_1 - x_e} \qquad (14)$$

$$\text{so } C = \frac{(25.39 - 0)10^{-4}}{(25.39 - 13.41)10^{-4}} = 2.12$$

4. Equilibrium Concentrations

Henry's Law constant = 30.77 in Hg/mole fraction

$y_1^* = Hx_1/P = (30.77)(25.39 \times 10^{-4})/(30.86) = 25.21 \times 10^{-4}$ mole fraction

$x_1^* = Py_1/H = (30.86)(73.71 \times 10^{-4})/(30.77) = 73.93 \times 10^{-4}$ mole fraction

5. Plate Efficiencies

$$E_{MV} = \frac{y_o - y_1}{y_o - y_1^*} = \frac{697.9 - 73.71}{697.9 - 25.21} = 92.8\%$$

$$E_{ML} = \frac{x_1 - x_2}{x_1^* - x_2} = \frac{25.39 - 0}{73.93 - 0} = 34.4\%$$

6. Liquid Flow Rate

Rotameter reading = 50

Calibrated rate = 16.0 gpm

L = (16.0)(8.33)/18 = 7.40 lb moles/minute

7. Vapor Flow Rate

Rotameter is calibrated in cfm for gas with a gravity of 0.877 at 60°F and 14.7 psi (ρ = 0.06678 lb/ft^3).

Molecular weight of gas flowing in rotameter
(17)(0.06979) + (18)(0.00929) + (28.9)(0.92092) = 27.97

Pressure in rotameter = 31.71 in Hg

Temperature in rotameter = 102.7°F

Density of gas = (31.71)(27.97)/(21.85)(562.7) = 0.07214 lb/ft^3

Rotameter reading = 120

Volumetric flow rate

$$Q = 120\sqrt{(0.06678)/(0.07214)} = 115.5 \text{ cfm}$$

G_o = (115.5)(0.07214)/(27.97) = 0.2977 lb moles/min

This is also the flow rate beneath the test tray.

$$G_1 = G_o(1 - y_o - y_{ho})/(1 - y_1 - y_{h1})$$

G_1 = (0.2977)(0.92092)/(0.96141) = 0.2852 lb moles/min

$$G_{avg} = \frac{G_o+G_1}{2} = \frac{0.2977 + 0.2852}{2} = 0.2915 \text{ lb moles/min}$$

8. Vapor Velocity

The vapor velocity is based on the active tray area between the inlet downcomer and the splash baffle, 0.615 sq ft.

$$u = \frac{(0.2915)(359)(29.92)(537.9)}{(60)\ (0.615)(30.86)(492)} = 3.01 \text{ ft/sec}$$

9. F Factor

Molecular weight of gas above test tray
(17)(0.007371) + (18)(0.03122) + (28.9)(0.96141) = 28.47

Average molecular weight = $\frac{27.97 + 28.47}{2}$ = 28.22

$$\rho_{avg} = \frac{(30.86)(28.22)}{(21.85)(537.9)} = 0.07410 \text{ lb/ft}^3$$

$$F = u\sqrt{\rho} = (3.01)(0.07410)^{1/2} = 0.818$$

10. Ammonia Balance on Tray

$$\frac{NH_3 \text{ out}}{NH_3 \text{ in}} = \frac{(G_1y_1+Lx_1)}{(G_oy_o+Lx_2)} = \frac{[(0.2852)(73.71x10^{-4})+(7.40)(25.39x10^{-4})]}{[(0.2977)(697.9x10^{-4})+(7.40)(0)]}$$

$$= 1.005$$

11. Residence Times

a. Gas Residence Time

$Z_f = 10.1$ inches

$Z_c = 3.95$ inches

$$t_G = \frac{(Z_f-Z_c)}{12\ u} = \frac{(10.1 - 3.95)}{(12)\ (3.01)} = 0.170 \text{ sec}$$

b. Liquid Residence Time

$$t = \frac{Z_c\ A}{12\ L_Q}$$

$$L_Q = \frac{(16.0)}{(7.48)(60)} \text{ cu ft/sec}$$

$$t_L = \frac{(0.395)(0.615)(7.48)(60)}{(12)(16.0)} 5.68 \text{ sec}$$

12. Transfer Units

a. Overall Gas Phase

$$N_{OG} = 1/2 \ln \frac{(1-y_1)}{(1-y_o)} - \ln (1-E_{OG}) \qquad (59)$$

Using E_{MV} as E_{OG},

$$N_{OG} = 1/2 \ln \frac{(1-0.007371)}{(1-0.06979)} - \ln (1 - 0.928) = 2.665$$

b. Liquid Phase

$$N_L = 55.4\ D_L^{1/2}\ F^{0.575} t_L \qquad (71)$$

$$D_L = 8.04 \times 10^{-5} \text{ ft}^2/\text{hr}$$

$$N_L = (55.4)(8.04 \times 10^{-5})^{1/2}(0.818)^{0.575}(5.68) = 2.513$$

c. Individual Gas Phase

$$\frac{1}{N_{OG}} = \frac{1}{N_G} + \frac{\lambda\,(1-x)_f}{N_L\,(1-y)_f} \qquad (52)$$

$$\lambda = \frac{HG}{PL} = \frac{(30.77)(0.2915)}{(30.86)\quad(7.40)} = 0.0393$$

$$\frac{1}{N_G} = \frac{1}{2.665} - \frac{(0.0393)[0 - 25.39\times10^{-4}]\ \ln\left(\frac{1 - 0.06979}{1 - 0.007371}\right)}{(2.513)\ \ln\left(\frac{1 - 25.39\times10^{-4}}{1 - 0}\right)[73.71 - 697.9]10^{-4}}$$

$$N_G = 2.785$$

13. Gas Phase Mass Transfer Coefficient

$$k'_G a = \frac{N_G}{t_G} = \frac{2.785}{0.170} = 16.34 \text{ sec}^{-1}$$

Calculations for the humidification runs were in the most part identical to those for the absorption runs and only the methods that differed are shown.

14. Vapor Sample Concentrations - Run 17

a. Inlet Sample

Moles dry air in sample = 121.05×10^{-5}

Water absorbed = 0.1157 grams = 1.4158×10^{-5} lb moles

Total moles in sample = $121.05 + 1.4158 = 122.4658 \times 10^{-5}$

$$y_o = \frac{1.4158}{122.4658} = 0.01156 \text{ mole fraction}$$

b. Outlet Sample

Calculations are the same as the inlet sample

$y_1 = 0.02907$ mole fraction

15. Equilibrium Concentration

Liquid temperature = 77.1 °F

Vapor pressure of water = 0.9374 in Hg

Pressure on tray = 31.41 in Hg

$y_I^* = (0.9374)/31.41 = 0.02984$ mole fraction

16. Plate Efficiency

$$E_{MV} = E_{OG} = \frac{(0.02907 - 0.01156)}{(0.02984 - 0.01156)} = 95.6\%$$

17. Individual Gas Phase Transfer Units

$$N_{OG} = N_G = -\ln (1-E_{OG}) \qquad (32)$$

$N_G = -\ln (1-0.956) = 3.171$

NOMENCLATURE

a	interfacial area, sq ft/cu ft gas holdup.
a'	interfacial area, sq ft/cu ft gas and liquid holdup.
$\bar{a}$	interfacial area, sq ft/cu ft liquid holdup.
A	constant in Equation (73).
A_1	function defined for Equation (17).
A_2	function defined for Equations (17) and (20).
b	constant in Equation (73).
c	constant in Equation (73).
c	concentration of solute in liquid, lb moles/cu ft.
c^*	concentration of solute in liquid in equilibrium with gas, lb moles/cu ft.
c_{BM}	logarithmic mean concentration of non-diffusing component.
C	mixing parameter defined by Equation (14).
C	function in Equation (66).
d	constant in Equation (73).
d	differential operator.
D_E	eddy diffusivity, ft^2/sec.
D_G	gas phase diffusivity, ft^2/sec.
D_L	liquid phase diffusivity, ft^2/sec.
D_s	bubble cap slot width.
E_a	apparent vapor plate efficiency in presence of entrainment.
E_{ML}	Murphree liquid efficiency.
E_{MV}	Murphree vapor efficiency.
E_o	overall column efficiency.
E_{OG}	vapor point efficiency.

E_{OL} liquid point efficiency

exp (x) e^x

F F factor, $u\sqrt{\rho_G}$, based on active bubbling area between inlet downcomer and splash baffle (0.615 sq ft).

G molar gas rate, lb moles/hr.

G_M molar gas velocity, lb moles/hr-sq ft.

h_L vertical distance between bottom of bubble cap slot opening and top of liquid flowing over weir.

H Henry's Law constant, atm/mole fraction, or in Hg/mole fraction.

H_{OG} height of an overall gas phase transfer unit, ft.

k_G individual gas phase mass transfer coefficient, lb moles/hr - sq ft - atm.

k_L individual liquid phase mass transfer coefficient, lb moles/ hr - sq ft - lb moles/cu ft.

$k'_G a$ individual gas phase mass transfer coefficient based on gas holdup, sec^{-1}.

$k_L \bar{a}$ individual liquid phase mass transfer coefficient based on liquid holdup, sec^{-1}.

K_{OG} overall gas phase mass transfer coefficient, lb moles/ hr - sq ft - atm.

$K'_{OG} a$ overall gas phase mass transfer coefficient based on gas holdup, sec^{-1}.

K_{OL} overall liquid phase mass transfer coefficient, lb moles/ hr - sq ft - lb moles/cu ft.

ℓn natural logarithm.

L molar liquid rate, lb moles/hr.

L_M molar liquid velocity, lb moles/hr - sq ft.

m slope of the equilibrium curve, dy*/dx.

M function defined for Equation (17).

n number of pools or mixing stages used in Equation (12).

n function defined for Equations (67) and (68).

N_A	rate of mass transfer of component A, lb moles/hr - sq ft.
N_G	number of individual gas phase transfer units.
N_L	number of individual liquid phase transfer units.
N_{OG}	number of overall gas phase transfer units.
N_{OL}	number of overall liquid phase transfer units.
p	partial pressure of solute in gas phase, atm.
p*	partial pressure of solute in gas in equilibrium with liquid, atm.
p_{BM}	logarithmic mean partial pressure of non-diffusing component in the gas phase.
P	total pressure, atm.
Q	volumetric flow rate, cu ft/min.
Q_B	fraction of liquid rate splashing upstream.
Q_F	fraction of liquid rate splashing downstream.
R	ideal gas law constant, atm - cu ft/lb mole - °R.
S	length of plate, ft.
t_G	gas residence time, sec.
t_L	liquid residence time, sec.
T	absolute temperature, °R.
u	linear gas velocity through column, based on active bubbling area between inlet downcomer and splash baffle (0.615 sq ft).
w	dimensionless distance along plate.
W_B	normalized distance of upstream liquid splashing.
W_F	normalized distance of downstream liquid splashing.
x	mole fraction solute in liquid.
x*	mole fraction solute in liquid in equilibrium with vapor.
x'	mole fraction solute in liquid, taken in a given horizontal plane.
x'*	mole fraction solute in liquid in equilibrium with vapor, taken in a given horizontal plane.

y	mole fraction solute in vapor.
y^*	mole fraction solute in vapor in equilibrium with liquid.
y'	mole fraction solute in vapor, taken in a given vertical plane.
y'^*	mole fraction solute in vapor in equilibrium with liquid, taken in a given vertical plane.
z	length of element through which diffusion occurs, ft.
Z	vertical distance through liquid or froth, ft.
Z_c	clear liquid height, in. or ft.
Z_f	froth height, in. or ft.
α	function in Equation (69).
β	mixing parameter defined by Equation (19).
β'	function in Equation (69).
γ	mixing parameter defined by Equation (16).
ϵ	entrainment, moles liquid/mole vapor.
λ	mG_M/L_M, slope of equilibrium line/ slope of operating line.
μ	viscosity, centipoises or lb/ft - hr.
φ	functional notation.
ρ	density, lb/cu ft.
ρ_{ML}	molar liquid density, lb moles/cu ft.
σ	surface tension

Subscripts

avg	average value
c	refers to calibrated value
e	sample taken between inlet and first row of bubble caps.
f	logarithmic mean value

G	gas phase
i	at the interface.
L	liquid phase.
n	stream leaving plate n.
0	entering plate 1 from below (gas).
1	on or leaving plate 1.
2	entering plate 1 from above (liquid).

BIBLIOGRAPHY

1. American Institute of Chemical Engineers Research Committee, "Second Annual Progress Report," University of Delaware (1954).

2. American Institute of Chemical Engineers Research Committee, "Second Annual Progress Report," University of Michigan (1954).

3. American Institute of Chemical Engineers Research Committee, "Third Annual Progress Report" (1955).

4. American Institute of Chemical Engineers Research Committee, "Addenda to the Third Annual Progress Report" (1956).

5. American Institute of Chemical Engineers Research Committee, "Fourth Annual Progress Report" (1956).

6. Anderson, J. E., Sc.D. Thesis, Massachusetts Institute of Technology (1954).

7. Anon., Petroleum Processing, 12, No. 1, 58 (1957).

8. Arnold, D. S., Plank, C. A. and Schoenborn, E. M., Chem. Eng. Prog., 48, 633 (1952).

9. Ashby, B. B., Ph.D. Thesis, University of Michigan (1955).

10. Badger, W. L. and Banchero, J. T., Introduction to Chemical Engineering, McGraw-Hill Book Company, Inc., New York (1955).

11. Begley, J. W., Personal Communication (1958).

12. Bolles, W. L., Petroleum Processing, 11, No. 2, 64; No. 3, 82; No. 4, 72; No. 5, 109 (1956).

13. Bowles, V. O., Petroleum Refiner, 33, No. 5, 197 (1954).

14. Bowles, V. O., U. S. Patent 2,692,128 (1954).

15. Bowles, V. O., Petroleum Refiner, 34, No. 7, 118 (1955).

16. Breitenbach, W. E., Bull. Univ. Wisconsin Eng. Exptl. Sta., Ser. No. 68 (1925).

17. Brown, G. G. and Associates, Unit Operations, Chapter 23, John Wiley and Sons, Inc., New York (1950).

18. Brown, J. W., B. S. Thesis, Massachusetts Institute of Technology (1954).

19. Byfield, A., S. M. Thesis, Massachusetts Institute of Technology (1939).

20. Chilton, T. H. and Colburn, A. P., Ind. Eng. Chem., 27, 255 (1935).

21. Chu, J. C., Petroleum Processing, 6, 39 (1951).

22. Chu, J. C., Petroleum Processing, 6, 154 (1951).

23. Cogan, M. H. R., U. S. Patent 2,711,308 (1955).

24. Colburn, A. P., Ind. Eng. Chem., 28, 526 (1936).

25. Crozier, R. D., Ph.D. Thesis, University of Michigan (1956).

26. Davies, J. A., Petroleum Refiner, 29, No. 8, 93; No. 9, 121 (1950).

27. Davies, J. A., Gordon, K. F. and Williams, Brymer, Notes for "Advances in Design and Operation of Distillation and Absorption Equipment," given at the University of Michigan, July, 1958.

28. Drickamer, H. G. and Bradford, J. R., Trans. Am. Inst. Chem. Engrs., 39, 319 (1943).

29. Friend, L. and Lemieux, E. J., Oil and Gas J., 54, No. 6, 88 (1956).

30. Garner, F. H., Ellis, S. R. M. and Luxon, E. S., J. Inst. Petrol., 43, 86 (1957).

31. Gautreaux, M. F. and O'Connell, H. E., Chem. Eng. Prog., 51, 232 (1955).

32. Gordon, K. F. and Sherwood, T. K., Chem. Eng. Prog. Symposium Series, No. 10, 15 (1954).

33. Huang, C. J. and Hodson, J. R., Petroleum Refiner, 37, No. 2, 103 (1958).

34. Hunt, C. d'A., Hanson, D. N. and Wilke, C. R., A.I.Ch.E. Journal, 1, 441 (1955).

35. Hutchinson, M. H. and Baddour, R. F., Chem. Eng. Prog., 52, 503 (1956).

36. Johnson, A. I. and Marangozis, J., Can. J. Chem. Eng., 36, 161 (1958).

37. Kammermeyer, K. and Lee, K. T., Paper presented at A.I.Ch.E. Meeting, Chicago, September, 1952.

38. Katzen, R., Chem. Eng., 62, No. 11, 213 (1955).

39. Kirschbaum, E., Dechema Monagraphien, 6, 19 (1933).

40. Kirschbaum, E., Distillation and Rectification, Chemical Publishing Company, New York (1948).

41. Lee, D. C., Petroleum Engineer, 26, No. 5, C 21 (1954).

42. Lewis, W. K. and Whitman, W. G., Ind. Eng. Chem., 16, 1215 (1924).

43. Lewis, W. K., Jr., Ind. Eng. Chem., 28, 399 (1936).

44. Marshall, W. R. and Pigford, R. L., Applications of Differential Equations to Chemical Engineering Problems, University of Delaware (1947).

45. Morgan, O. M. and Maass, O., Can. J. Research, 5, 162 (1931).

46. Murphree, E. V., Ind. Eng. Chem., 17, 747 (1925).

47. Norman, R. L., Personal Communication (1958).

48. Nutter, E., Petroleum Engineer, 26, No. 5, C 6 (1954).

49. O'Connell, H. E., Trans. Am. Inst. Chem. Engrs., 42, 741 (1946).

50. Oliver, E. D. and Watson, C. C., A.I.Ch.E. Journal, 3, 37 (1957).

51. Perry, J. H., Ed., Chemical Engineers Handbook, Third Edition, McGraw-Hill Book Company, Inc., New York (1950).

52. Perry, J. H., Ed., Chemical Engineers Handbook, Third Edition, Section 8, McGraw-Hill Book Company, Inc., New York (1950).

53. Perry, J. H., Ed., Chemical Engineers Handbook, Third Edition, Section 12, McGraw-Hill Book Company, Inc., New York (1950).

54. Robinson, C. S. and Gilliland, E. R., Elements of Fractional Distillation, 4th Edition, Chapter 17, McGraw-Hill Book Company, Inc., New York (1950).

55. Robinson, D., Ph.D. Thesis, University of Delaware (1958).

56. Samaniego, J. A., Oil and Gas J., 52, 161 (April 26, 1954).

57. Sherwood, T. K., Ind. Eng. Chem., 17, 745 (1925).

58. Sherwood, T. K. and Pigford, R. L., Absorption and Extraction, 2d Edition, McGraw-Hill Book Company, Inc., New York (1952).

59. Sherwood, T. K. and Pigford, R. L., Absorption and Extraction, 2d Edition, Chapter V, McGraw-Hill Book Company, Inc., New York (1952).

60. Sherwood, T. K. and Pigford, R. L., Absorption and Extraction, 2d Edition, Chapter VIII, McGraw-Hill Book Company, Inc., New York (1952).

61. Stone, H. L., Sc.D. Thesis, Massachusetts Institute of Technology (1953).

62. Talvalkar, S. G., Personal Communication (1958).

63. Thrift, G. C., Chem. Eng., 61, No. 5, 173 (1954).

64. Treybal, R. E., Mass-Transfer Operations, McGraw-Hill Book Company, New York (1955).

65. Treybal, R. E., Mass-Transfer Operations, Chapter 2, McGraw-Hill Book Company, New York (1955).

66. Warzel, L. A., Ph.D. Thesis, University of Michigan (1955).

67. West, F. B., Gilbert, W. D. and Shimizu, T., Ind. Eng. Chem., 44, 2470 (1952).

68. Westkaemper, L. E., Ph.D. Thesis, University of Michigan (1955).

69. Wharton, L., B. S. Thesis, Massachusetts Institute of Technology (1955).

70. Whitman, W. G., Chem. Met. Engr., 29, 146 (1923).

71. Williams, G. C., Stigger, E. K. and Nichols, J. H., Chem. Eng. Prog., 46, 7 (1950).

72. Willard, H. H. and Furman, N. H., Elementary Quantitative Analysis, 3d Edition, D. Van Nostrand Company, Inc., New York (1940).